1963

Automatic interpretation of the clinical electrocardiogram

Morris Henry Mericle
Iowa State University

AUTOMATIC INTERPRETATION OF THE CLINICAL ELECTROCARDIOGRAM

by

Morris Henry Mericle

A Dissertation Submitted to the

Graduate Faculty in Partial Fulfillment of

The Requirements for the Degree of

DOCTOR OF PHILOSOPHY

Major Subject: Electrical Engineering

Approved:

Signature was redacted for privacy.

In Charge of Major Work

Signature was redacted for privacy.

Head of Major Department

Signature was redacted for privacy.

Dean of Graduate College

Iowa State University
Of Science and Technology
Ames, Iowa

1963

TABLE OF CONTENTS

INTRODUCTION

General

History

It has been known for many years that a measurable amount of electric current is associated with activity of the heart. Ludwig and Waller, in 1892, experimented with the capillary electroscope and recorded this electromotive force from the precordium. Einthoven's description, in 1903, of the string galvanometer, a sensitive and quantitative instrument, stimulated a sudden increase in both clinical and experimental studies of electrocardiography. This type of magnetic galvanometer has remained useful, although, in more recent times, electronic amplifiers, oscillographs, and cathode ray tubes have been employed with much greater utility and a greater degree of accuracy.

The present concept of the theory of electrocardiography is based on data collected from many sources. Some of the main sources of information are:

1. Clinical data collected on patients during life and correlated with information found at necropsy.
2. Physiologic observations on the intact hearts of experimental animals, such as the frog, turtle, dog, and cat.
3. Study of isolated muscle strips.
4. Studies on the giant axon of the squid, as well as other nerves, by neurophysiologists.
5. Studies on the large one-celled plant.

Present day studies of electrocardiography of interest to the engineer are being accomplished primarily in the following areas:

1. Automatic recording.
2. Spatial vectorcardiography.
3. Automatic diagnosis by digital computer.
4. Electrical models of the heart.

Utilization of modern concepts of data acquisition and processing can advance the concept of the electrocardiogram, increase its usefulness, and provide a method of economically handling a high volume of patient traffic.

Purpose

The investigation of automatic interpretation of the clinical electrocardiogram is being accomplished as a project for the heart station of Iowa Methodist Hospital. In a major hospital, the patient traffic is heavy, and a great deal of clinical data becomes available from those treated. For purposes of research by the heart station, it is highly desirable to acquire an electrocardiogram on each patient, for purposes of classification, diagnosis, and statistical studies.

The present method of electrocardiogram analysis is manual. Technicians measure and record all pertinent parameters from the electrocardiogram. This is time-consuming, and permits recording and analysis of only a relatively small percentage of the patient traffic. This investigation has consisted of two major portions. The first has been the utilization of an IBM 1620 computer to diagnose the principal heart diseases. The diagnosis is checked by cardiologists for verification and a more detailed

analysis. Generally, the normal, manually measured clinical parameters have been utilized, and the diagnostic logic of the cardiologist duplicated on the computer. The second portion has been the study of the methods of automatically measuring the electrocardiogram, and furnishing a diagnosis directly, without the interposition of technicians. This method must be accurate, economical, and within the capabilities of a reasonably sized computer.

There are two levels of objective in the program. The first is the overall objective to furnish, on a routine, automatic basis, electrocardiograms, together with their associated classifications (diagnoses) to a large number of patients constituting the traffic. This is intended to serve, not as a complete diagnosis, but rather, as a routine indicator of the heart condition of the patient, and in some cases, to discover evidence of heart disease not previously suspected.

However, the more fundamental, the basic objective of this dissertation is the investigation of the use of correlation techniques in the recording and diagnosis of the electrocardiogram. Such techniques permit utilization of a much greater amount of the information available in the electrocardiogram than the information contained in the normal clinical parameters. This should permit a reduction in the number of leads required per patient, since the correlation technique yields information on the exact nature of the wave shape, as well as the normally recorded clinical parameters. Work has been done on both the automatic recording of the electrocardiogram, and on the use of correlation techniques in interpretation, however, it is felt that the technique utilizing the

repetitive pulse technique is novel, and holds promise for simplification of the automatic recording techniques.

Scope

The scope of this dissertation has been limited to investigation of the usefulness of correlation techniques for achieving a diagnosis of the electrocardiogram. It does not treat all the system aspects of the problem, nor the selection and fabrication of hardware. Therefore, it is confined to the following areas:

1. Investigation of the waveform under consideration.
2. Determination of diagnostic criteria, with their associated classification.
3. Comparison of the methods being presently used to solve this problem.
4. Investigation of the correlation techniques with application to this specific problem.
5. Analysis and selection of data acquisition techniques, with the associated logic of recognition.
6. Application of diagnostic criteria to data.
7. Analysis of results obtained.

The Clinical Electrocardiogram

General waveform

A typical electrocardiogram waveform is shown in Fig. 1. The parameters normally measured by the examining cardiologist are also indicated and tabulated on the same figure. The configuration shown, of

Figure 1. The normal clinical electrocardiogram shown with parameters

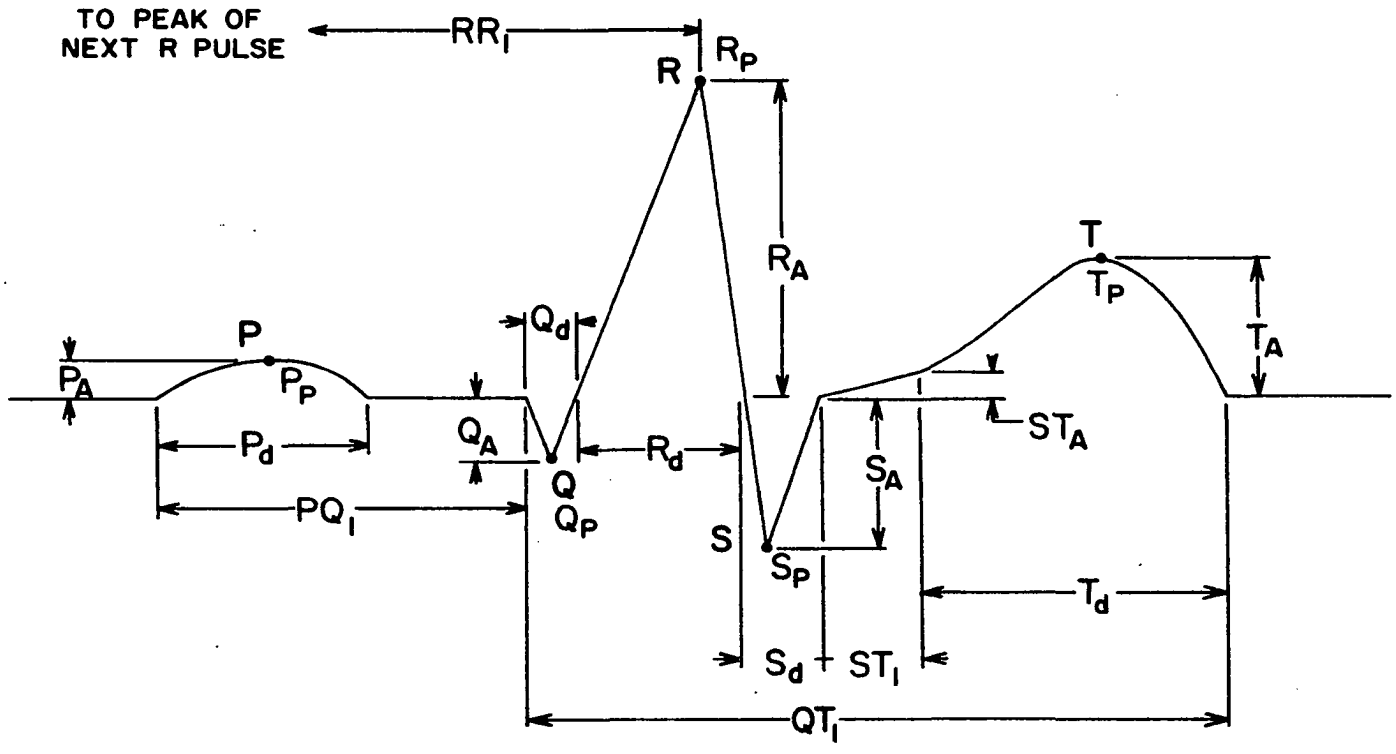

AMPLITUDES	DURATIONS	INTERVALS
P_A	P_d	PQ_I
Q_A	Q_d	ST_I
R_A	R_d	QT_I
S_A	S_d	RR_I
T_A	T_d	
ST_A		

course, varies from patient to patient, and varies with the position of the lead being measured. In order to extract the required information from the electrocardiogram, there are normally twelve leads employed per patient. This gives 180 available measurements per patient, although, for the diagnosis utilized in this project, only 49 measurements are required.

Measurements

The measurements are taken from contacts placed on different points of the body, which sense differences in potential generated between the points as various electrical actions occur in the heart. The output of the contacts then appears across a galvanometer, and the deflection of the galvanometer forms the electrocardiographic waveform. In the present day instruments the output of the sensors is usually amplified and recorded either on a Sanborn recorder, displayed on a cathode ray oscilloscope, or both. The normal connections for these leads, together with their nomenclature are shown by Fig. 2.

The standard leads, I, II, and III are attached in the following manner. Lead I measures the potential rise between the right and left wrist, lead II the potential rise between the right wrist and left leg, and lead III the potential rise between the left wrist and left leg. Any potential rise measured in a pair of these standard leads is the scalar sum of the potential rises of the other two pairs of leads. In accordance with Burch and Winsor (2) this is called Einthoven's Law. In actuality it is merely Kirchhoff's voltage law stated with reference to the particular system employed in electrocardiography. The precordial chest leads, V1,

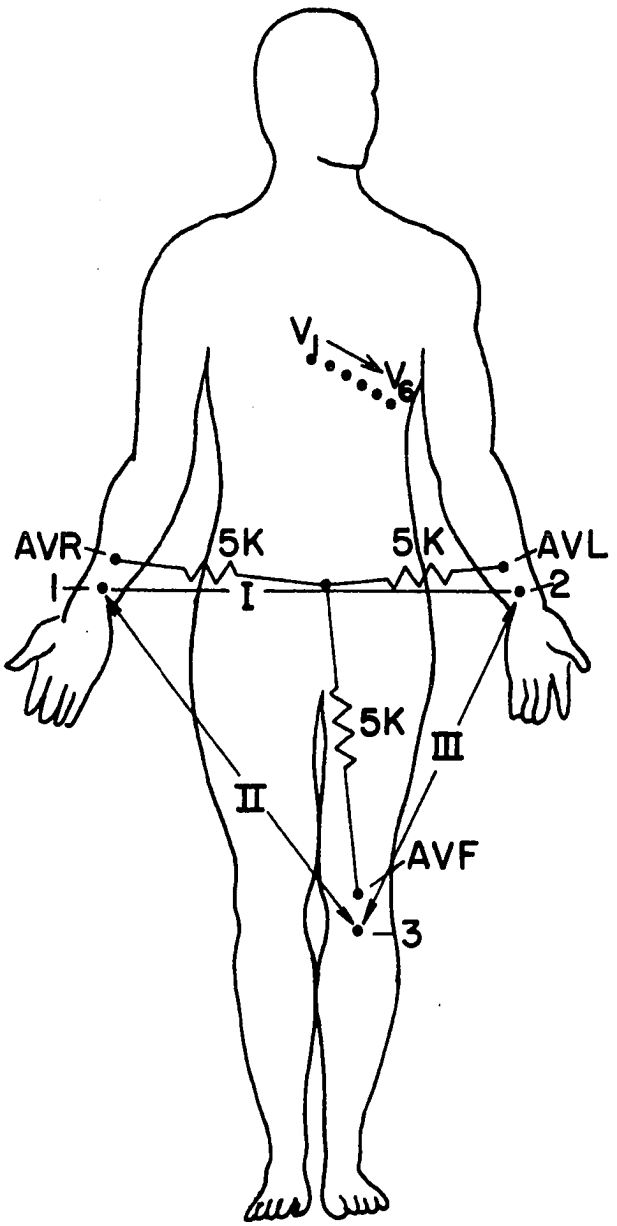

Figure 2. Electrocardiograph contact locations

V2, V3, V4, V5, and V6 are placed on the chest in the positions shown in Fig. 2. These are unipolar leads, which utilize a reference point, placed at the neutral of the wye formed by the three resistors placed between the neutral point and the electrodes placed on the left wrist, left leg, and right wrist. Each branch of the wye consists of a 5 K resistor between the electrode and the neutral point. The galvanometer then measures the potential difference between this neutral point and the various points on the chest cavity. The unipolar leads AVF, AVL, and AVR employ the same reference point as the precordial leads, but the exploring electrodes are placed on the left leg, left wrist, and the right wrist respectively. The proper combination of waveforms from the various data acquisition points permits the cardiologist to precisely determine not only the magnitude, but also the direction of the electric vector in the heart, as the heart cycle takes place. Specific determination of the direction and magnitude of the electric vector will not be made here, as the clinical uses of vectorcardiography are limited at present.

Waveform generation mechanisms

The waveform discussed herein will be that of standard lead I, as shown in Fig. 1. The waveforms generated in the other leads are caused by identical mechanisms, but the shape may appear completely different as a result of the location of the sensor. The clinical electrocardiogram is not a smooth single waveform, as can be seen by inspection of Fig. 1. Rather, it is a series of repetitive pulses associated together because each pulse is the manifestation of a specific action in a single organ. The pulses to be considered are the P-wave, the QRS complex, and the

T-wave. The model of the heart to be considered is the simplest model, the dipole, consisting of a single electric net vector as described by Burch and Winsor (2). The action of this model of the heart is explained in the subsequent paragraphs of this section. Although neither complete nor accurate, this model is sufficient to explain the waveform.

The various voltage pulses are caused by a change in the charge distribution of the heart itself. When the muscle is relaxed, the cellular structure is in the "polarized" state. This state is characterized by positive and negative charges existing in doublets across the individual cell walls of the muscle, as shown in Fig. 3a, and in greater detail in Fig. 3d.

When activated by a stimulus, according to Burch and Winsor, the resistance of the walls is lowered, and the charges migrate through the walls of a finite thickness, giving rise to a cardiac current. The result of this is the "depolarized" state, shown in Fig. 3c, which immediately precedes contraction of the muscle. Fig. 3d shows the progress of the depolarization wave during electrical action in the heart. Similarly, stimuli cause, after contraction of the muscle, a repolarization wave, resulting in return of the cardiac musculature to the polarized state.

The voltages which appear on the electrocardiogram are those caused by these current sources within the heart. According to Geselowitz (7), a multipole model of the heart electric vector may be postulated, and a mathematical model analyzed. A first order approximation to this multipole is the dipole model used in conventional electrocardiography. The voltages pulses result from a region of excitable muscle tissues in the

Figure 3. Charge distribution in the heart

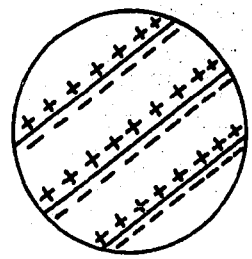

(a)

CHARGE DISTRIBUTION IN "POLARIZED" (RELAXED) STATE

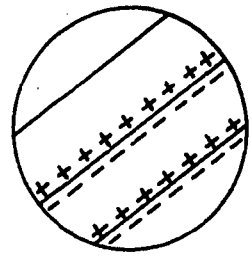

(b)

CHARGE DISTRIBUTION DURING "DEPOLARIZATION" (ACTUATING) STATE

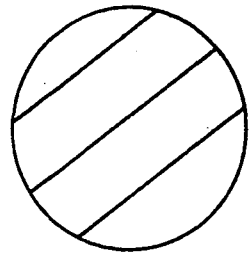

(c)

CHARGE DISTRIBUTION DURING "DEPOLARIZED" (ACTUATED) STATE

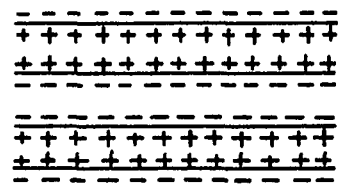

(d)

INDIVIDUAL CELL STRUCTURE DURING "POLARIZED" STATE

heart called the pacemaker, which acts as a free running current pulse generator. Currents are carried through the regions of the heart by an electrical conduction system, the Purkinje network, and cause the surrounding tissue to change state as described above, resulting in the contraction and relaxation of the heart which causes the pumping action.

It will be noted that the polarization and depolarization processes in the heart are the opposite of each other, and each produces a voltage wave. It would be expected, therefore, that if the polarization wave procedded in the same direction as the depolarization wave, that a voltage would be generated in the opposite direction to that obtained from the depolarization. However, generally, the direction of the wave varies in the polarization process from that of the depolarization process, and the polarization process is generally taking place at a slower rate than the depolarization process, hence the magnitude of the generated voltage wave may be smaller than that of the depolarization wave, as well as being in a different direction.

Since the size of the heart, and the extent of the rate of change of charge on the charge configuration affect the total amount of voltage generated during the cardiac cycle, this generated voltage becomes proportional to the heart activity. Thus, a voltage pulse of high amplitude and long duration would indicate a greater amount of heart activity associated with that given pulse as compared with that of a pulse manifesting a smaller amplitude and duration. Hence, one measure of heart activity would be the area of a given voltage pulse. Since the amount of heart activity is directly related to the condition and size of the organ, the knowledge of the area of a given pulse might serve as a possible

basis of diagnostic criteria to be applied to the analysis of the condition of the organ. The parameters presently utilized, as listed in Fig. 1, consist of maximum amplitudes and durations of the pulses, neither of which by itself is directly associated with total heart activity. The maximum amplitude merely specifies the maximum rate of change related to the charge configuration, while duration indicates the total length of time required for either the polarization or depolarization process, regardless of the magnitude of the pulse. To more closely evaluate the significance of the area, an idea must be gained as to the shape of the pulse. This would suggest the usefulness of the correlation function approach. The usefulness of these normal clinical parameters lies in the ease of measurement when manual techniques are utilized. The manual determination of area is lengthy and inefficient. However, use of the normally measured clinical parameters requires subjective analysis of many interrelated empirical relationships, with no fundamental theory which can be applied. This can be seen in the explanation of the present method of computer diagnosis, which appears in a later section.

Specific voltage pulses

As has been stated above, the electrocardiogram waveform is a series of voltage pulses. At the beginning of the cardiac cycle, the organ is in the polarized state, and no voltage pulse is present. The first pulse in the cardiac cycle is the P-wave. It represents the depolarization of the auricular musculature, and spreads from the sinoauricular (SA) node to the atrioventricular (AV) node. Its maximum amplitude does not usually exceed 2.5 mv, with an average value of 0.55 mv, and its duration

does not normally exceed 0.11 second. The depolarization actions, as well as the repolarization actions usually originate in the nodes. These are specific points within the heart musculature which, when excited, initiate the depolarization and repolarization processes. They may be excited by "pacemakers" or another polarization or depolarization process.

Following the P-wave, there is a delay in the transmission of the impulse at the AV node, and this is represented by a segment of zero voltage in the waveform. It does not normally exceed 0.10 second for adults. It, plus the P-wave duration, usually is designated the PQ (PR) segment. Also included in this segment is the auricular repolarization wave, but it takes place relatively slowly, and the size of the musculature is small, so the segment does not usually noticeably exhibit this action, and is usually considered to be of zero amplitude.

Following the PQ segment, the QRS complex is the depolarization complex of the ventricular musculature. It consists, usually, of an initial downward deflection, the Q-wave, an initial upward deflection, the R-wave, the initial downward deflection after the R-wave, the S-wave, and a second upward deflection (not utilized in this study), the R'-wave. The duration of the QRS interval does not normally exceed 0.10 second. The amplitudes vary with the lead, but averages follow for lead I: Q = 0.36mv, R = 5.5mv, and S = 1.5mv. The complex nature of this depolarization wave arises from the non-homogeneity of the ventricular musculature, and the direction of propagation of the accession wave.

Following the QRS complex is a segment, usually zero, but sometimes

rising with time, called the ST segment. It represents the time that the ventricular musculature is in the depolarized state.

Following the ST interval is the T-wave, which represents the ventricular repolarization. Its average height is 2.0mv, with a maximum of 5.5mv.

Use of the Electrocardiographic Waveform

General

The electrocardiographic waveform is used by the cardiologists as a very significant piece of data in the diagnosis of heart disease. Naturally, many additional data are required and utilized in arriving at a final diagnosis, but it is indicated in the literature that the electrocardiogram is a powerful supplementary tool used to classify the patient into one of four broad categories. These categories are:

1. Normal.
2. Slightly suggestive of myocardial disease.
3. Strongly suggestive of myocardial disease.
4. Definite evidence of myocardial disease.

According to Burch and Winsor (2), in most cases, it has definitely been established that myocardial damage always results in a deviation in the depolarization and the repolarization processes, hence results in an altered waveform on the electrocardiogram.

Present method of computer diagnosis

At Iowa Methodist Hospital a method has been devised, and is in present use, employing a digital computer for diagnosis of heart disease. This method has been in use for both children and adults for several

months. An actual evaluation of the method has not been made, since many changes in the computer program have been made from time to time. However, the computer diagnosis has agreed with the findings of a panel of cardiologists in most cases. Actual overall figures are not available, but in one group of children of about 20, agreement was reached between the computer and the panel in all but 4 cases, and two of these were explainable by careful analysis of the input data to the computer. This method utilizes the normal clinical parameters (amplitudes and durations) for the full set of leads shown in Fig. 1 and Fig. 2, although, as was previously stated, only 49 of the readings are actually utilized in the diagnosis.

The clinical parameters are measured and recorded on special cards by technicians. An example of this card is shown on Fig. 4. The data contained on these cards is then punched onto data cards and fed into the computer, where the diagnosis is effected. The output is typed on a card identical to that shown in Fig. 5. The items checked in the diagnosis are clearly shown in Fig. 5, and will not be restated here.

The method of diagnosis is generally to measure the parameters, compute a quantitative value which represents the total effect of all the parameters on a given myocardial condition, and classify these quantitative results into categories which correspond to the nearest description of the condition. For instance, heart rate is computed from the RRI interval, and classified into the appropriate frequency range, and a written tag furnished on the diagnosis form. This is descriptive of the heart rate in medical terminology. This is a very simple example of a

Figure 4. Data card for recording electrocardiograms

NAME_____ HOSP.#_____ RESEARCH #_____ AECG

Date ECG taken_____ Age_____ Attending Physician_____

2 R-R_____ _____ _____ P-R Int._____ _____ _____

QRS_____ _____ _____ Q-T_____ _____ _____ II P Duration_____

	P	Q	R	S	ST SEG.	T	Intri.Defl.	STD.
I								
II								
III								
AVR								
AVL								
AVF								
V1								
V2								
V4								
V6								

Figure 5. Electrocardiogram analysis form

NAME OF PATIENT	HOSPITAL NO.	AGE OF PATIENT	DATE OF TRACING	RESEARCH NO.
HEART RATE	BRADYCARDIA	MINIMAL TACHYCARDIA	MODERATE TACHYCARDIA	MARKED TACHYCARDIA
P-R INTERVAL	ABNORMALLY SHORT	BORDERLINE DELAY	MINIMAL DELAY	PROLONGED INTERVAL
AXIS	NORMAL	RIGHT	LEFT	INDETERMINATE
RIGHT VENTRICULAR HYPERTROPHY	NO HYPERTROPHY	POSSIBLE HYPERTROPHY	PROBABLE HYPERTROPHY	RIGHT HYPERTROPHY
LEFT VENTRICULAR HYPERTROPHY	NO HYPERTROPHY	POSSIBLE HYPERTROPHY	PROBABLE HYPERTROPHY	LEFT HYPERTROPHY
Q-T CORRECTED FOR RATE	NORMAL INTERVAL	BORDERLINE INTERVAL	PROLONGED INTERVAL	
T-WAVES	BORDERLINE	ABNORMAL		
MYOCARDIAL INFARCTION POSTERIOR	CANNOT BE EXCLUDED	PROBABLE	TYPICAL PATTERN	OLD
MYOCARDIAL INFARCTION ANTERIOR	CANNOT BE EXCLUDED	PROBABLE	TYPICAL PATTERN	OLD
MISCELLANEOUS FINDINGS	BUNDLE BRANCH BLOCK, RIGHT	BUNDLE BRANCH BLOCK, LEFT	PAROXYSMAL TACHYCARDIA	WOLF-PARKINSON-WHITE

This interpretation has been done by a digital computer. It has not been examined by a cardiologist. It should not be considered a final interpretation. The machine has not been programmed to recognize most arrhythmias, electrolyte disturbances, and certain other abnormalities. The checked interpretations have been calculated after allowing for the age of the patient.

JOHN E. GUSTAFSON, M. D.

ECG ANALYSIS FORM IMH NO. 1

PRINTED BY THE STANDARD REGISTER COMPANY, U.S.A.

classification procedure.

Referring to the adult standards, Appendix A, one can see the criteria used. The mechanization of these criteria is shown in the several flow charts also contained in Appendix A. The standards for children are similar, and the flow charts for the children's program are practically identical in structure. These standards are combined standards from many standard medical references, using, in part, the information contained in Burch and Winsor (2), and Zeigler (20). These were combined by Dr. J. E. Gustafson of Iowa Methodist Hospital to furnish the criteria presently utilized. These have been modified, as required, during the period the computer diagnostic method has been in operation.

The entire method of diagnosis rests on the successive comparison of the computed quantity with a series of threshhold values λ_n, and classification of the result into one of n + 1 categories as defined by the values λ_n. Associated with each of these categories is a descriptive tag, defining the category in medical terminology. For purposes of this dissertation, this is the method which will be employed in the automatic interpretation scheme, since it has been highly successful in practice, and since the quantities which will be found by the automatic method can be used in a similar manner. These values of λ_n are those listed as criteria in Appendix A.

METHODS OF ANALYSIS

Present Approaches to Problem

A review of the literature covering the automatic recording, measurement, and interpretation of the clinical electrocardiogram shows that a large amount of work is being done in this area, with many techniques in use. Although the analytical techniques for accomplishing the measurement and interpretation vary, most of the equipment requirements are similar. There are three distinct techniques reported, each quite different in the method of analysis utilized.

At the National Bureau of Standards, as reported by Taback (16), a measurement and recording technique is in operation which utilizes a sampler operating at a frequency of 1000 samples per second. The sampled data is converted to digital form by an analogue-to-digital converter, and stored on magnetic tape. The filtering of the data is accomplished by means of a moving average computed by a digital computer, forty samples wide. The average of forty samples is taken as the value of the signal at the sample point being considered. This produces an attenuation versus frequency characteristic of $\left|\frac{\sin 0.040\omega}{0.040\omega}\right|$, which causes the curve to fall to zero at 25 cycles per second, thus eliminating the effects of high frequency noise. The onset and offset of the various pulses are found by the criterion that three successive rises (or drops) in the averages constitute the beginning (or end) of a given pulse. This yields pulse heights and durations, the same data utilized in the manual measurement methods.

The U. S. Public Health Service is undertaking a second effort, and

this effort is described by Caceres (4) and Steinberg (15). The general method is similar to that previously described, except that the data are first recorded on analogue tape, transported, played back on analogue tape, and then digitized. After the data are in digital form, it is fed directly to a digital computer for analysis. Initially, as reported, a digital filtering scheme was used, wherein at each sample point a parabola was fitted to the sample point, and 8 adjacent samples, 4 ahead and four behind the sample point under consideration. This gave a least squares fit to a high degree of accuracy, but, at a rate of 625 samples per second, required 25 minutes per waveform to accomplish the filtering. Since this was obviously impractical, analogue filtering was used in the later stages of the project. This scheme utilizes the filtered waveform, and its derivative, to accomplish the pattern recognition. The parameters ultimately extracted are those clinical parameters listed in Fig. 1.

A third technique, first proposed by Martinek (11), as defined by Stark (14) utilizes information theory techniques. Martinek proposed use of a large number of sensors to accurately determine the potential distribution of the heart, using the multipole model for the heart. The output of the sensors was optically correlated with the cataloged waveforms of a number of specific heart diseases. The disease having the highest correlation coefficient was selected as the diagnosis. This used correlation of the entire electrocardiogram, and presented the problem of a large catalogue, and an extremely difficult normalization problem. No results were given in either of these papers, as they were proposed methods.

A modification of the correlation technique was proposed by Stark. This consisted of a system similar to the first two described, using correlation techniques. The quantized data was split into several pulses, and cross-correlated against the output of a random number generator. An adaptive selection scheme was employed, wherein the cataloged waveform, starting with the random numbers, was modified to give successively higher correlations functions, until convergence is reached. The use of these random numbers was for two purposes. The first was for the demonstration of a true adaptive system, as one aspect of the problem of artificial intelligence, and the second was for the purpose of reducing the memory space required for catalogues. Each pulse was normalized on both the time base and the amplitude base, so a limited set of numbers was required. It will be noted that this is a refinement over previous techniques in that the cataloging problem is reduced by the correlation of the individual pulses. The diagnostic method proposed was using the Schmitt orthogonal lead system, and was within the area of spatial vectorcardiography. No results were given, as this was also a proposed system, so the effectiveness of this method has not yet been evaluated.

The methods described above are generally in chronological order, and show a gradual evolution from the obvious solution of the problem to the more sophisticated application of modern techniques of information theory. The use of clinical parameters, although duplicating the work of the cardiologist, ignores additional information contained in the signal. In the diagnosis by the experienced cardiologist, any additional bits of data may be considered, consciously or unconsciously, in arriving at a final

diagnosis. However, the present standards do not consider all the information content of the signal, and if successful machine diagnosis is to be made, all the information present should be used.

The progress toward more advanced techniques of data acquisition and interpretation should result in a reduction of the equipment required, as the sampling rate can be lowered as a result of utilization of a priori knowledge of the probable signal structure and content.

Proposed Method for Iowa Methodist Hospital

The general method to be utilized in this project also consists of a sampling and quantizing, and storage process. The proposed system is shown in Fig. 6. This method of data scanning and acquisition is the simplest and least expensive which can be used, and it is certainly adequate for measurement and recording of current data. For scanning historical data, which are recorded on charts, an optical scanner would be required. While the use of old data, where diagnosis and prognosis could be compared with later case histories of the patients is highly desirable for improvement of the diagnostic criteria, it is not considered that this is of paramount importance in this project. Rather, the establishment of a method for using present diagnostic criteria in an efficient manner is the initial goal.

The electrocardiograph will, for automatic recording purposes, necessarily provide a means for the entering, by the operator, of a digital code into the storage medium. These data entered in code would consist of patient name, patient number, and other pertinent facts necessary for

POSSIBLE IMH ECG RECORDING CONFIGURATION

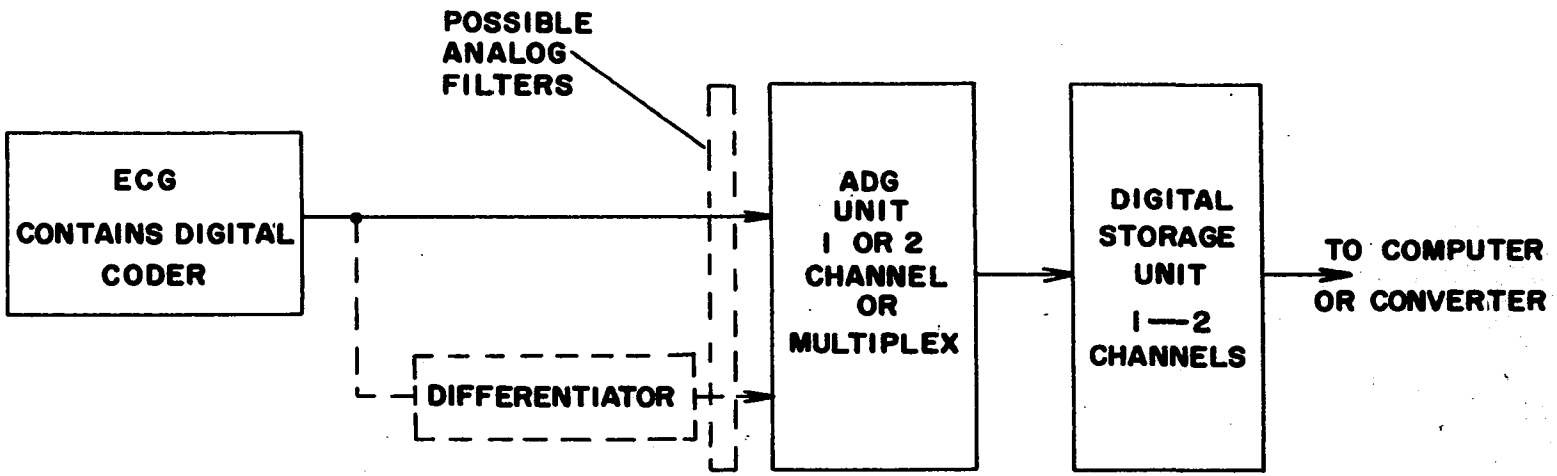

Figure 6. Proposed ECG recording unit

proper identification of the electrocardiogram. The analog waveform may require some filtering in the actual model, and perhaps the waveform must be differentiated in order to furnish a base point for measurement and sample counting. The output of a differentiating circuit will be operated on by logical circuitry, designed to pick the highest negative derivative magnitude. Investigations by the U. S. Public Health Service has established that this negative maximum of the derivative always occurs on the negative slope of the R wave, on all waveforms, whether normal or abnormal. Therefore, it can be used as a time base point on the electrocardiogram waveform.

The analog signal will then be quantized by an analog-to-digital converter. The usual resolution for the converter is an accuracy in quantization to one part in 1024. This has proved successful in the projects previously described, and will be initially utilized in this system. The sampling rate for this project will be 250 samples per second. An analysis of the most critical pulse, the Q wave, is made in Appendix B, and this frequency was selected. Since an analogue-to-digital converter is not available on this project, data from the U. S. Public Health Service project will be utilized. The basic sampling rate on this data will be 500 samples per second, and, by sorting, sampling rates of 250 and 125 samples per second will be used, and the results compared, although the rate of 500 samples per second is apparently higher than required.

The output of the quantizer will be stored in digital form. The storage in digital form will provide a means for proper synchronization of the data, and will avoid one basic difficulty encountered by the Public

Health Service project. That project was formed to accept data from numerous sources, and as a result, the data were recorded in analog form on tape, and played back on another analog tape transport into the converter. This introduced an extremely difficult problem of flutter and wow (low frequency noise) into the signal at frequencies close to the most critical frequencies of the pulses. This very much increased the difficulty of pattern recognition. It is considered that direct digital recording will eliminate much of this low frequency noise problem.

The system outlined above will serve as a basis for acquisition of the data to be used in the analysis to follow. Further discussion of the hardware to be used does not appear to be warranted, since the crucial problem is the actual method of analyzing a signal which must be extracted from a combination of signal and noise.

The problem of implementing the system previously described is relatively routine, in that no special purpose equipment is required, and careful design of the subsystems will result in a suitable data acquisition system. The central problem lies in the utilization of the digitized data properly. The data must be used to reconstruct the basic waveform from the sampled signal with the superimposed noise, and to interpret the waveform into information meaningful to the cardiologist. This latter requirement may require the normal clinical parameters, or the interpretation of the data into actual diagnoses, or a combination of both. The problem thus may be split into three interdependent areas, that of extraction of the signal from the sampled data containing both signal and noise, that of interpretation of the electrocardiogram, and that of

performing an actual diagnosis.

Although these three problems cannot be strictly separated, they will be dealt with separately at first. Thus, the discussion will concern signal extraction, pattern recognition, and diagnosis in separate sections, then expand the ideas developed therein into an overall method of analyzing the data.

EXTRACTION OF SIGNAL BY CORRELATION

Development of General Method

Previous work

The methods previously discussed utilized several techniques for extraction of the signal from a combination of signal plus noise. The first method, by the National Bureau of Standards, employed a moving average to characterize the signal. This amounts to a linear approximation to the signal, but requires a high sampling frequency to minimize the effects of wild sample points. The second method, by the Public Health Service, employed analogue filtering to remove the objectional frequency components of the noise from the combination of signal plus noise. One disadvantage of both of these methods is that frequency components of the signal in the frequency bands stopped by the filtering are also removed. The parabolic fitting method, also employed by the Public Health Service, uses a mean square error criterion, which is superior to the other two methods, but requires excessive computation.

Correlation techniques

In order to optimize a given system, some error criterion must be selected. In the cases discussed above, two criteria were mentioned, the linear minimization of error, and the mean square minimization of error. The mean square error is realistic, and describes a valid performance criterion for a large number of systems and it is mathematically convenient to use.

The use of correlation techniques, which was undertaken by Stark (14)

and Martinek (11) furnishes a mean square error criterion and does so without excessive computation. The use of correlation techniques is further discussed by Bendat (1), Davenport (5), Goldman (8), Horwitz (10), Truxal (17), and Turin (18). The use of such techniques is attractive because of the possibility of utilizing a combination of digital and analogue filtering techniques to accomplish the extraction of signal from the combination of signal plus noise. Therefore the correlation techniques will be investigated in detail.

Correlation techniques can be shown to furnish an approximation to the signal in that they furnish a mean square error minimization between the signal, and the combination of the signal plus noise. Several approaches may be taken to demonstrate this property, and a probabilistic approach is shown as supplementary material in Appendix E. However, a different approach to the problem may be taken, which demonstrates that the signal to noise power ratio is maximized by the correlation technique. The approach taken utilizes matched filters in the same manner as Turin (18).

If $s(t)$ is any physical waveform, consider, by definition, that a filter which is "matched" to this waveform is one having an impulse response $h(\tau) = ks(\Delta - \tau)$, where k and Δ are arbitrary constants. The transfer function of this matched filter, which is the Fourier transform of the impulse response is,

$$H(j\omega) = \int_{-\infty}^{\infty} h(\tau)e^{-j\omega\tau}\, d\tau$$

$$= k\int_{-\infty}^{\infty} s(\Delta - \tau)e^{j\omega\tau}\, d\tau$$

$$= k\left[\int_{-\infty}^{\infty} s(\tau')e^{j\omega\tau'}\, d\tau\right]e^{-j\omega\Delta}$$

under the substitution $\tau' = \Delta - \tau$. Now, the spectrum of $s(t)$ is

$$S(j\omega) = \int_{-\infty}^{\infty} s(t)e^{-j\omega t}\, dt$$

Comparing the last two equations, we have

$$H(j\omega) = k\, S(-j\omega)e^{-j\omega\Delta} = k\, S^*(j\omega)e^{-j\omega\Delta}$$

Thus, the matched filter under discussion has a transfer function which is the complex conjugate of the spectrum of the signal to which it is matched.

Let us examine such devices to determine whether or not they provide an optimization of the signal-to-noise ratio. Consider that a waveform $x(t)$ consists either entirely of white noise, $n(t)$, or of white noise $n(t)$ plus a signal of known form. It is desired to make the decision as to which of these cases is true by passing $x(t)$ through a linear filter. Thus, the output of the filter should consist of a component $y_n(t)$ plus a component $y_s(t)$, due to the noise and signal components respectively of

$x(t)$. The output should be considerably greater if $s(t)$ is present. This can be accomplished by specifying that the filter make the instantaneous power in the output $y_s(\Delta)$, (where Δ is at a specific time t), a maximum with respect to the average power in $n(t)$ at time $t = \Delta$.

Assuming that $n(t)$ is stationary, the average noise power at any instant is the integrated power under the noise power density spectrum at the filter output. If $G(j\omega)$ is the transfer function of the filter, then the output noise power density is

$$\frac{N_0}{2} \left| G(j\omega) \right|^2$$

where $N_0/2$ is the amplitude of the noise power spectral density. The output noise power is therefore

$$\frac{N_0}{4\pi} \int_{-\infty}^{\infty} \left| G(j\omega) \right|^2 \, d\omega$$

Further, if $S(j\omega)$ is the input signal spectrum, then $S(j\omega)G(j\omega)$ is the output signal spectrum, and $y_s(\Delta)$ is the inverse Fourier transform of this, evaluated at $t = \Delta$, that is

$$y_s(\Delta) = \frac{1}{2\pi} \int_{-\infty}^{\infty} S(j\omega)G(j\omega)e^{j\omega\Delta} \, d\omega$$

The ratio of the squared second equation to the first is the power ratio which is to be maximized

$$\rho = \frac{\pi \left[\int_{-\infty}^{\infty} S(j\omega) G(j\omega) e^{j\omega\Delta} \, d\omega \right]^2}{N_0 \int_{-\infty}^{\infty} |G(j\omega)|^2 \, d\omega}$$

Since the integral in the numerator is real $[ys(\Delta)]^2$, and identifying $G(j\omega)$ with $f(x)$ and $S(j\omega)$ with $g(x)$ in the Schwarz inequality

$$\left| \int f(x) g(x) dx \right|^2 \leq \int |f(x)|^2 dx \int |g(x)|^2 dx$$

we obtain

$$\rho \leq \frac{1}{\pi N_0} \int_{-\infty}^{\infty} |S(j\omega)|^2 \, d\omega$$

Since $S(j\omega)^2$ is the energy density spectrum of $s(t)$, the integral above is the total signal energy E in $s(t)$. Then

$$\rho \leq \frac{2E}{N_0}$$

In the case that $f(x) = kg^*(x)$, i.e., when

$$G(j\omega) = kS^*(j\omega) e^{-j\omega\Delta}$$

the Schwarz inequality becomes equal on both sides, hence the equations which follow the Schwarz inequality all become equalities. This results in a maximum signal energy for a given noise energy. In case the noise is not white, the following holds

$$G(j\omega) = \frac{k\, S^*(j\omega) e^{-j\omega\Delta}}{\left|N(j\omega)\right|^2}$$

This follows because if the input, $x(t)$ is passed through a filter with a transfer function $N(j\omega)$, the noise component at its output will be white. However, the signal component will be distorted, now having the spectrum $S(j\omega)/N(j\omega)$. The cascade connection of the noise-whitening filter and this matched filter is indeed the solution stated above. Thus we have shown that the matched filter approach does provide a maximum value of the signal-to-noise power ratio.

That the matched filter technique provides the same information as the correlation functions can be seen from the following. The response to an input $s(t)$ of a linear filter with an impulse response $h(\tau)$ is, by convolution

$$\int_{-\infty}^{\infty} h(\tau)s(t - \tau)\, d\tau$$

If $h(\tau) = s(-\tau)$, with no time delay, then

$$y_s(\tau) = \int_{-\infty}^{\infty} s(-\tau)\, s(t - \tau)\, d\tau$$

Making the substitution $(t - \tau) = \tau'$, we have

$$y_s(t) = \int_{-\infty}^{\infty} s(\tau')\, s(t + \tau')\, d\tau'$$

Considering the finite form over a period T of a single pulse, and shifting forward by τ' gives

$$y_s(t) = \frac{1}{2T} \int_{-T}^{T} s(\tau') \, s(t + \tau') \, d\tau'$$

It will be noted that this form is exactly the same as the form of the finite autocorrelation function developed independently in Appendix E. If the filter was not exactly matched to s(t), but rather to $s_1(t)$, the average output of the matched filter becomes the continuous crosscorrelation function as defined in the following equation.

$$y(t) = \frac{1}{2T} \int_{-T}^{T} s_1(\tau') \, s_2(t + \tau') \, d\tau'$$

The development in the preceding paragraphs, although carried out in order to show that correlation techniques do indeed provide for a maximization of signal power with respect to noise power, also hold promise for future development on this project, since it may be possible to build analog matching filters in order to further minimize the computation required by the digital computer. However, more information regarding the required impulse response function must be acquired before implementation of such an analog system can be attempted.

In the preceding paragraphs, and in Appendix G, we have shown that the correlation functions do indeed represent a minimization of a mean square error in the case of linear dependence between variables. We shall assume this linear dependence in the problem under investigation, and utilize the crosscorrelation function as a measure of the dependence of the two functions.

We can now summarize some of the properties of correlation functions which will be useful later. Properties of the autocorrelation function are:

1. The autocorrelation function is an even function ($\theta(\tau) = \phi(-\tau)$).
2. The autocorrelation function has a maximum at $\tau = 0$.
3. $\phi(0)$ is the average power of the time function.
4. If a signal contains periodic components (or a dc value), the autocorrelation function contains components of the same periods (or a dc component).
5. The autocorrelation function is equal to the sum of the autocorrelation functions of the individual frequency components.
6. A given autocorrelation function can correspond to any number of time functions, however each time function has only a single autocorrelation function.
7. The autocorrelation function of the derivative of f(t) is the second derivative of the autocorrelation function of f(t).

Some properties of the crosscorrelation function are:

1. The crosscorrelation function is not an even function.
2. $\phi_{12}(\tau) = \phi_{21}(-\tau)$.
3. $\phi_{12}(\tau)$ does not necessarily posses a maximum at $\tau = 0$.

These properties are summarized in Truxal (17).

Since we are dealing with a system in which the input waveforms are

sampled, and then quantized into numerical form, the data to be analyzed is in a discrete form. Therefore, in accordance with the development of Appendix G, the discrete autocorrelation function becomes

$$\phi_{11}(j) = \lim_{N \to \infty} \frac{1}{2N + 1} \sum_{k = -N}^{+N} x_K \, x_{K + j}$$

and the crosscorrelation function between two waveforms, 1 and 2 becomes

$$\phi_{12}(j) = \lim_{N \to \infty} \frac{1}{2N + 1} \sum_{k + -N}^{+N} x_K \, y_{K + j}$$

Application of correlation techniques to the electrocardiogram

Having shown that the correlation techniques discussed above will lead to a minimization of the error in the mean square sense, let us investigate the applicability of such techniques to the waveform of the electrocardiogram. We note the following facts about the waveform:

1. It is approximately periodic.
2. It is composed of several pulses.
3. Except for the ST segment, the noiseless value between pulses equals zero.
4. It possesses certain common characteristics, which are always present, regardless of the patient being recorded.
5. Since the heart rate varies, and the width of the individual pulses is not proportional to the heart rate, a search must be made before application of the correlation techniques.

With these characteristics in mind, let us briefly discuss some of

the implications. The periodicity of the wave, and, further, the periodicity of the individual pulses simplifies the correlation functions. If the period of the heart rate, at the time of recording is (R-R) = T, the crosscorrelation function in the continuous case simplifies to

$$\phi_{12}(\tau) = \frac{1}{T} \int_{-T/2}^{T/2} g_1(t) g_2(t + \tau)\, d\tau$$

and in the discrete case to

$$\phi_{12}(j) = \frac{1}{2N + 1} \sum_{k = -N}^{N} x_K y_{K + j}$$

Thus, it is necessary to perform correlation over a period T, as the same information is repeated for the next cardiac cycle. Furthermore, since a specific pulse occurs only once during each cardiac cycle, the entire cycle need not be covered, since the zero value of the ordinate at points outside the interval $2T_s + T_c < T$ contributes nothing to the value of the correlation function. T_c is the width of the cardiac pulse, and T_s the width of the standard pulse being correlated with the cardiac pulse. Therefore, the required correlation is considerably reduced. Between pulses, the value of the waveform voltage is essentially zero, although the noise will usually be present. Since the noise is assumed to be uncorrelated with the signal, the crosscorrelation figure for the zero voltage line will be zero.

In order to apply correlation techniques to this problem, it is necessary to utilize some standard pulses to correlate the waveform pulse with. Although waveforms vary from lead to lead, and from patient to

patient, inspection of a large number of waveforms suggests that the P and T waves are shaped very much like sinusoids, and that the QRS complex is built up of triangles. Therefore, for the initial stages of this investigation, wave shapes of this type will be used as the catalogued pulses against which the cardiac pulses will be correlated. By initially using these pulses which are describable in an analytical manner, we can, through simple subroutines, simplify the standardization of waveforms, and simplify the mathematical procedure involved in the actual correlation. After the basic technique is in workable form, extension to the method can be made, in order to more accurately define the exact shape of the pulses.

Now, in order to render the correlation computation meaningful, several conditions are necessary. First, the most important condition to be satisfied is an area criterion. If the standard P wave, for instance, were correlated against a P wave of larger amplitude and duration, i.e., one indicative of greater heart activity, it would give a greater value of the crosscorrelation function than one of less amplitude, even though the waveshape of the pulse of less amplitude might more closely approximate that of the standard wave. The critical factor is the area, and some technique must be developed to normalize the waves being correlated. As an initial iteration on the problem, waves will be picked which are indicative of the mean values tabulated for various groups of patients, and used as a standard. For instance, reference to Burch (2) and Appendix D shows that, for normal adults, the following values are typical for the P wave.

Lead	Avg. Amplitude	Range (Min. to Max.)	Duration	Range (Min. to Max.)
I	0.55 mv	0-1.1	0.08 sec	0.06 - 0.11
II	1.25 mv	0.3-2.5	0.08 sec	0.06 - 0.11
III	0.80 mv	-1.0-2.0	0.08 sec	0.06 - 0.11

Thus we shall store these values in the computer as a standard for the particular lead under consideration. If lead I were being checked, the standard against which the electrocardiogram would be compared would be, for diagnostic purposes, 1.1 sin x, where x will be some angle determined by the index of the discrete correlation function.

Having fixed certain standards, an indication of the meaning of the correlation function is in order. First, for pulses having the same wave-shape, the crosscorrelation function becomes the autocorrelation function. For a wave of the same area and same time base (identical pulse) this autocorrelation function would be a maximum value which could be attained in correlating two pulses of the same area. Now, the autocorrelation function of a periodic pulse is periodic, reaches a maximum at $\tau = (0)$, and is an even function about this point. This zero point occurs at the point of coincidence of the pulse peaks. Thus, in the case of a function such as sin ωT, the autocorrelation is $\frac{1}{2}$ cos ωT, which demonstrates the statements listed above. Additionally, since the autocorrelation function is even, it is necessary only to perform the correlation until a maximum is reached, and the symmetry yields the descending portion of the correlation function. Now, if the time base is identical, but the second function is k sin ωT, the value of the autocorrelation function becomes $\frac{k^2}{2}$ cos ωT.

Thus, a wave of the correct time base, but different area, if of the same shape, will indicate this area by the value of the autocorrelation function.

Consider, however, the case where the waveshapes are not identical. In order to analyze this case, some assumptions must be made. Two useful assumptions are as follows:

1. The time base of the standard pulse is the same as that of the pulse being measured, or can be directly related to it.
2. The effects of various deviations of the shape of the pulses from the standard pulses can be catalogued and taken into account.

If these assumptions can be justified and/or implemented, any given pulse can be correlated with the standard pulse, and the correlation function interpreted in terms of meaningful values of heart activity, and, in addition, a reconstruction of the pulse furnished with some degree of accuracy.

The program description of the computation of the crosscorrelation functions is shown in Appendix C. It is now necessary to investigate the problem of logic associated with the pattern recognition program, because prior to any application of the correlation techniques, it is necessary to have proper indexing of the sample points, and to know where in the sequence of samples to perform the several correlations required. Also, the waves must be normalized in amplitude and time prior to the correlation in order to easily interpret the results of the correlation computation. Prior to discussion of the logic of recognition, however, a preliminary study of

some experimental results of the correlation computations will be made, in order to justify the assumptions previously made, and to determine whether the correlation techniques themselves will be useful in formulation of the logic of recognition.

Correlation Studies and Data

Correlation results

In order to determine the characteristics of correlation functions for use in this study, a number of these functions were computed in accordance with the program outlined in Appendix C. Some of these correlation functions are plotted in the accompanying figures.

The program was originally checked by computation of the autocorrelation function of a sine wave. Analytical computation of this wave yields an autocorrelation function for the sine wave $E \sin \omega t$. With $E = 1$, the program, utilizing 41 data points and a sine wave pulse yielded a value of 0.4885. This is an error of 2.3% from the correct value of 0.500, and represents a typical P-wave computation at 500 samples per second. The error arises, of course, from the trapezoidal integration used. The manual measuring method used by the cardiologists on this wave is approximately $\pm$ 5%, so the program accuracy is well within the limits required. This curve is shown in Fig. 7.

The next study undertaken was the study of the triangular wave. The study was undertaken to ascertain the effects of a non-isoceles triangle on the correlation function, and to determine the effects of shape variation on a mathematically tractable pulse shape. The pulse selected was

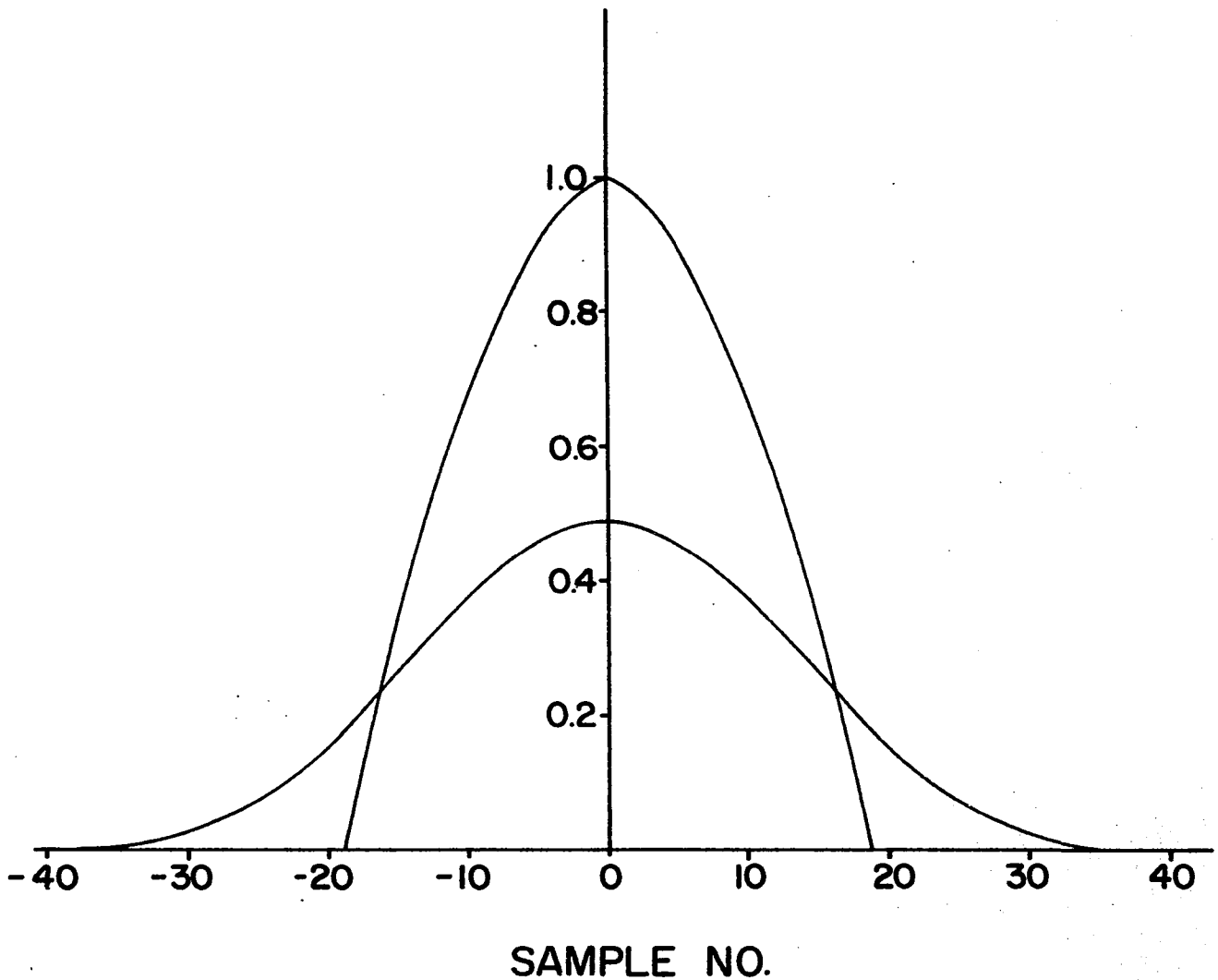

Figure 7. Sine wave autocorrelation

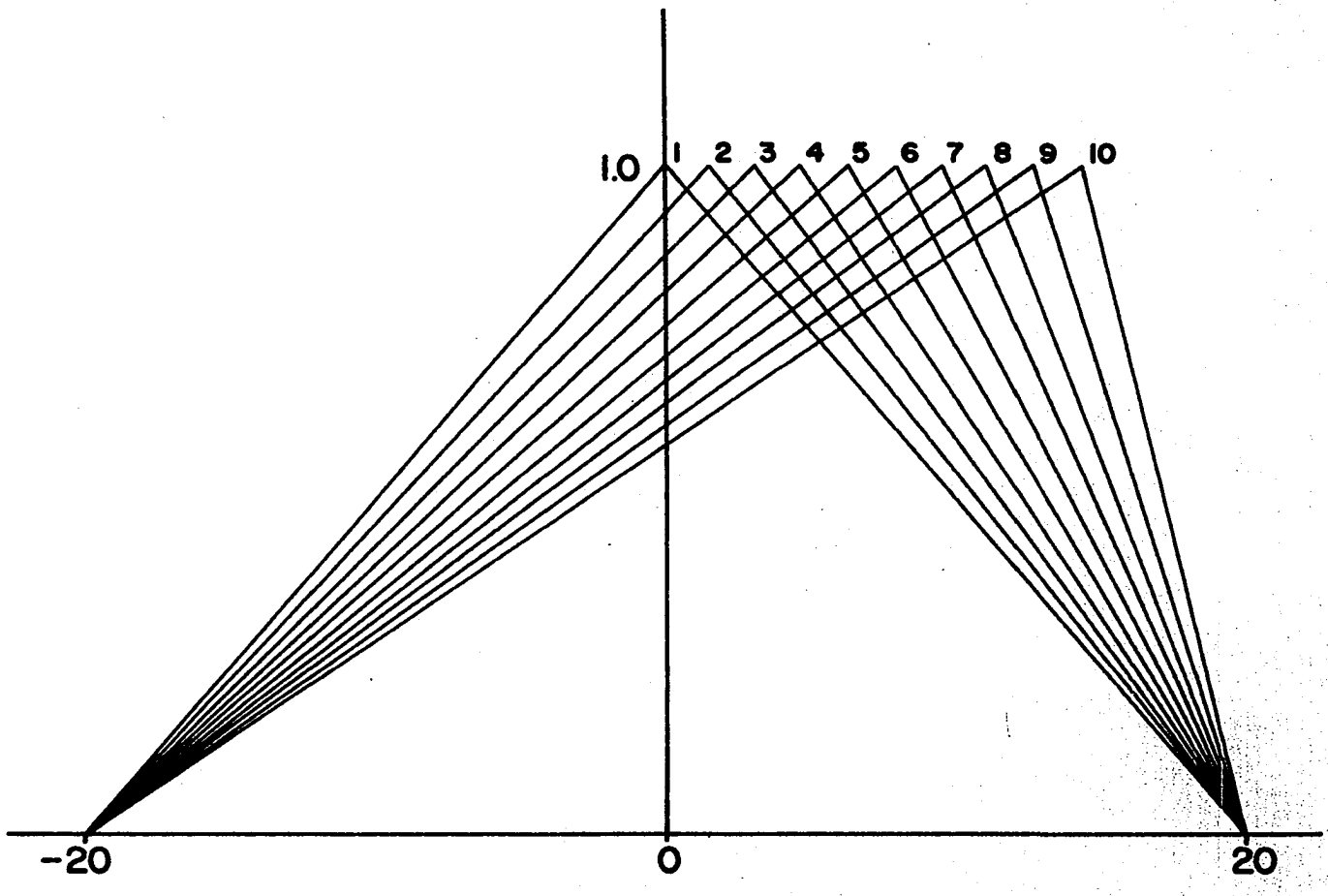

Figure 8. Triangular pulses

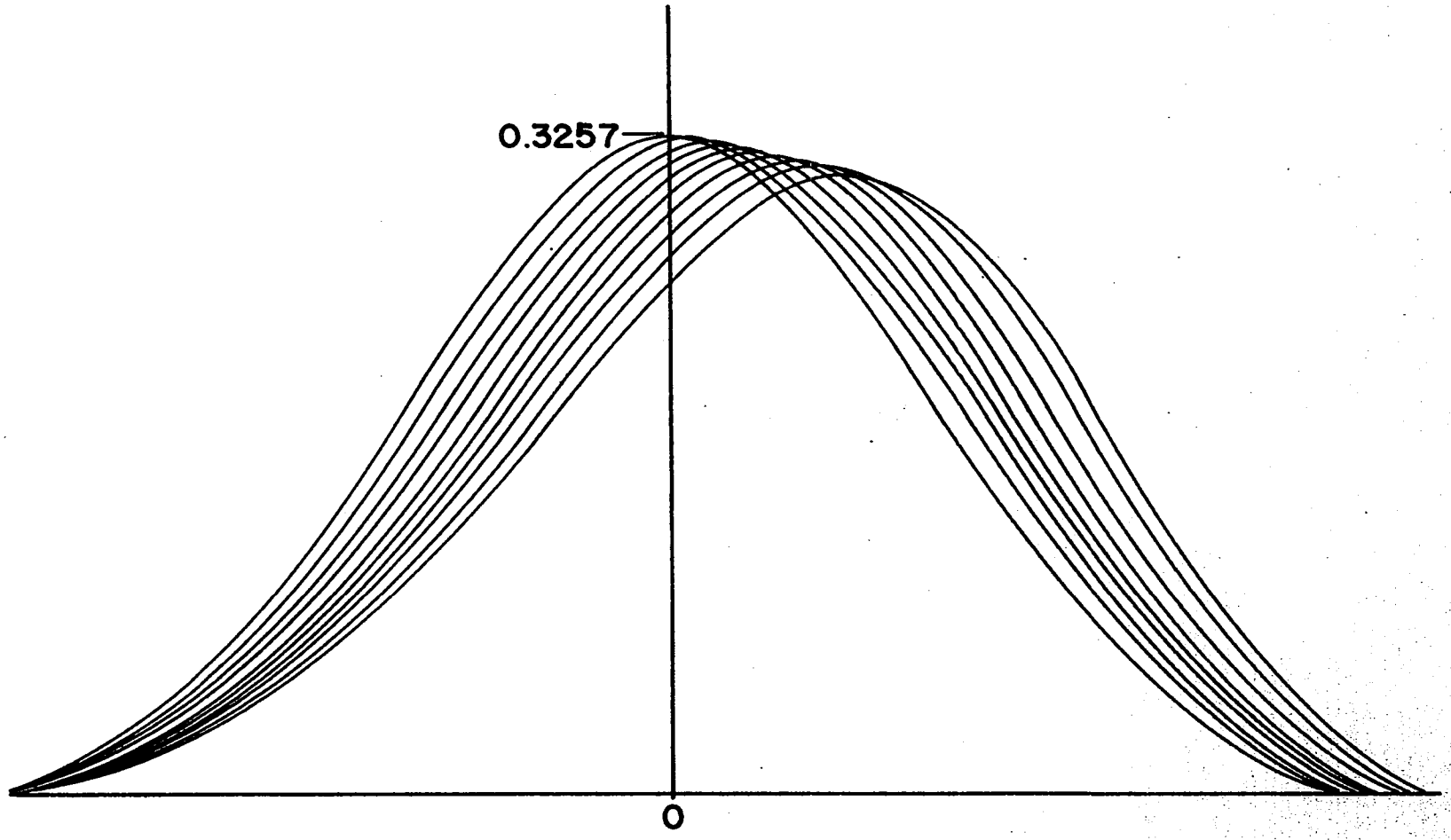

Figure 9. Triangular pulse crosscorrelation

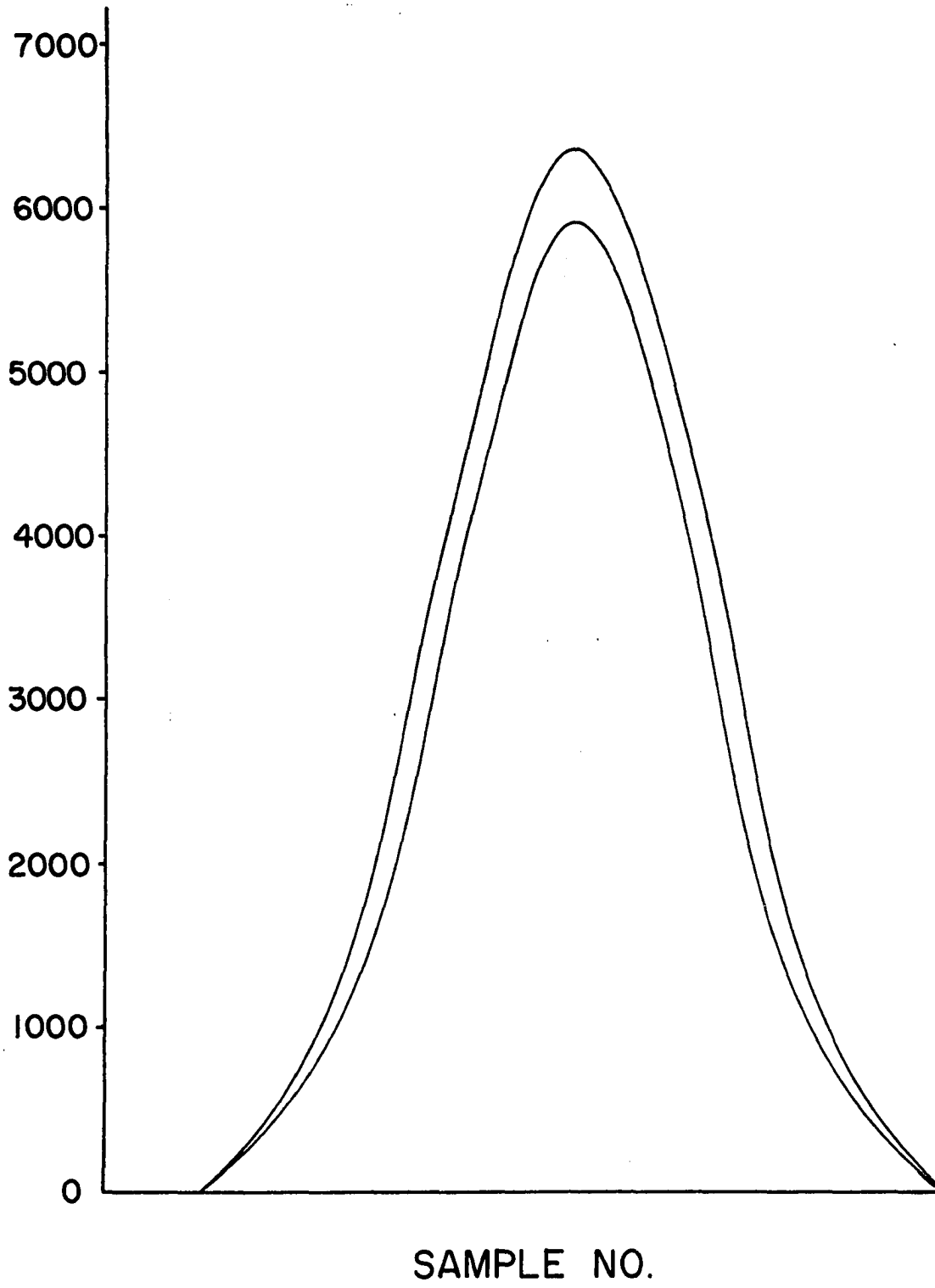

Figure 10. R-wave correlation

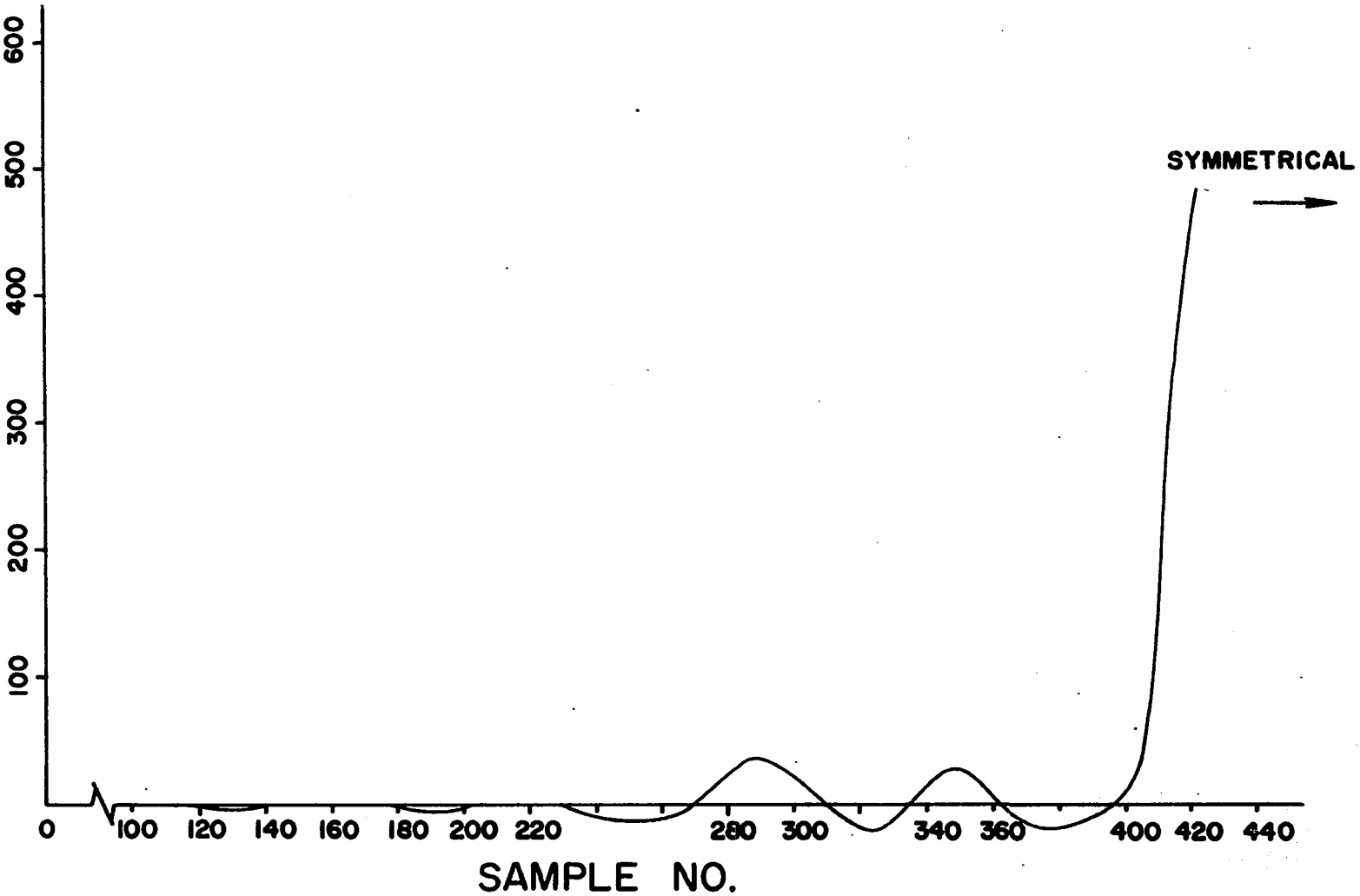

Figure 11. Autocorrelation of entire ECG wave

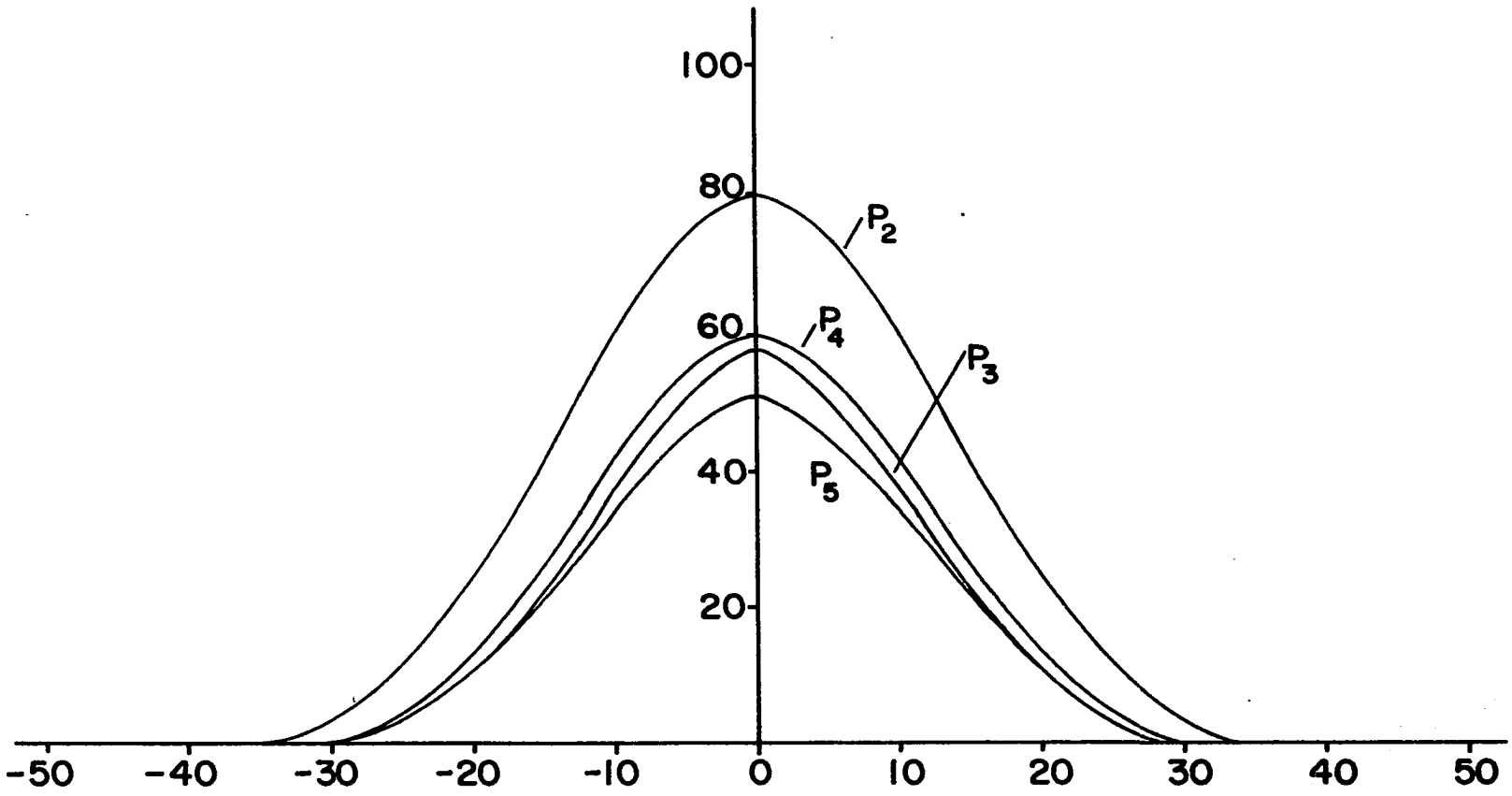

Figure 12. P-wave correlations (auto)

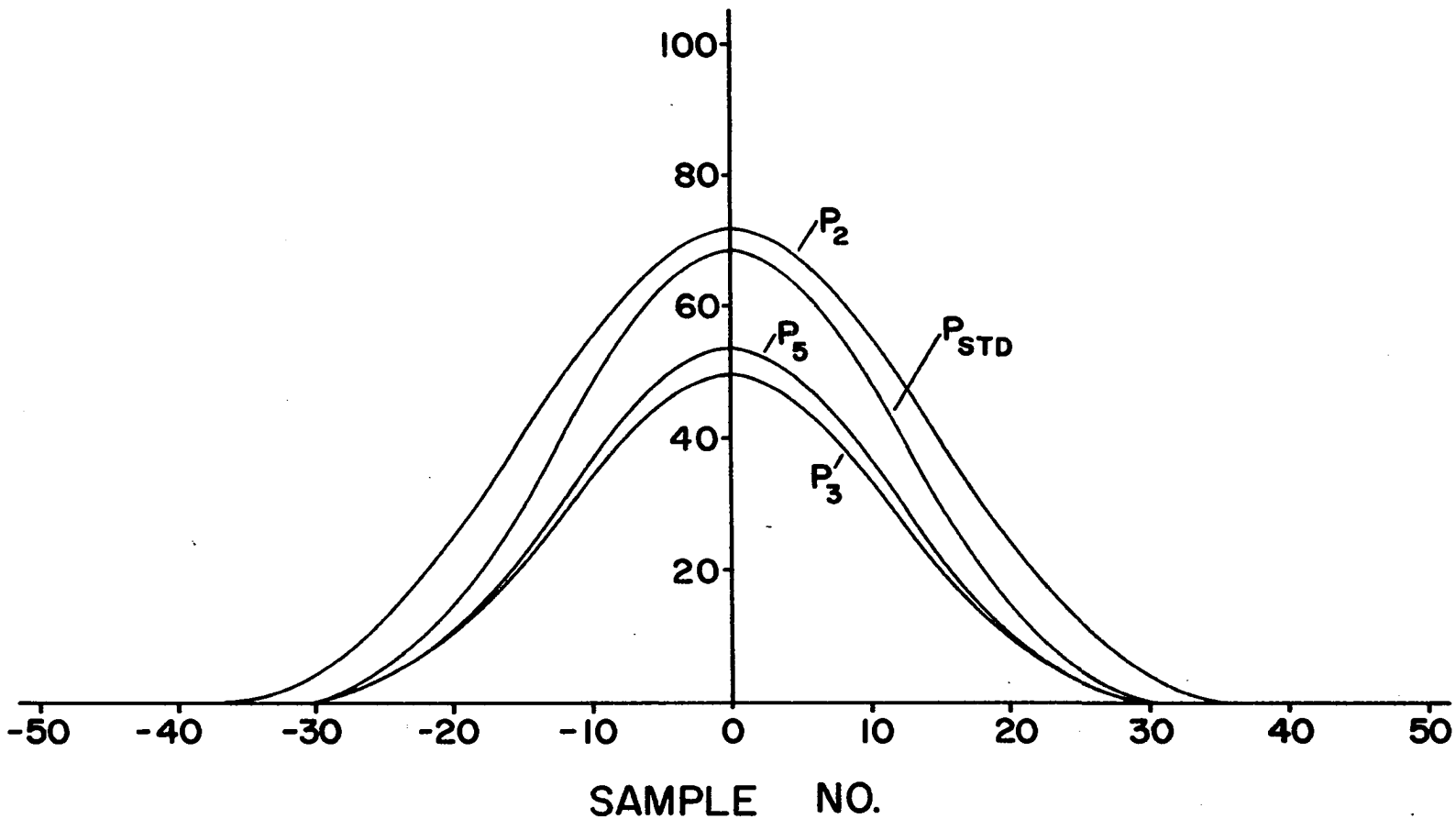

Figure 13. P-wave autocorrelation-smoothed data

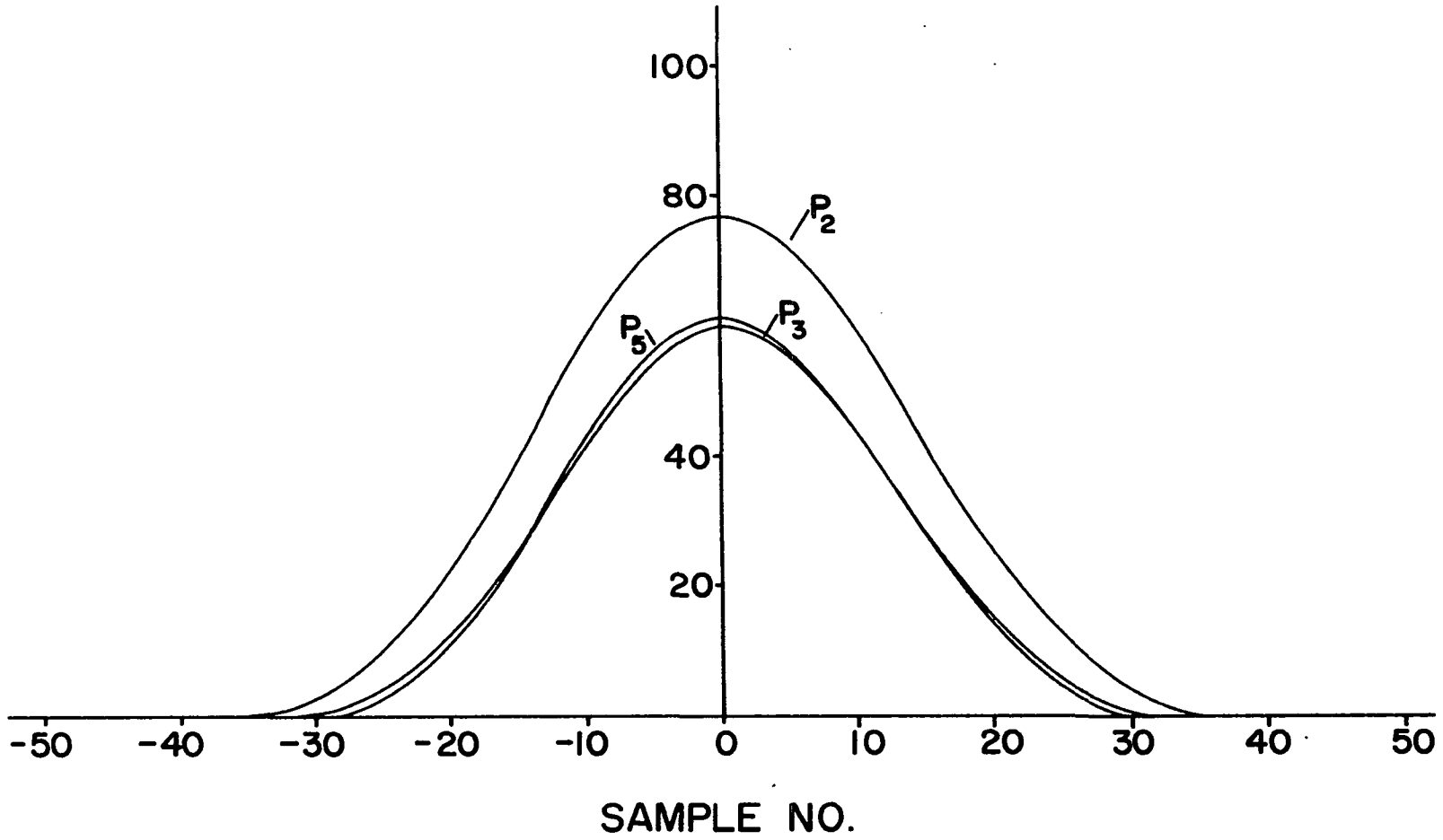

Figure 14. P-wave crosscorrelation-smoothed

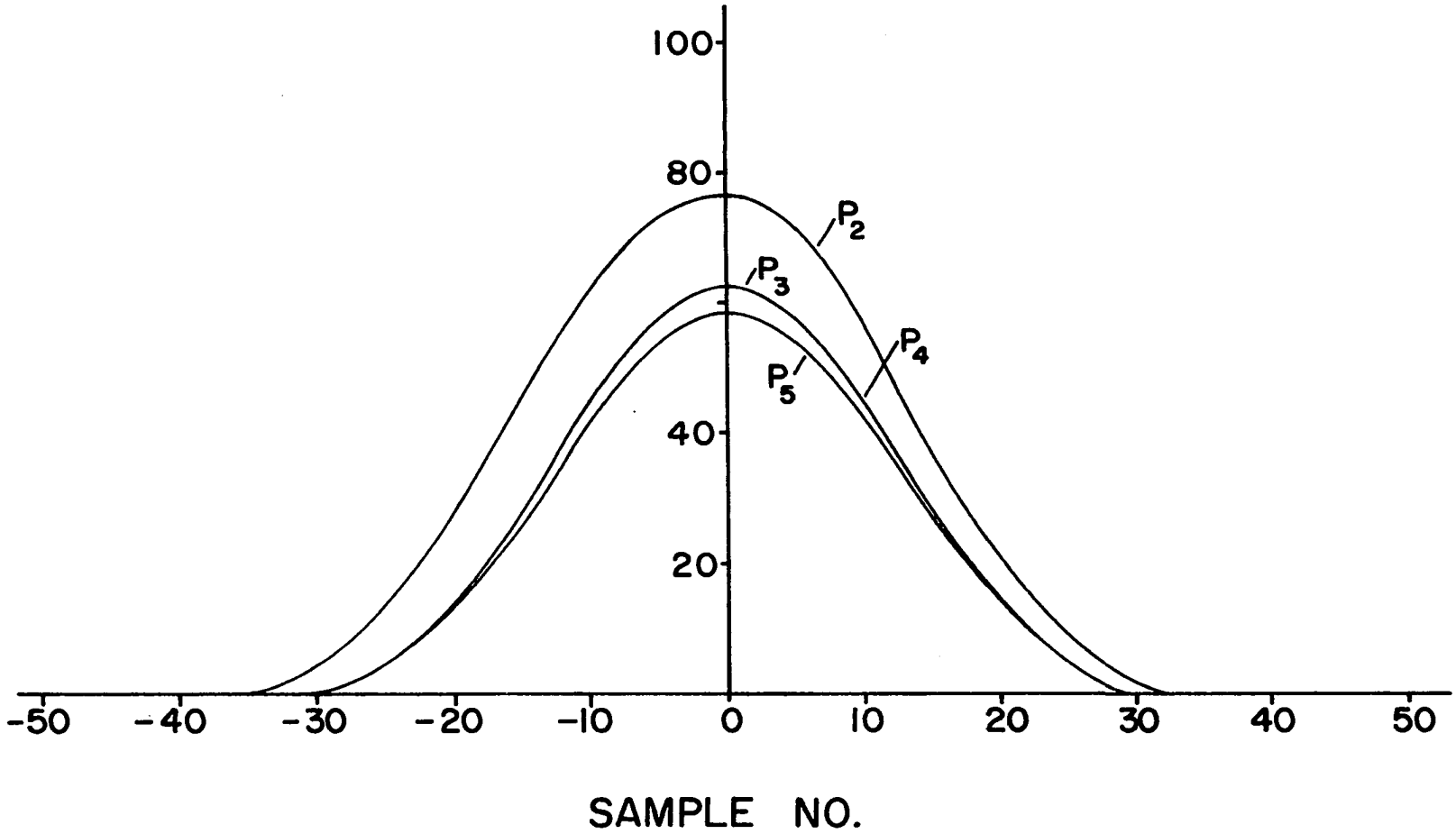

Figure 15. P-wave crosscorrelation

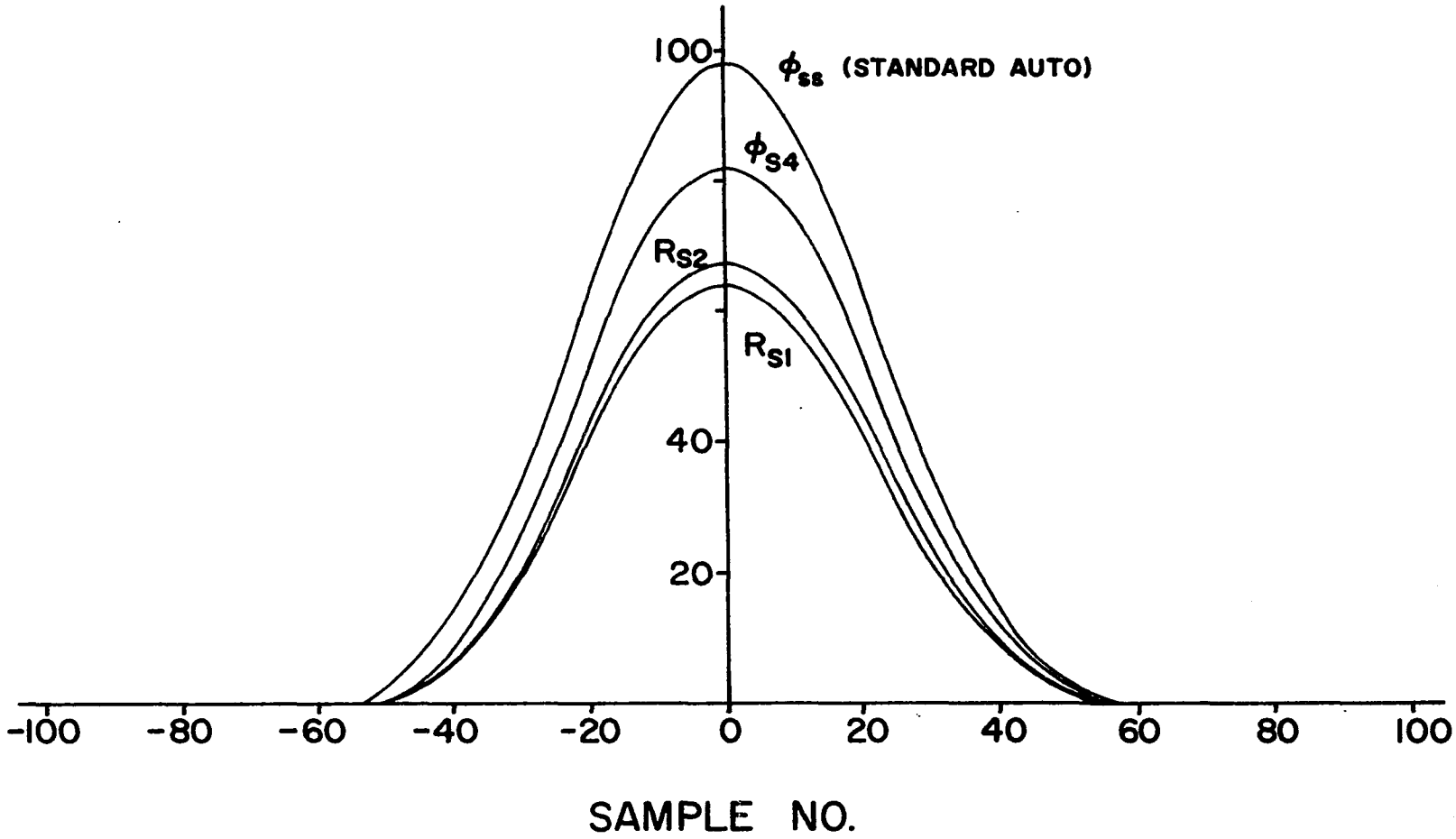

Figure 16. Correlations, T-waves

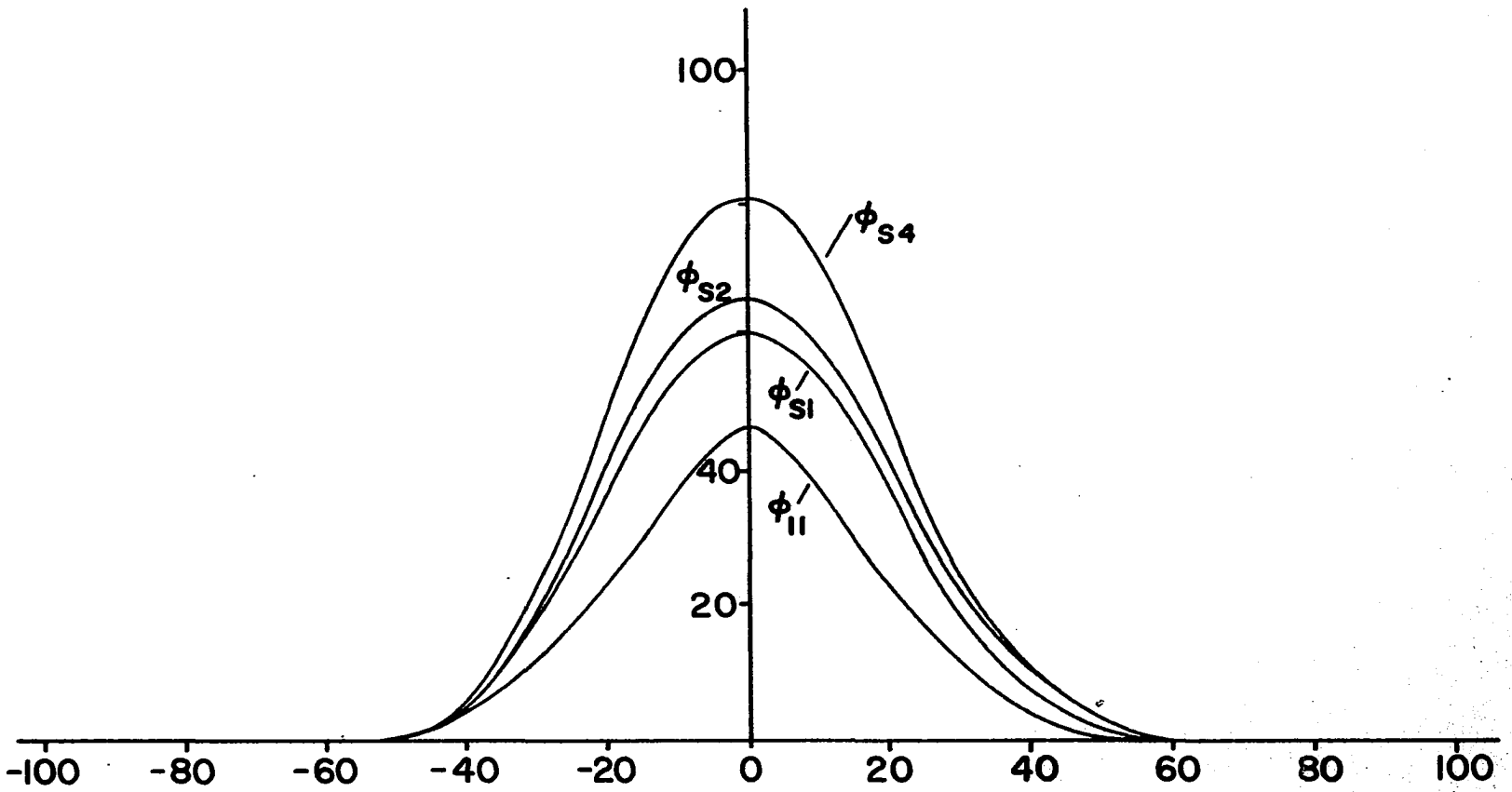

Figure 17. T-wave correlation-smoothed

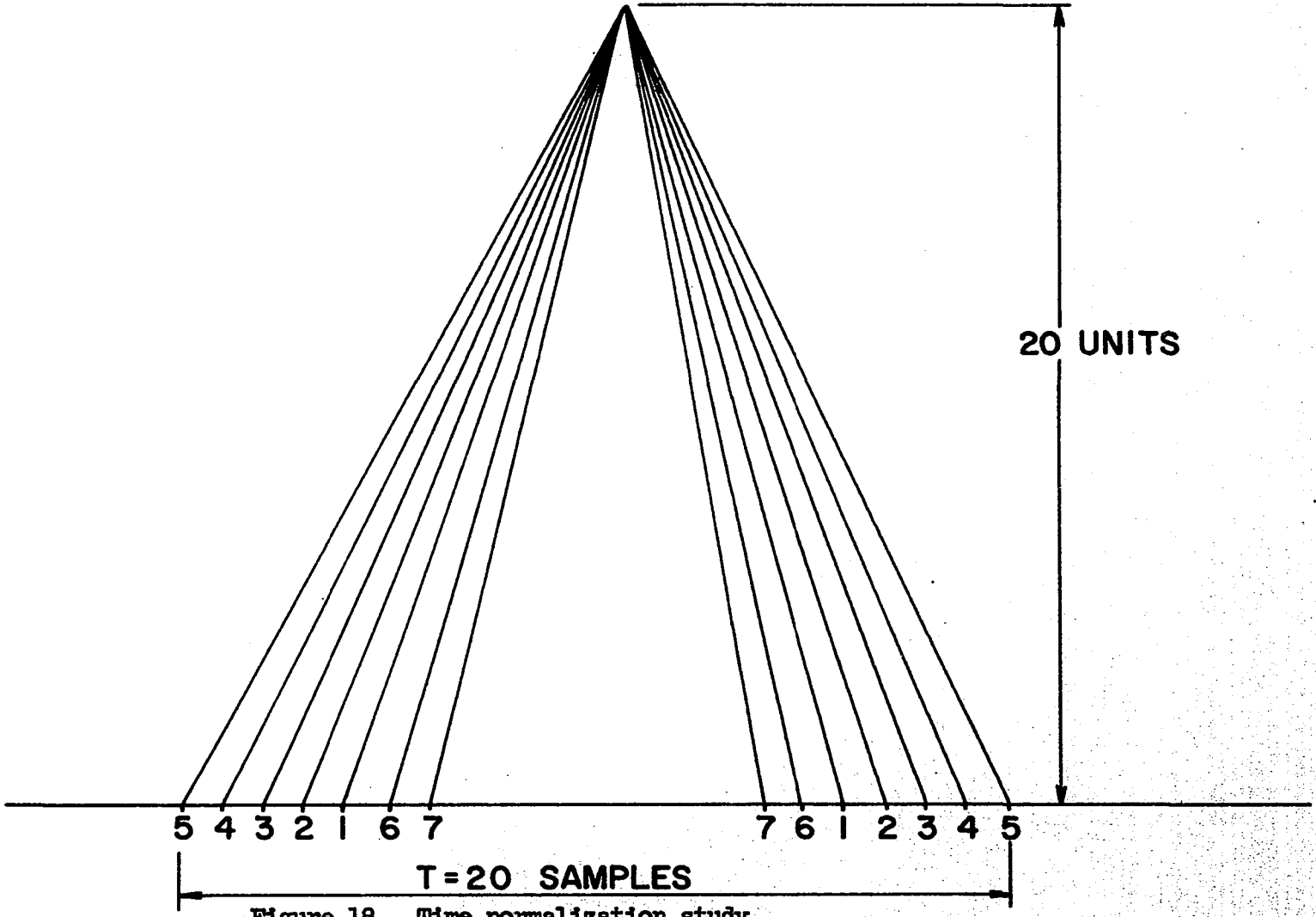

Figure 18. Time normalization study

triangular in nature, with a pulse width of 40 samples. An isoceles triangle with peak at sample No. 21 was chosen as pulse No. 1, the triangles of the same area were successively offset to sample No. 38, chosen as pulse No. 10. Autocorrelation functions were computed for pulses 1 through 10, and crosscorrelation functions between pulse 1 and all other pulses. The results can be summarized by Fig. 19. This shows that the autocorrelation function remains substantially constant, and that the crosscorrelation function decreases as the offset between wave peaks increases, as shown by Fig. 19, curve a. Only three significant figures were utilized in this computation, and more accurate input data would serve to smooth the curve.

Some additional information can be gained from this study. It is necessary to determine the shift on the time axis of the peak of the correlation function as a function of the separation of the peaks of the pulses being correlated with each other. This is a linear 1 to 1 relationship between the peak sample shift of the crosscorrelation function and the sample difference between the peak of the pulses being crosscorrelated, under the conditions that the pulses are normalized on the time base.

The results of these studies can be summarized by the set of curves defining the maximum value of the crosscorrelation function of a controlled area as a function of the peak shift in the pulses, and of the shift in the correlation function peak with respect to the peak shift in the the pulses. These relationships can be used in a table lookup scheme in the diagnosis for (a) altering the standard waveform, and (b) correcting the value of

the maximum correlation function to correspond to the shift in peaks of the pulses.

The next study performed was the R-wave of the QRS complex of the electrocardiogram. These pulses are shown in Fig. 24. In this complex, the primary (R) wave appears triangular. A triangular standard wave was selected, with an amplitude close to (larger) than the R-waves. The R waves were raw sampled data, and slightly irregular, because of the presence of noise, so a standard triangular wave approximating the envelope of the data pulse was selected. This data is actual sampled data from the U. S. Public Health Service project. It will be noted that the data has not been normalized, since the scale factors were not made available to this project. The following results were obtained for the successive R waves of a single lead.

Wave	Area	Autocorrelation	Crosscorrelation (with R_{std})
R_{std}	5810	6374 (6374)	
R_1	5118	5629 (7230)	5944 (5230)
R_2	5470	6404 (7210)	6340 (5970)
R_3	5530	6553 (7220)	6414 (6100)
R_4	5349	5367 (6470)	6092 (5620)
R_5	5553	6537 (7170)	6402 (6090)

The first figures tabulated under the correlation functions are the raw data, and the figures in the parentheses are the correlation functions corrected to reflect the differences in area of the waves. Since the waves are all in the same lead, approximately the same corrected value

of correlation functions appears for all waves except R_4 (which appears to be in error). This is consistent with expectations of periodic electrocardiograms. It will be further noted that the autocorrelation functions for the R-waves are higher than those for the standard waves, which indicates that the waves are not truly triangular in nature, but rather are more sharply peaked than the triangular pulses, which is consistent with the results of previous studies. Previously, for the same area, autocorrelation functions were computed for three pulses, the square wave, the sine wave, and the triangular wave. The ratio of autocorrelation function to the area squared for the three pulses respectively were 1.000, 1.240, and 1.333. Therefore, for these R-waves, one would expect the optimum standard to be more peaked than a triangle, perhaps consisting of two parabolic segments. However, for ease of computation, the first standard will remain the triangular wave, and the consequent reduction of the value of the crosscorrelation function accounted for in the diagnostic standards. Referring to Fig. 10, it can be seen that the crosscorrelation function peak corresponds to the sample No. as the autocorrelation peak, hence there is very little shift from an isoceles triangle. Any small shifts can be handled by the appropriate factor given by Fig. 19.

Additional studies were performed on the P-wave, and the results are shown in Figs. 12, 13, 14, and 15. The data used is shown in Fig. 22. Both the actual data points and the smoothed (linear) data points shown in Fig. 22 were utilized. The standard wave pulse was a sinusoid, which appears to be generally close to the form of most P-waves. The results are summarized below.

Original Sampled Data

Wave	Area	Autocorrelation	Crosscorrelation (with P_{std})
P_{std}	774	69 (69)	
P_2	916	81 (58)	76 (64)
P_3	646	58 (83)	58 (69)
P_4	708	61 (72)	63 (69)
P_5	644	51 (73)	57 (69)

Smoothed Data

P_{std}	774	69 (69)	
P_2	942	72 (51)	76 (63)
P_3	668	50 (67)	60 (69)
P_4	678	54 (70)	60 (68)

It will be noted that the deviations of values is greater in this case than with the R-waves. Inspection of the data in Fig. 22 shows that there was a base change in wave P4. P2, P3, and P5 occurred in the same lead and should be fairly repetitive, but it is noted that P2 is much larger in area, with a broader peak, which gives a lower value of the corrected correlation function. This, according to Steinberg (15) is the most difficult pulse to identify and measure, and has given difficulty on the U. S. Public Health Service project. In the case of P2, no reason except patient variation between heartbeats can be ascertained. Fortunately, in the initial portions of this investigation, great precision is not required on the P-wave measurement in order to secure a successful

diagnosis, as, in general, presence or absence and general form are the only diagnostic criteria needed for the diseases being considered. Later utilization of correlation techniques in more refined and extensive diagnoses will undoubtedly require more precise definition of the P-waves.

Inspection of the corrected values of autocorrelation and crosscorrelation of the above pulses indicates that a sine wave is a fairly good approximation, and inspection of the Figs. 21 through 26 indicates that the P-waves are very symmetrical, so that sine waves shall continue to be used as a reasonable standard pulse, and will probably serve as a usable standard for most diagnoses.

The T-waves of the same original sampled data were studied, with the results tabulated below. The data utilized were those shown in Fig. 23, in original form, and smoothed, as shown thereon. Results on these waves are somewhat inclusive because of the shift of the baseline data of the sampled data electrocardiograms. The standard wave selected was again a sine wave.

Wave	Area	Autocorrelation	Crosscorrelation (with T_{std})
T_{std}	11,710	98 (98)	
T_1		47	64
T_2	1,310		67
T_4	1,454		82
T_1(smoothed)			61
T_2(smoothed)			66
T_4(smoothed)			81

No corrections are shown to the results listed above, since a changing baseline on the data invalidated many of the results with the original data used. Inspection of Figs. 16 and 17 pictorially indicates the same results as those summarized above. Inspection of these figures show a shift of about 5 data points to the right on the crosscorrelation functions from the autocorrelation functions, however. This is indicative of the skewed nature of the T wave. Modification of the standard wave is indicated, but the initial study will utilize the curve shown in Fig.19 to modify the value of the crosscorrelation function in order to compensate for this shift, and a sine wave standard will also be utilized in this case.

As a check on studies made by previous investigators, an autocorrelation study was made on the entire electrocardiogram waveform, as shown in the data of Fig. 21. The first half (the second being symmetrical) of this is shown in Fig. 11. The shape of this curve can be explained from inspection of Fig. 11 and Fig. 21. At the maximum positive value of the autocorrelation function, at the right side of 11, the wave is aligned with itself. At the first negative minimum, the T wave is opposite the depressed ST segment, and the P-wave is opposite the PR interval. A smaller relative positive maximum occurs when the P and R waves are aligned, and a negative minimum occurs when the P and R waves are aligned with the ST segment. A positive maximum occurs again when the T and R waves are aligned, and a negative minimum occurs thereafter when the P wave is opposite the ST segment.

The presence of these relative maxima and minima in the autocorrelation

function can serve to identify the presence or absence of the various pulses, as well as their direction (positive or negative). Additionally, with the use of some logical operations the locations of the various pulses can be ascertained. In one scheme of diagnosis presented by Martinek (11), given myocardial diseases may establish specific types of overall autocorrelation functions which may be classified. However, the computation of correlation functions is lengthy. In an average ECG waveform, sampled at 500 samples per second, 400 individual samples may be expected. In order to compute the autocorrelation function of sampled data of this length, $2N^2$ multiplications and additions are required to compute half the symmetrical correlation function. This, for N = 400, results in 320,000 multiplications and an equal number of additions. If the waveform is broken up into specific pulses, with N = 40, this results in 3200 operations each of multiplication and addition, a saving of 99% in computer time, and a saving of a great deal of memory space. As previously pointed out, advantage will be taken of this saving, and the correlation of only individual pulses taken.

An additional study was performed in conjunction with the pattern recognition study which is of interest in this section. This study was to determine the effects on the value of the correlation function of an improper normalization on the time axis, resulting either from an error occurring in the logic of recognition, or the use of a standard waveform not correctly matched to the pulse which is being correlated. The pulses under consideration are shown in Fig. 18. The following data were taken on this study.

Figure 19. (sample shift)/(pulse sample length)

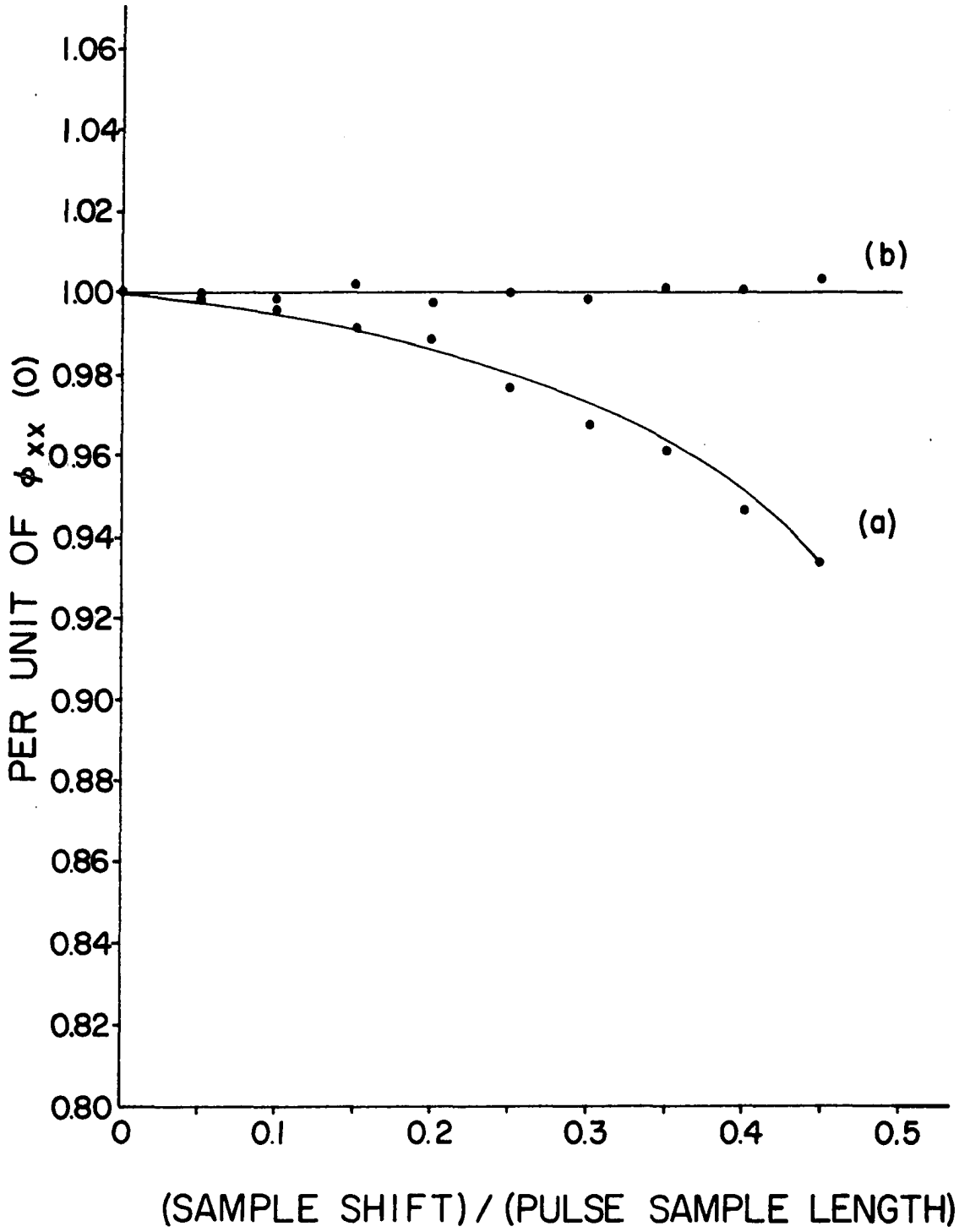
1.06
1.04
1.02
1.00
0.98
0.96
0.94
0.92
0.90
0.88
0.86
0.84
0.82
0.80
PER UNIT OF ϕ_{xx} (0)
(b)
(a)
0
0.1
0.2
0.3
0.4
0.5
(SAMPLE SHIFT) / (PULSE SAMPLE LENGTH)

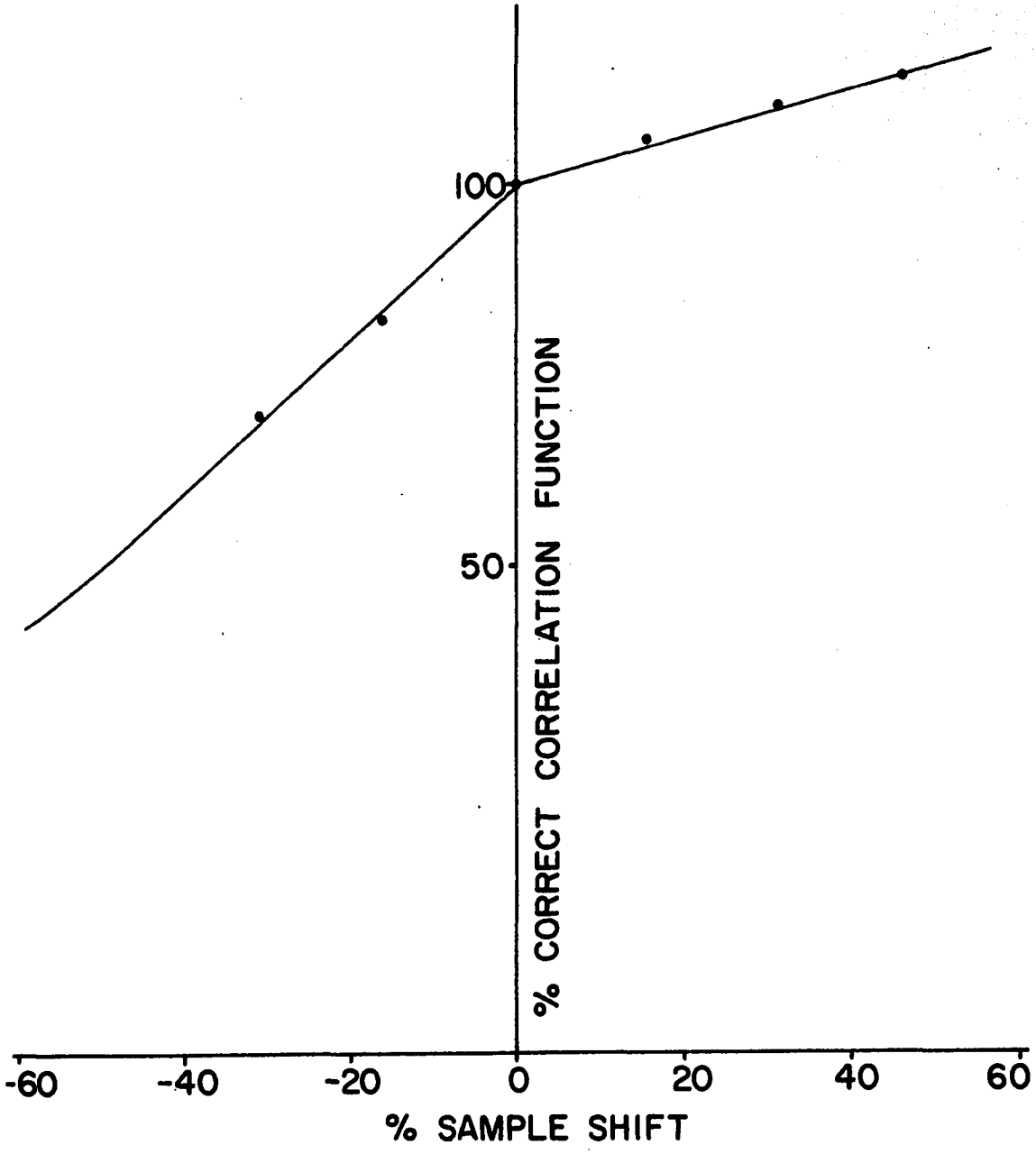

Figure 20. Effect of normalization

Pulse	Autocorrelation	Crosscorrelation	Area	% Sample Change
1 - 1	8212 (0.5680)		120	
2 - 2	9402 (0.4700)		140	
3 - 3	10819 (0.4225)		160	
4 - 4	12075 (0.3730)		180	
5 - 5	13522 (0.3380)		200	
6 - 6	6682 (0.6682)		100	
7 - 7	5482 (0.8575)		80	
1 - 2		8705 (0.5180)		0
1 - 3		9168 (0.4780)		+15.4
1 - 4		9461 (0.4380)		+30.8
1 - 5		9759 (0.4070)		+46.2
1 - 6		7302 (0.6080)		-15.4
1 - 7		6338 (0.6600)		-30.8

The parentheses show the values of the correlation functions after correction for area differences. The pertinent results of this study are indicated in Fig. 20. It will be noted that the values of the correlation functions, of different pulses varying in time base, but of constant maximum amplitude, exhibit approximately a piecewise linear relationship on each side of the correct value. The break in the curve occurs because of the higher percentage change at below the unity value. This curve furnishes a correction which can be applied to the correlation function when the time base is either improperly normalized as a result of the logic of recognition, or furnishes a basis for interpreting the correlation

functions when no normalization whatsoever is used. This would permit the use of median values as standards and use of this correction to change the values. It can be seen that a possibly large saving in computation time might result.

Data

Samples of the data utilized in this investigation are shown in Figs. 21 through 26. During the early stages of the project, it was decided to use the sampled data available from the U. S. Public Health Service project. On this project, an analogue-to-digital converter was available with print-out, at any sampling frequency desired. A small amount of this data was made available, and a sample of one waveform of one lead is shown in Fig. 21.

Fig. 21 shows a plot of the sampled data. The original data furnished was at a sampling frequency of 500 samples per second, but, for purposes of plotting, every other data point was chosen, giving an effective sampling frequency of 250 samples per second. The individual wave pulses shown in Figs. 22, 23, and 24 show all data points (500 samples per second). This data was very useful initially on the project because it furnished an illustration of the noise inherent in the electrocardiogram. As can be seen from inspection of this data, the noise components are relatively small with respect to the signal components, and do not present a difficult problem for signal detection.

However, it was difficult to transport the data in large quantities between projects, and the numerical format was unsuitable for direct use in the 1620, and required additional conversion prior to use on the

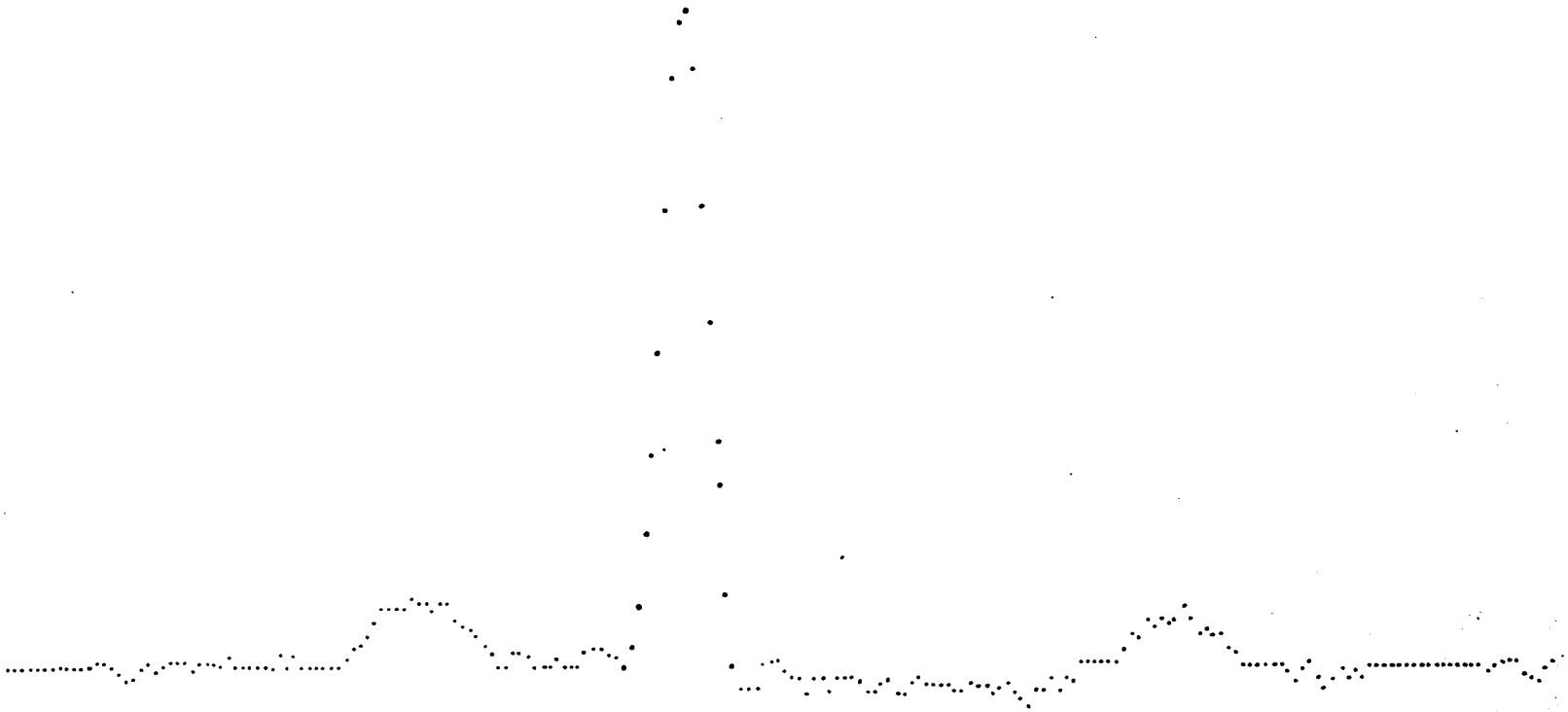

Figure 21. Sampled data - ECG

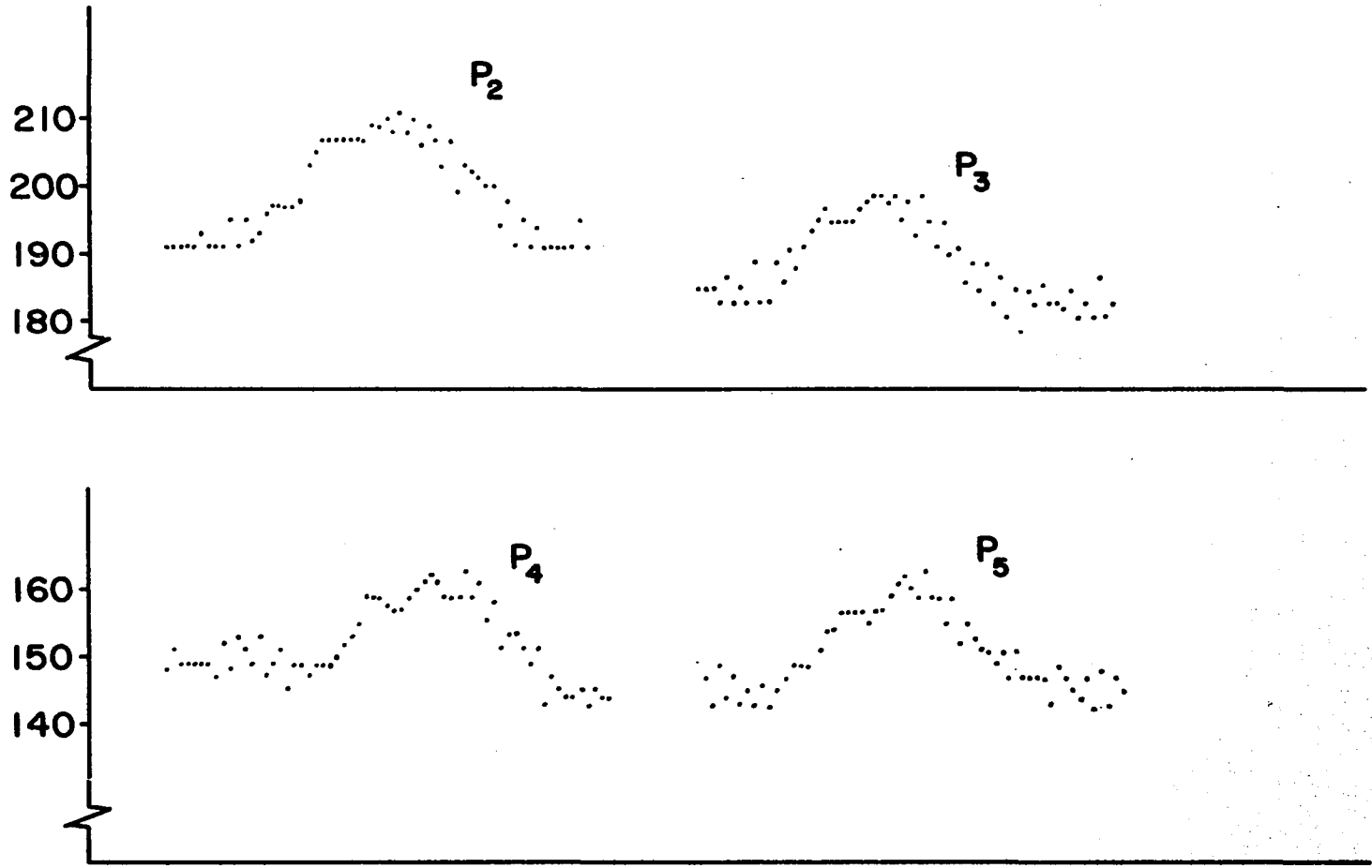

Figure 22. Sampled data - P-waves

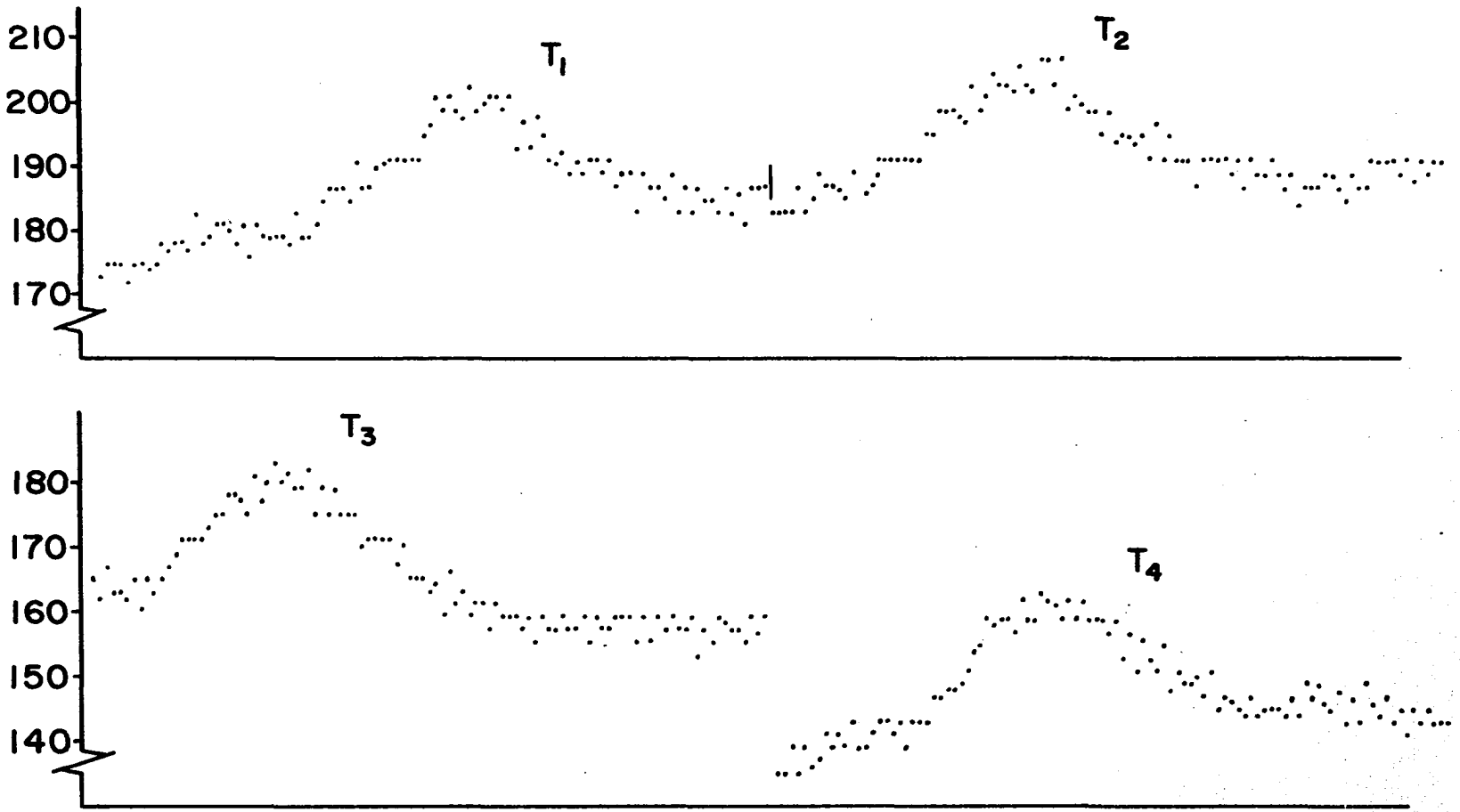

Figure 23. Sampled data - T-wave

Figure 24. Sampled data - R waves

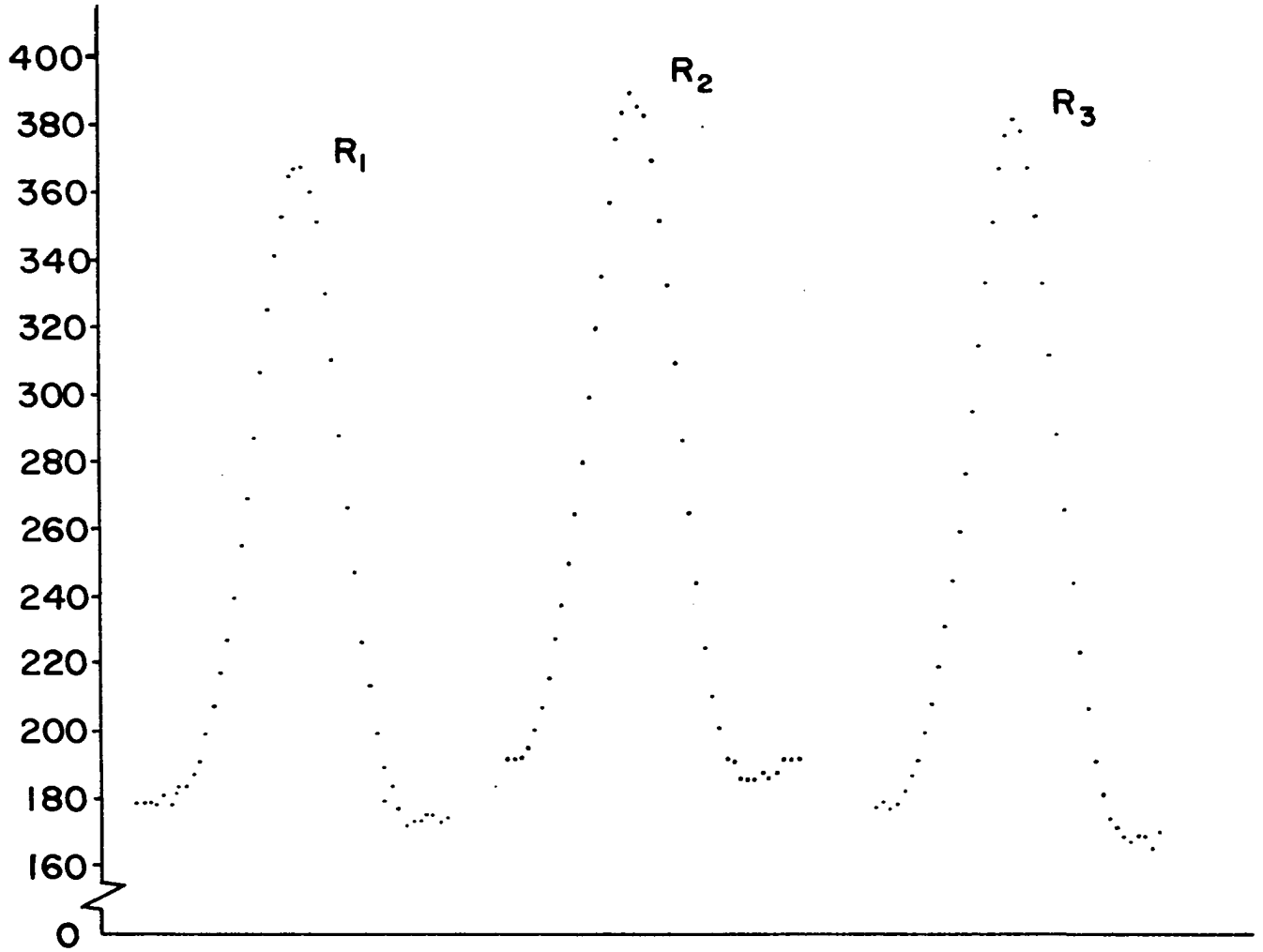

SAMPLED DATA - R WAVES

Figure 24. Sampled data - R waves (continued)

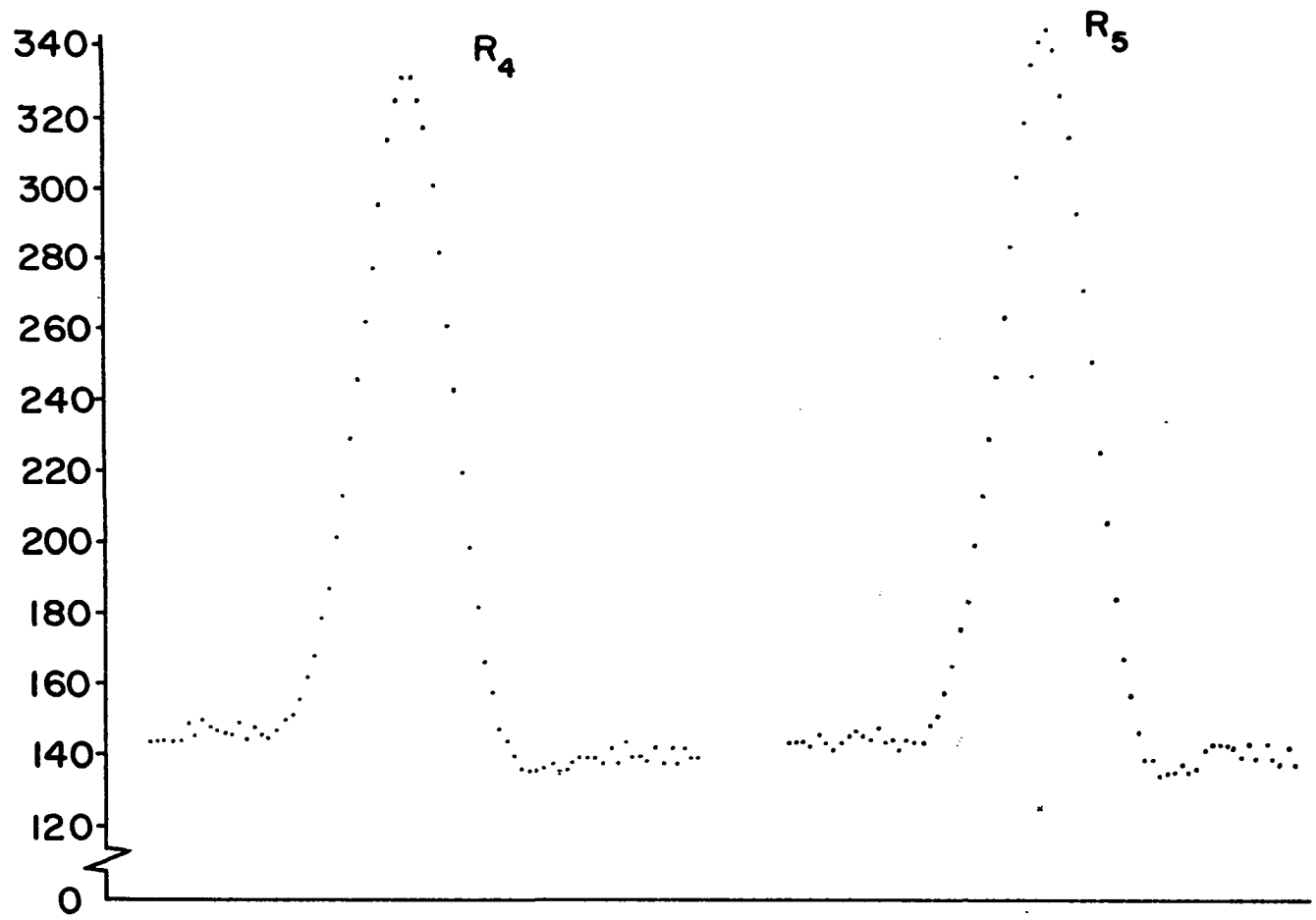

SAMPLED DATA- R WAVES

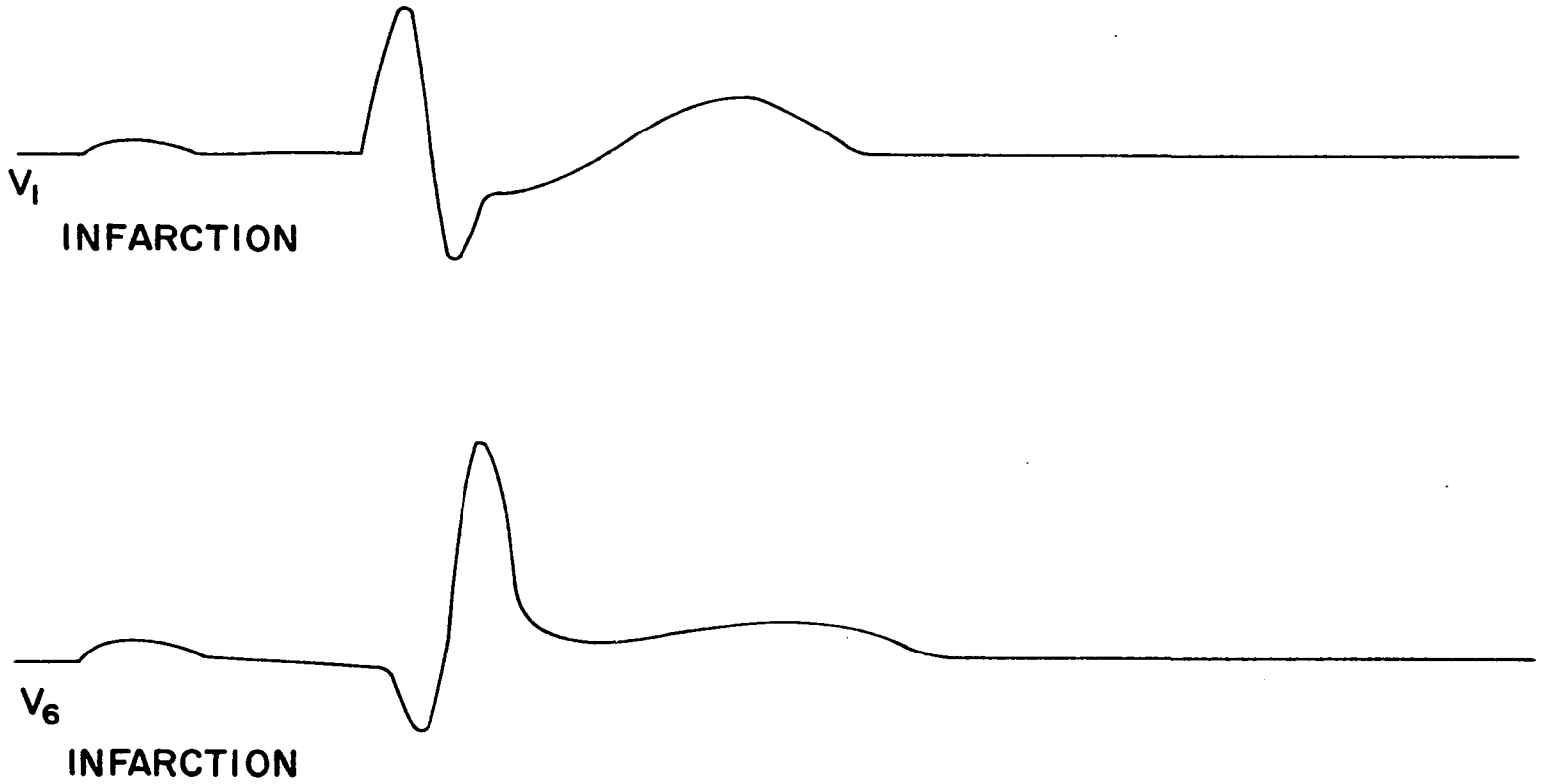

Figure 25. Sampled (hand) data for use in program

Figure 26. Actual ECG data

IOWA METHODIST HOSPITAL
RAYMOND BLANK MEMORIAL HOSPITAL FOR CHILDREN

Patient: _____ Age: _____ Room No. 424

Date Taken: 4-8-62 Dr. L. F. Staples Hosp. No. 219-637

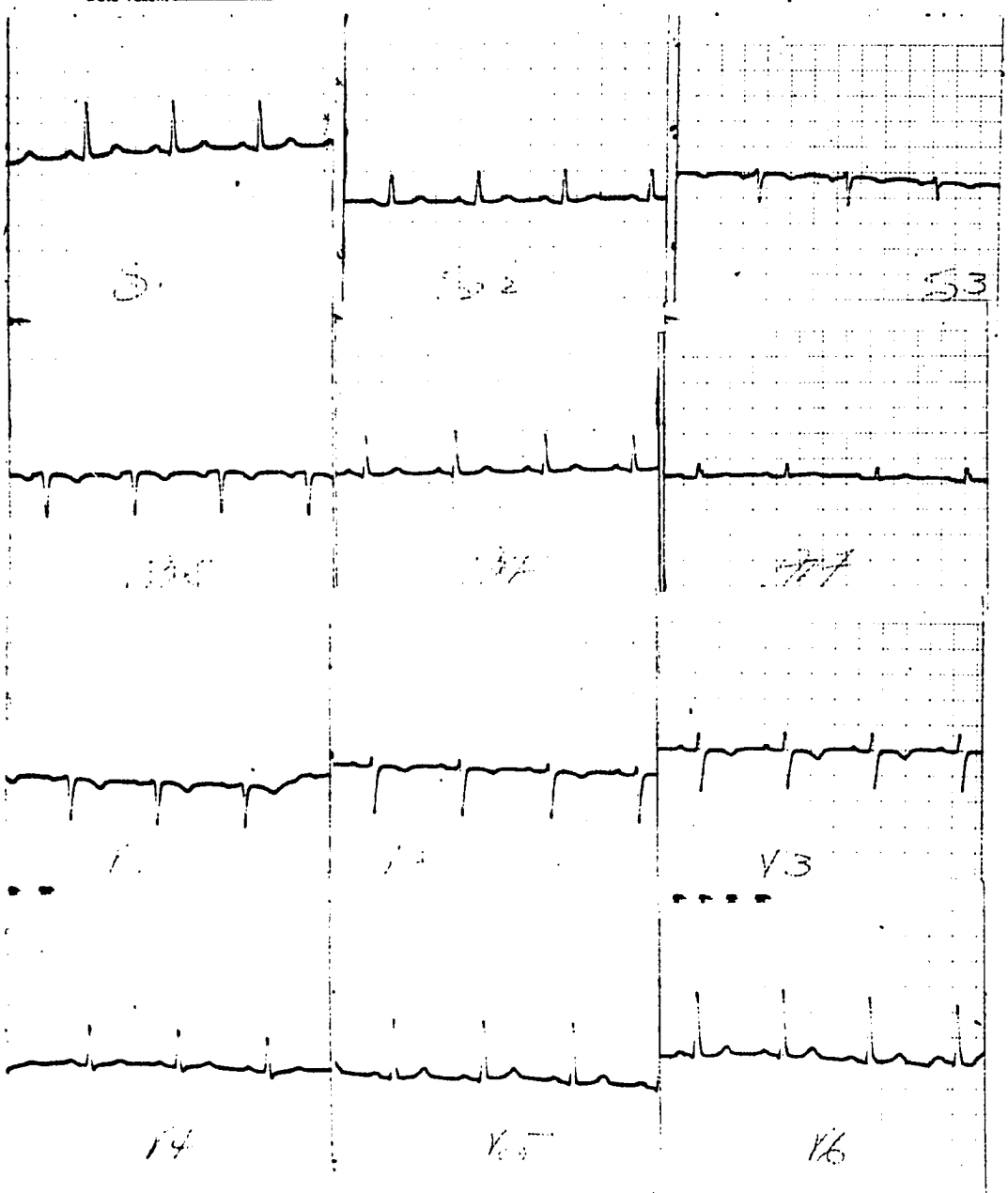

MR-17

ELECTROCARDIOGRAPH REPORT

project. These disadvantages, coupled with the lack of supporting data such as scale factors and lead number designations forced discontinuance of use of this data. An additional difficulty presented by this data is that the baseline shifts at low frequencies because of the flutter and wow in the analogue tape recorder used on the project, as previously explained. The data which was available was used to study the correlation routines, and the results were discussed in a previous section.

It will be noted, in Figs. 22, 23, and 24, that a visually approximated average was taken of the data, and these points used in computation of the correlation functions. No attempt was made to provide a statistical fitting of this curve to the sampled data, as this is the purpose for which the correlation functions are to be employed. Rather, this smoothing, performed by inspection, was for the purpose of determining its effect on the correlation functions, in magnitude and shape.

The results of the smoothing on the correlation functions was very slight, and suggested an alternative, slower, method of data acquisition. It was proposed to use the data available at Iowa Methodist Hospital from patients tested at the Heart Station. This data is available in the form shown in Fig. 26, and consists of the patient's identification, the 12 electrocardiograms, and an analysis, which appears on the back of the mounting sheet for the records. This provides a guide to checking the results of the diagnoses, as well as the necessary records. However, the data, taken directly from the electrocardiograph, is unsuitable, and must be converted to digital form.

Since the results of the smoothing indicated very little change in

the correlation functions as a result, it was decided to carefully measure the waveforms from the electrocardiograms, expand them on both the time and amplitude scales, and pick samples from the expanded plots to give the data in usable digital form. Although the scale is approximately 1/4 that actually used in the project, an example of this expansion is shown on Fig. 25. Values were picked at proper sampling intervals, recorded, and put onto punched cards for use in the computer. The studies which follow use data of this type.

Logic of Recognition of the Electrocardiogram

Discussion of recognition

The problem of automatic interpretation of an electrocardiogram is a specific case of a larger general class of problems in pattern recognition. Fundamentally, the problem of pattern recognition, according to Minsky (25) is to find a set of quantities associated with a given pattern which remain invariant under various transformations. Such quantities might therefore be recognizable under conditions of translation, rotation, dilation along any or all axes, and be independent of superimposed noise.

The basic approach in the recognition is to match the various patterns against prototypes, or catalogued patterns. A more general and powerful method is the property list method, wherein each pattern is subjected to a series of tests, each test detecting some property of heuristic importance. These properties must be invariant under the previously listed transformations. The problem of pattern recognition then consists of discovering the properties and combining them in a meaningful

manner to build up the pattern recognition system.

This system, on this project, will initially use correlation techniques to match the various patterns against prototypes, and combine these results to classify the cardiographic data. The classes selected will be various disease categories, as well as normal categories. Thus, only the complete classification of a waveform constitutes pattern recognition.

In order to best implement the program, two initial steps are necessary. First, advantage must be taken of all a priori knowledge available concerning the waveform. Second, a search program must be initially undertaken in order to increase the a priori knowledge, and to indicate any additional steps necessary before application of the fitting and classification techniques. Use of such preliminary knowledge permits minimization of the computation required. The a priori knowledge of the waveform is listed in the following paragraph.

Referring to Fig. 1, the electrocardiogram waveform possesses certain characteristics common to all these waveforms, regardless of the patient, or the lead. These characteristics may vary considerably, but they are present in all cases, and have points of similarity. Some of these characteristics are listed below:

1. The following pulses are present in some degree and shape in all cases.
   a. P wave
   b. Q wave
   c. R wave
   d. S wave

e. T wave

f. ST segment

2. In the USPHS program it was definitely established by Steinberg (15) that the highest derivative is negative and exists between the R wave and the T wave. This is always the case, and is always repeatable.

3. It has been definitely established, both fundamentally and experimentally that the interval between the T wave and the P wave establishes a baseline of zero heart activity.

4. Inspection of a large number of electrocardiograms supports the fact that the P and T waves are generally of a nearly sinusoidal nature, and the QRS complex is composed of pulses generally triangular in nature. Quantitative results are shown in a previous section.

There are several ways to institute the search phase of the program. The simplest is that used by the National Bureau of Standards, and reported by Taback (16). This consists of using a moving average along the waveform for a preliminary smoothing, and the program used for this investigation is shown in Appendix F. Originally, a combination of counting and moving average was used on the raw sampled data, but trial showed that the computation of the moving average over the entire waveform was very simple, and required little computation time, so this method is utilized in this investigation.

The moving average provides a preliminary smoothing, but, by its nature, results in the loss of specific information. When a pulse is

encountered, the average, taken over two points on each side of the point under consideration, reduces the amplitude of the pulse, and increases its duration. Therefore, it is necessary to use some additional logic to determine the correct pulse width. At a sampling frequency of 250 samples per second, in this project, the P-wave is increased by two samples, the R-wave by 4 samples, and the T-wave by two samples. Therefore, account must be taken of the fact when interpretation of this search is undertaken. The primary value of utilizing the results of this initial smoothing for recognition purposes lies in the elimination of the point-to-point variations due to noise, which would cause great difficulty in formulation of the logic of recognition. This was the trouble with the original method shown in Appendix F.

After the moving average has been computed, the necessary additional logic can be listed. It is assumed that a synchronizing circuit has located the point of maximum negative derivative, the quantity described above. The sampling rate is 250 samples per second. Using the maximum negative derivative as the time base point, and the interval between the repolarization of the ventricular musculature and the depolarization of the auricular musculature as the baseline of zero heart activity, the starting point in time, after a preliminary count, is a point on this zero base line. Proceeding from this point in time, the first pulse to be encountered is the P-wave. The logic of recognition of the P-wave follows.

P-wave recognition

1. Locate sample (address at N) flagged as point of maximum

negative derivative.

2. Beginning with sample (N-100), check values of successive samples.
3. If 10 values of successive samples are constant (difference < 0.01 mv), take the average value of these 10 samples as zero value, X.
4. Subtract X from all values of samples, and restore in original locations.
5. Flag first sample where absolute value $\geq$ 0.01 mv.
6. Are next three successive samples absolute values > 0.01 mv, and increasing?
7. If not, proceed with comparison of successive samples.
8. If yes, flag sample N_1. This defines the beginning of the P wave.
9. If N_1 occurs later than N-30, indicate "No P-wave present" and go to QRS recognition.
10. Continue comparison with zero.
11. Does a subsequent value (later than N_1 + 10) become < 0.01 mv?
12. If no, go to step 18.
13. If yes, flag first sample where absolute value < 0.01 mv, or where sign changes. Call it N_2.
14. Compare next 5 values with zero. Is the absolute value $\leq$ 0.01 mv? If no, go to step 18.
15. If yes, find the maximum absolute value of samples between N_1 and N_2.

16. If maximum absolute value of sample > 2 mv and occurs later than sample (n - 30), indicate "No P-wave present".
17. Compare maximum value from zero. If negative, indicate "Negative P-wave", if positive, indicate "Positive P-wave".
18. If no, indicate "Baseline shift, no P-wave possible" (if heart rate < 110 beats per second). Go to QRS recognition.
19. $P_d = (N_2 - N_1)\ (0.004)$
20. Continue comparison with zero to proceed to QRS complex.

After recognition of the P-wave has been completed, the next pulse to be checked is the QRS complex. This consists of the initial downward pulse, the Q wave, the initial upward pulse, the R-wave, and the initial downward pulse following the R-wave, the S-wave. The logic of recognition of this complex follows.

QRS recognition

1. Commencing with the last sample in P-wave recognition sequence, compare absolute value of sample with 0.0^4 mv.
2. Are next three samples > 0.04 mv?
3. If no, continue comparison routine until step 2 gives yes.
4. If yes, flag first sample > 0.04 mv.
5. Compare values previous to flagged sample of 4, with absolute value $\leq$ 0.01 mv.
6. Flag sample previous to that of 5 as N_3. This defines the beginning of the Q-wave or the R-wave.

7. Is the sample flagged in $4 < 0$? If yes, this marks the beginning of the Q-wave. If no, go to step 11.
8. Continue comparison of absolute sample values with zero until sign changes.
9. Flag sample immediately previous to the sign change as N_4. This defines the end of the Q-wave and the beginning of the R-wave.
10. Compute $Q_d = (N_4 - N_3)\ (0.004)$
11. If 7 is no, this marks the beginning of the R-wave. Relabel N_3 as N_4 and indicate "No Q-wave".
12. Continue comparison of absolute values with zero until sign changes or value $\leq$ 0.01 mv.
13. If no sign change, indicate "No S-wave".
14. Flag sample at which sign changes and label N_5. This defines the end of the R-wave and the beginning of the S-wave.
15. Compute $R_d = (N_5 - N_4)\ (0.004)$.
16. Continue comparison of absolute values with zero.
17. Are absolute values of samples > 0.10 mv.
18. If no, indicate "No S-wave".
19. If yes, continue comparison with zero for 30 successive samples.
20. Does absolute value become < 0.05 mv?
21. If yes, define sample with minimum absolute value in this interval as N_6. This defines the end of the S-wave.
22. Compute $S_d = (N_6 - N_5)\ (0.004)$.

23. If no, indicate "Depressed ST segment", and compute average of next 10 samples as y, the value of the ST segment. Depressed ST segment should be indicated if the absolute value > 0.05 mv.

After the durations and structure of the QRS complex have been determined, it is necessary to recognize the ST segment, and the presence and duration of the T-wave. If the value Y, computed above, exceeds 0.5 mv, a depressed ST segment exists. The beginning of the ST segment will be defined by the sample N_5 if no S-wave exists, and by N_6 if an S-wave is present. The end of the ST segment, and beginning of the T-wave is defined as the point where the sample value differes from the value of the ST segment by more than 0.5 mv. The end of the T-wave is defined as the point at which the T-wave returns to a value of less than 0.1 mv different from the baseline of zero heart activity. The logic of recognition follows.

T-wave recognition

1. Compare samples after either N_6 or N_5 with Y.
2. If the difference of the absolute values of the samples from the value Y, or the value of the sample $N_6 < 0.03$, for 10 successive times, the T-wave is beginning.
3. Flag the sample at which the difference exceeds 0.05 mv.
4. Successively compare samples with standard, and proceed to the point where the difference is 0.01 mv, and continue 10 more samples.
5. Flag this sample from 4.

6. Is the sample number flagged in 3 minus the sample number flagged in 5 less than 10?
7. If no, flag the sample 5 samples previous to the sample flagged in 3, and designate this as N_7. This defines the end of the ST segment.
8. If yes, flag the sample at which the difference becomes less than 0.01 mv.
9. Does the sign of the samples change during the previous comparison?
10. If no, ignore. Signify "No T-wave".
11. If yes, designate this sample (where sign changes) as N_8, the start of the T-wave.
12. Compare sample values with zero, forward from sample N_8.
13. Is the absolute value of the sample < 0.05 mv?
14. If no, continue comparison.
15. If yes, define point of minimum difference as N_9. This defines the end of the T-wave.
16. Find the maximum [value - V] between N_7 and N_8. This is the peak of the T-wave. Flag it N_{10}.
17. Compute $(N_{10} - x)$ to get the value of the peak.
18. Is this value > 0?
19. If yes, indicate "Positive T-wave".
20. If no, indicate "Negative T-wave".
21. Compute $T_d = (N_9 - N_8)\ (0.004)$.

22. Compute $(N_3 - N_1)$ (0.004) = PQ (If Q-wave present).

23. Compute $(N_4 - N_1)$ (0.004) = PR (If Q-wave absent).

24. Compute $(N_6 - N_3)$ (0.004) = QRS_d (If Q-wave present).

25. Compute $(N_6 - N_4)$ (0.004) = QRS_d (If Q-wave absent).

26. Compute $(N_7 - N_6)$ (0.004) = ST_d.

27. Compute $(N_8 - N_3)$ (0.004) = QT (If Q-wave present).

28. Compute $(N_9 - N_4)$ (0.004) = QT (If Q-wave absent).

Applications and results

The flow diagram for the series of operations outlined immediately above will not appear in block diagram form in Appendix F, as the logic of the steps contained can be followed in the text.

After the moving average has been computed, and the logic of recognition applied in order to define the presence or absence of various pulses, the preliminary steps are complete. A technique similar to this is termed "point recognition" by Stark (14). The presence or absence of the various pulses, together with their directions characterizes the general nature of the electrocardiogram pattern, and furnishes an initial partial classification of the waveform. It further provides a criterion as to whether to correlate a given waveform or not, and whether to expect, when the correlation functions are computed, a positive or negative waveform. Thus, this general characterization of the wave is useful both in the minimization of the required computation, and the establishment of preliminary criteria of use in classifying the results of the correlation

studies.

The calculation of the various durations of time is of equal importance in the logic of recognition. It is first necessary to know these durations in order to utilize them in diagnoses of some of the common heart abnormalties, and second, it is necessary to know the duration of the pulses in order to provide a normalization on the time base to render the correlation functions meaningful. Without some sort of normalization procedure, the interpretation of the correlation functions is practically impossible to achieve with any degree of accuracy. Normalization of the amplitudes can be done by the methods outlined previously in the section covering correlation studies.

The factor introducing the largest problem in the procedure described herein is that of normalization on the time base. The normalization of amplitude can be effected by simple arithmetic operations involving the area of the pulse, which is easily computed. However, the amplitude normalization is possible only after normalization on the time base has been effected. The normalization of the time base can be effected, in the proposed system, in one of several ways. First, the time normalization can be accomplished by the specification of the proper time interval for the standard, and the values of the standard adjusted for the proper number of samples. This requires a recomputation of the sample values for the standard for each pulse on which correlation is to be performed. This requires a large amount of computer time, unless adequate memory space is available to select proper standards without recomputing the sample values. Second, if the pattern recognition routine is run first,

and a second pass in real time made, with the sampling rate adjustable, and governed by the results of the recognition program, this variable sampling interval can provide the correct number of samples in the sampled electrocardiogram waveform to effect the normalization in this manner. A third alternative is to select, as standards, the pulses with a number of samples approximating the mean number of samples in each pulse for which the correlation functions are to be computed. Since this study is primarily concerned with the feasibility of this general correlation technique, only the first and third methods will be investigated herein, as implementation of a variable speed sampler must be delayed until a data acquisition system is available. Under these constraints, the diagnostic methods will be investigated in the following section. Results of this program are shown in Tables 1 and 2.

Table 1. Pattern recognition results, V1

Quantity	LVH	RVH	Infarction	N1	N2	N3
P-wave	-	+	+		+	+
Q-wave						
R-wave	+	+	+	+	+	+
S-wave	-		-	-	-	-
T-wave	-	-	+		-	+
ST_d	0.120	0.120	0.076		0.104	0.144
QT	0.220	0.180	0.152		0.200	0.212
T_d	1	0.100	0.140		0.224	0.148
QRS_d	0.100	0.065	0.076	0.100	0.096	0.068
PR	0.160	0.216	0.148	0.120	0.160	0.120
Q_d						
ST	-0.40		-0.80			
R_d	0.020	0.065	0.036	0.040	0.036	0.026
S_d	0.080		0.040	0.060	0.060	0.042
P_d	0.080	0.060	0.060		0.068	0.052

Not present if no sign is indicated. A blank means a measurement cannot be taken.

\+ Present and positive in sign

\- Present and negative in sign

All results in seconds except ST, in MV.

Table 2. Pattern recognition results, V6

Quantity	LVH	RVH	Infarction	N1	N2	N3
P-wave	+	+	+	+	+	+
Q-wave	-		-		-	-
R-wave	+	+	+	+	+	+
S-wave		-			-	
T-wave	+	+	+	+	+	+
ST_d	0.140	0.124	0.080	0.176	0.136	0.216
QT	0.240	0.244	0.168	0.228	0.228	0.280
T_d		0.140	0.136	0.176	0.224	0.148
QRS_d	0.100	0.120	0.088	0.052	0.092	0.064
PR	0.160	0.176	0.160	0.180	0.160	0.132
Q_d	0.032		0.032		0.020	0.020
ST	-0.80		0.60			
R_d	0.068	0.040	0.056	0.052	0.040	0.044
S_d		0.080			0.032	
P_d	0.080	0.060	0.060	0.068	0.100	0.072

Not present if no sign is indicated. A blank means a measurement cannot be taken.

\+ Present and positive in sign

\- Present and negative in sign

All results in seconds except ST, in MV.

DIAGNOSIS

Discussion of Factors Affecting Electrocardiogram

Cardiac states

Diagnosis will be initially on a limited number of heart defects. These follow the same order as those in the manual program, with the exception of infarction. It has not been possible at this date to consistently furnish diagnoses of infarction on the manual program, and further investigation of the criteria must be made before setting standards. This investigation will be delayed until a data acquisition system is available to the project. The disease states to be investigated are:

Normal

Atrioventricular (AV) Block

Bundle Branch Block (Right and Left)

Ventricular Hypertrophy (Right and Left)

These three diseases to be investigated are of a long term nature, and may not be evident to the patient in an overt manner, whereas the presence of an infarction will be apparent to both the patient and the physician. Therefore, there is considerable merit in a study of the six states listed above. A brief discussion of each of these five abnormalties follows, together with some of the basic diagnostic criteria.

A normal waveform is one whose descriptive parameters fall within normal limits, and will not fall within the classifications including any of the abnormalities listed above, or infarctions. There is a wide variation of the parameters describing the normal pattern, so, a pattern

will be classified as normal if it does not fall within any of the abnormal classifications.

The PR interval represents the time required to depolarize the auricular musculature plus the delay in the AV node, plus the time required to depolarize enough ventricular muscle to produce sufficient current to cause the beginning of the QRS complex. It is dependent upon heart rate. A long transmission time indicates a partial atrioventricular block, which is a definite indicator of cardiac disease. Since the length of the PR interval is used in the recognition program described in the previous section, this value can be used with the standards listed in Appendix A to furnish a diagnosis. Heart rate can be computed from the assumed synchronizing circuit referred to previously. This does not require use of the correlation techniques.

Bundle branch block is the complete or partial interruption of transmission of the depolarization wave through the transmission network of the ventricles, consisting of the bundle of His and the Purkinje (arborization) network. After depolarization of the auricular musculature is complete, the wave passes through a node called the bundle of His, thence to the Purkinje network to be transmitted to the right and left ventricular muscle fibres. The bundle of His includes a right and left portion, as does the Purkinje network, for transmission of the wave to the right and left ventricles respectively. When the bundle of His is affected, transmission to the Purkinje network is impossible, and this condition is called complete bundle branch block. If the lesion occurs in the Purkinje network itself, or in the transmission between the Purkinje network and

the ventricular muscles, partial or incomplete bundle branch block results. Either of these conditions can occur in either the right or left bundles. The effects of each are lessened cardiac efficiency, and each can be identified by the pattern in the proper precordial leads.

The effects of bundle branch block show up on the electrocardiogram as a widening of the QRS complex caused by the delay in transmission through the system. This widens the QRS complex over the normal limit, and, since the normal upper limit of duration of the QRS complex is 0.11 sec., a duration greater than this is indicative of bundle branch block. This is not conclusive evidence, however, for transmission may be taking place over an alternate path, causing premature activation of the QRS complex. This is called the Wolf-Parkinson-White syndrome, and, if this is present, results in a shortened PR interval of less than 0.09 seconds in duration. In order to further isolate the state into right or left bundle branch block, it is necessary to consider an additional term, that of intrinsicoid deflection. The amplitude of the intrinsicoid deflection represents the difference in potential between the endocardial and epicardial surfaces of the myocardium subadjacent to the precordial electrode during depolarization. This is a very rapid process, occupying practically no time, hence is marked in time by the maximum negative derivative. This furnishes an excellent index with which to localize the block. Thus, if $QRS_d > 0.11$ sec., and the intrinsicoid V6 (over the left ventricle) > 0.08, and $TV6 < 0$, and $QV6 = 0$, a diagnosis of left bundle branch block can be made, as shown in Appendix A. If $QRS_d > 0.11$ sec., and intrinsicoid $V1 > 0.04$, right bundle branch block

is present. Some additional conclusions can be drawn concerning bundle branch block.

Since bundle branch block represents a retardation in the actuation of the ventricular musculature, if complete bundle branch block appears in both sides, the heart will completely cease to function. Therefore, complete bundle branch block can exist in only one side, not both. Second, since hypertrophy represents over activity and overdevelopment of one or both of the ventricles, and bundle branch block precludes this over activity, the two states are infrequently found in a given side. Therefore, if bundle branch block exists in either side of the heart, hypertrophy cannot exist in that same side. Conversely, however, presence of bundle branch block in a given side of the heart probably increases the tendency toward hypertrophy in the opposite side, as that ventricle will have additional load thrown on it.

As can be ascertained from the foregoing discussion, neither of the two basic conditions described required the use of correlation techniques. The criteria require only information available from the logic of recognition. Both hypertrophy, left and right, and infarction, posterior and anterior, will result in patterns requiring use and interpretation of the results of correlation techniques. As has been previously stated, however, infarction is a heart attack, and, when it occurs, requires the immediate attention of a physician and hospitalization. Therefore it is of less immediate concern than hypertrophy, the most common of all abnormalities. Simply stated, hypertrophy is essentially heart strain caused by extended periods of hypertension and result in over development

and over activity of one or both the ventricles. The patient suffering from this abnormality may be unaware of it, hence the great application of a routine computer technique to find this condition, so that corrective measures can be effected.

Right ventricular hypertrophy causes a widened QRS complex and a late intrinsicoid deflection because of the thickened walls of the right ventricle. The QRS complex is mainly positive in V1, with a late intrinsicoid deflection. In V6 the R-wave tends to be low, the intrinsicoid deflection early, and the S-wave wide, slurred, and great in amplitude according to Burch (2). These changes are characteristic of hypertrophy caused by pulmonary obstruction. That due to an increased volume of output causes a different pattern. There is a wide, slurred, and prominent R-wave in V1, and a wide, prominent, and slurred S-wave in V6.

Left ventricular hypertrophy causes a domination of the right ventricle by the left ventricle. The QRS complex, consists primarily of negative deflection of great amplitude in V1, and a positive deflection of great amplitude in V6. As the hypertrophy, both left and right, increases, the QRS complex progressively widens.

From the immediately foregoing discussion, it can be seen that the correlation functions hold great promise. Both types of hypertrophy cause a widening of the QRS time base, and an increase in amplitude of the pulses, hence an increase in area. Since the correlation function magnitudes are roughtly proportional to the square of the area of the pulse, if the time base is normalized, as shown under correlation studies, hypertrophy would be expected to be indicated by a marked increase in the

correlation functions of the QRS complex. With these considerations, the results of the correlations are tabulated in the following sections.

Results

General discussion

The expanded data for the electrocardiograph was correlated pulse by pulse, after the recognition was performed. The basic data obtained is tabulated in the first two tabulations, and corrected data is tabulated in subsequent tabulations.

The first tabulation is autocorrelation of the various pulses for the following waveforms, leads V1 and V6:

Right Ventricular Hypertrophy	(1)
Left Ventricular Hypertrophy	(1)
Infarction	(1)
Normal	(3)

No attempt was made to normalize these, and the amplitudes were expanded to provide easy reading and to further provide convenient numbers for the correlation routine presently being utilized. Since it is not the purpose of this initial study to set up absolute standards, interpretation in terms of the magnitudes of the clinical parameters was not attempted.

Tabulation of results

Table 3 shows the results of the computation of the autocorrelation functions of the pulses defined by the recognition program. Table 4 shows the results of these computations when crosscorrelation was performed with certain standard waveforms. The standards used were as follow:

P-wave	21 samples	100 maximum amplitude	sine wave
R-wave	15 samples	200 maximum amplitude	triangle, isoc.

Just as the waveforms were altered in amplitude, and amplitude scale, so were the standards. These results could be altered by normalizing the amplitudes by consideration of the pulse areas, but the diagnosis does not depend on this at this stage of the project. In later stages, when enough data is available, more specific standards can be set, and exact diagnostic limits prescribed, as in the manual method. However, adequate data is not presently available to set specific standards, so relative standards will indicate the possibilities of use of correlation in diagnosis.

Table 3 corrects the crosscorrelations of Table 4 for differences in the time base, since the standards were not normalized. It was desired to examine the problem of what information could be gained by using standard pulses of median sample widths. The use of the time-normalized pulses as a standard is well illustrated by the results of the autocorrelations performed. Table 6 shows the further correction to take into account the deviation of the peaks of the actual pulses from those of the standard pulses. Both the corrections made in Tables 5 and 6 were made by application of the curves developed in the section on correlation studies.

Examination first of the autocorrelation functions shows their usefulness in diagnosis of hypertrophy, both left and right. Considering right ventricular hypertrophy first, it will be noted that lead V1 yields a large R-wave correlation, very much larger than any other cardiac state except infarction. However, it possesses no S-wave, whereas infarction contains a very substantial S-wave. Lead V6 contains a substantial R-wave,

as indicated by the correlation function, and the largest S-wave by a great margin. This, coupled with the fact that the QRS complex is widened to a value of 0.12 seconds differs from all other patterns in the correlation computation. However, the intrinsicoid (located between the R and S-waves) is less than 0.08 sec., so left bundle branch block is eliminated. The size of the correlation functions, indicating great right ventricular activity, eliminate right bundle branch block. Thus, in this definite case of right ventricular hypertrophy, all other possibilities are eliminated by the combination of the results of the correlation computation and application of the logic of recognition. The results of the crosscorrelation yields exactly the same conclusion. These conclusions are exactly what would be expected from the description of the symptoms of right ventricular hypertrophy, as previously stated.

Left ventricular hypertrophy also stands out as a distinct pattern. The lead V1 exhibits a very large S-wave, larger than all other cases considered. The lead V6 indicates an extremely large value of the correlation function of the R-wave, as expected. This indicates a widening and thickening of the QRS complex, associated with great cardiac activity, as outlined in the previous description of electrocardiographic manifestations. Checking the results of the logic of recognition, the presence of a depressed ST segment is evident, which further classifies this waveform into the correct category.

The pattern of infarction does not stand out from the normal except in lead V1, where large S and large R-waves are both present. This is expected from the criteria utilized in the manual program, but insufficient

Table 3. Autocorrelation functions

Pulse	RVH	N1	N2	N3	LVH	Infarction
Lead V1						
P	39		26	57	122	18
Q						
R	2345	16	107	70	16	4074
S		1777	374	3393	5878	3163
T	308		308			634
Lead V6						
P	16	46	153	41	71	60
Q			28	45	94	872
R	2437	11202	817	537	44720	7770
S	2284		14			
T	780	330	678	135		273

work has been done in classification of infarction to make a direct statement about this cardiac state.

The normal waveforms exhibit wide variations in the correlation functions, but none of those associated with the abnormal cardiac states under examination. A great deal of data must be run in order to set up specific numerical quantities to automatically classify into the various cardiac states, and combine the results of both the logic of recognition and the correlation studies into a consistent, accurate diagnostic tool. However, clear patterns emerge through use of the logic of recognition and the

Table 4. Crosscorrelation functions

Pulse	RVH	N1	N2	N3	LVH	Infarction
Lead V1						
P	357		322	393	743	247
Q						
R	5435	455	1183	766	333	5544
S		1777	2214	5495	9663	6327
T	837		1397			1614
Lead V6						
P	232	413	903	419	579	443
Q			433	588	1044	3177
R	4429	11267	2605	2256	26541	9645
S	5281		438			
T	1774	1326	2022	764		1024

correlation techniques, and these can be more closely classified as additional data becomes available.

Table 5. Crosscorrelation functions corrected for time base differences

Pulse	RVH	N1	N2	N3	LVH	Infarction
Lead V1						
P	327		307	343	743	228
Q						
R	5435	513	1000	678	277	4730
S		2100	2610	4870	13800	5610
T	927	2150				1560
Lead V6						
P	213	430	1100	407	579	427
Q			360	490	1075	3080
R	4850	11850	2300	2060	31600	9450
S	6670		452			
T	1860	1470	2770	787		985

Table 6. Crosscorrelation functions corrected for time base difference and peak difference

Pulse	RVH	N1	N2	N3	LVH	Infarction
Lead V1						
P	327		307	343	782	228
Q						
R	5570	513	1000	697	277	4730
S		2120	2610	4870	13800	5610
T	980		2150			
Lead V6						
P	213	442	1100	407	585	432
Q			360	490	1082	3150
R	4880	11950	2300	2060	31800	9650
S	6850		452			
T	1860	1470	2790	787		985

CONCLUSIONS

In this study of techniques for automatic interpretation of the clinical electrocardiogram, the correlation techniques have been applied to the problem of pattern recognition, and have been shown to be of great value in the classification of the waveform into various cardiac states, both normal and abnormal. The greatest immediate use of these techniques to date has been in hypertrophy, a finding in agreement with other investigators (14). This was the primary purpose of this study.

Of equal importance, in implementation of this study, is the application of preliminary smoothing and the use of a logic of recognition to discern the location and nature of the waveform under interpretation. This program can be refined to any degree demanded by the requirements of the electrocardiographic classification.

It has been shown that crosscorrelation techniques with standards can be corrected to a certain extent, when the differences are small, in order to give realistic values to the correlation functions. Much the same information is available from the crosscorrelation computation as is available from the autocorrelation computation. However, the investigation conducted so far has not utilized the correlation techniques to extract all the information inherent therein.

A more complete catalogue of standard waveforms should be available, with ability to normalize on both a time and amplitude basis included. Further, some capability of using successively closer standards should be built into the technique. Either a complete adaptive system could be used,

or a logical set of catalogued values capable of normalization be furnished. Only when the closest possible fit between the pulse being checked and the standard is achieved can the full amount of information be gained, and the ultimate purpose of this project be achieved. That purpose is the utilization of more information from the electrocardiogram than is presently used.

It is considered that the techniques outlined herein constitute a good framework from which to build up the studies of the clinical electrocardiogram. The use of the correlation technique does not preclude use of the logic of recognition to implement the present program of amplitudes, utilizing the present diagnostic standards. Neither does it preclude the investigation of significance of the area as a diagnostic tool. These investigations require no major modifications.

One of the limitations on this investigation was the fact that the entire program could not be implemented on the computer in one pass, as the memory was not of sufficient size. In the near future, this will be corrected. In order to render this method economical to use in the hospital on a routine basis, further investigation should be made of the possibility of utilizing analogue, or digitally-controlled filters, in order to perform the correlation by actual filters, instead of simulating the matching filter technique by computation of the correlation functions.

ACKNOWLEDGEMENTS

The author wishes to express his appreciation to the many people who furnished suggestions during the project. Of particular help, however, on the Electrical Engineering Staff, were Dr. V. W. Bolie, who suggested the general project, and Dr. R. G. Brown, who served as major professor on the dissertation, and whose suggestions during the project and guidance in preparation of the dissertation were invaluable. The project supervisor, Dr. J. E. Gustafson, of Iowa Methodist Hospital, furnished the computer, the medical supervision and guidance, and the financial support for the entire project. Much of the detailed programming and computer operation was provided by Jerry Balm, my colleague on the project.

SELECTED REFERENCES

1. Bendat, J. E. Interpretation and application of statistical analysis for random physical phenomena. Institute of Radio Engineers Transactions on Bio-Medical Electronics BME-9: 31-43. 1960.

2. Burch, G. E. and Winsor, T. A primer of electrocardiography 4th ed. Philadelphia, Pa., Lea and Febiger. 1960.

3. _____, Abildskov, J. A. and Cronvich, J. A. Spatial vector-cardiography. Philadelphia, Pa., Lea and Febiger. 1960.

4. Caceres, C. A. How can the waveforms of clinical electrocardiogram be measured automatically by a computer? Institute of Radio Engineers Transactions on Bio-Medical Electronics BME-9: 21-22. 1962.

5. Davenport, W. B. and Root, W. L. An introduction to the theory of random signals and noise, New York, N. Y., McGraw-Hill Book Co., Inc. 1958.

6. Feller, W. An introduction to probability theory and its applications 2nd ed. Vol. 1 New York, N. Y., John Wiley and Sons, Inc. 1960.

7. Geselowitz, D. B. Multipole representation for an equivalent cardiac generator. Institute of Radio Engineers Proceedings. 48: 75-79. 1960.

8. Goldman, S. Information theory. New York, N. Y., Prentice Hall, Inc. 1955.

9. Hawkins, J. K. Self-organizing systems - a review and commentary. Institute of Radio Engineers Proceedings. 49: 31-48. 1961.

10. Horwitz, L. P. and Shelton, G. L. Pattern recognition using auto-correlation. Institute of Radio Engineers Proceedings. 49: 175-185. 1961.

11. Martinek, J., Yeh, G. C. K. and Carmine, R. A new system for electro-cardiographic recording, analysis, and diagnosis. Institute of Radio Engineers Transactions on Medical Electronics ME-6: 112-116. 1959.

12. Minsky, M. Steps toward artificial intelligence. Institute of Radio Engineers Proceedings. 49: 8-30. 1961.

13. Papoulis, A. The Fourier integral and its applications. New York, N. Y., McGraw-Hill Book Co., Inc. 1962.

14. Stark, L., Okajima, M. and Whipple, G. H. Computer pattern recognition techniques: electrocardiographic diagnosis. ACM Communications 5: 527-532. 1962.

15. Steinberg, C. A., Abraham, S. and Caceres, C. A. Pattern recognition in the clinical electrocardiogram. Institute of Radio Engineers Transactions on Bio-Medical Electronics BME-9: 23-30. 1962.

16. Taback, L., Mardon, E., Mason, H. L. and Pipberger, H. V. Digital recording of electrocardiographic data for analysis by a digital computer. Institute of Radio Engineers Transactions on Medical Electronics ME-6: 167-171. 1959.

17. Truxal, J. G. Automatic feedback control system synthesis. New York, N. Y., McGraw-Hill Book Co., Inc. 1955.

18. Turin, G. L. An introduction to matched filters. Institute of Radio Engineers Transactions on Information Theory IT-6: 311-329. 1960.

19. Young, T. Y. and Huggins, W. H. The intrinsic component theory of electrocardiography. Institute of Radio Engineers Transactions on Bio-Medical Electronics BME-9: 214-221. 1962.

20. Zeigler, R. F. Electrocardiographic studies in normal infants and children. Springfield, Ill., Charles C. Thomas. 1951.

APPENDIX A

Manual Diagnosis Flow Charts

The adult standards and flow charts for mechanization of the manual diagnostic criteria for the adult electrocardiogram are shown in the following pages.

General Criteria, Adult Electrocardiograms

Even though the diagnosis performed herein is to be on the childrens' electrocardiograms, the adult version has been shown here since the flow charts are practically identical in each case, and the adult standards contain the flow charts for myocardial infarction, which is not present in children.

Table 7. Adult diagnostic standards

Heart Rate

Bradycardia - - - - - - - - - - - - less than 60

Minimal Tachycardia - - - - - - - - 100 - 120

Moderate Tachycardia - - - - - - - 121 - 160

Marked Tachycardia - - - - - - - - 161 - 210

Probable paroxysmal over 210

P-R Interval

Rate	Abnormally short	Borderline	Minimal Delay	Prolonged Interval
<80	< 0.10	0.20	0.21 - 0.22	> 0.22
80-110	< 0.10	0.20	0.20 - 0.21	> 0.21
>110	< 0.10	0.20	0.19 - 0.20	> 0.20

Table 7. Adult diagnostic standards (continued)

Axis

The axis computation is shown in the accompanying flow chart.

Hypertrophy

The criteria for right and left ventricular hypertrophy follow.

Q-T Interval

Q-T corrected = Q-T/ R-R	< 0.44, check normal interval
	0.44 - 0.48 check borderline interval
	> 0.48, check prolonged interval

T-Waves

Omit in the presence of hypertrophy 2, 3, or 4, myocardial infarction 1-4 or bundle branch block.

Borderline	Abnormal
T1 = 0.5 or	T1 = 0.5 or
TaVL (if RaVL is > 2SaVL) 0.5 to -0.5	TaVL (if RaVL > 2SaVL and > 8) > -0.5
TaVF, TV4, and TV6 same as for TaVL	TaVF, TV4, and TV6 same as for TaVL

Infarction

The criteria for posterior and anterior myocardial infarction follow.

Wolf-Parkinson-White

P-R interval < 0.09 and QRS over 0.10

Table 7. Adult diagnostic standards (continued)

Block

The criteria for right and left bundle branch block follow.

Detailed Criteria, Adult Electrocardiograms

The detailed criteria for several cardiac conditions follow. This collection of criteria was not gained from a single source, but rather was compiled by Dr. Gustafson from many sources, and modified as program requirements dictated changes and additions to the criteria. However, many of the criteria can be checked in Burch (2), and for the childrens' electrocardiograms by Ziegler (20).

Block

LBBB	RBBB
QRS > 0.11 and	QRS > 0.11 and
Intrinsicoid V6 > 0.08 and	Intrinsicoid V1 > 0.04
No Q in V6 and	
TV6 < 0	

If RBBB present, RVH not possible

If LBBB present, LVH not possible

Axis

If mean electrical axis falls in the first quadrant, check left.

If mean electrical axis falls in second quadrant, check indeterminate.

If mean electrical axis falls in third quadrant, check right.

If mean electrical axis falls in fourth quadrant, check normal.

The computation of the axis accompanies the flow chart for the program.

Table 7. Adult diagnostic standards (continued)

Hypertrophy

Left Ventricular Hypertrophy (LVH)

A. (RV6 - 10)4

B. (SV1 - 8)3

C. (Intrinsicoid V6 - 0.04)(100)8

D. (0.1RV6-TV6)0.5(RV6) TV6 no less than -2(TV6 less than -2, make it -2).

E. (RaVL - 10)3

F. (RaVF - 20)3

G. (0.1RaVF - TaVF)0.2RaVF Only if RaVF and RV6 are over 10.

Left ventricular hypertrophy degree is indicated by the sum of the above.

Right Ventricular Hypertrophy (RVH)

H. (RV1 - 6)4

I. (SV6 - 7)3

J. (Intrinsicoid V1 - 0.04)100(8)

K. (RaVR - 5)3

L. [RV1/(RV1 + SV1) - 0.30]10(RV1 - 3)

M. (0.1RV1 - TV1)0.3RV1 If RV1/(RV1 - SV1) greater than 0.7 and RV1 greater than 10.

Right ventricular hypertrophy is indicated in degree by the sum of the above.

Table 7. Adult diagnostic standards (continued)

Degree of Hypertrophy

Degree	0	1	2	3	4
LVH Total	30-49	50-70	71-90	91-110	Over 110
RVH Total	5-10	11-40	41-70	71-90	Over 90

Anterior Infarction

Cannot be excluded

RV2 < RV1, or

RV4 < RV2, or

Q1 > 0.15R1, or

QaVL > 0.15RaVL (RaVL > 4), or

TV4 or TV6 < -1.5

Probable

Q > 2 in V1, or V2, or

Q1, aVL, V4, or V6 > 0.25 succeeding R and T same lead less than 0.5

Typical

Q1, aVL, V1, V2, V4, or V6 > 0.25 succeeding R and T segment $\geq$ 3

Old

R = 0 in V1, V2, V4, or V6, or

Q > 0.25RaVL, V4, V6, and ST segment 0 and T wave > 0

Posterior Infarction

Cannot be excluded

Q2, Q3, or QaVF over 0.15 - 0.25 R same lead, and

T2, or TaVF less than -1.0

Table 7. Adult diagnostic standards (continued)

Probable

Q2, Q3, or QaVF over 0.25 succeeding R and ST segment same lead elevated 1mm (if R same lead less than 5, call "cannot be excluded")

Typical

Q2, Q3, or QaVF over 0.25R2, R3, RaVF, and T wave same lead less than 0 in T2, or T3, or TaVF

Old

Q2, Q3, or QaVF over 0.25 succeeding R, and ST segment 0, and T wave > 0

Figure 27. General logic flow

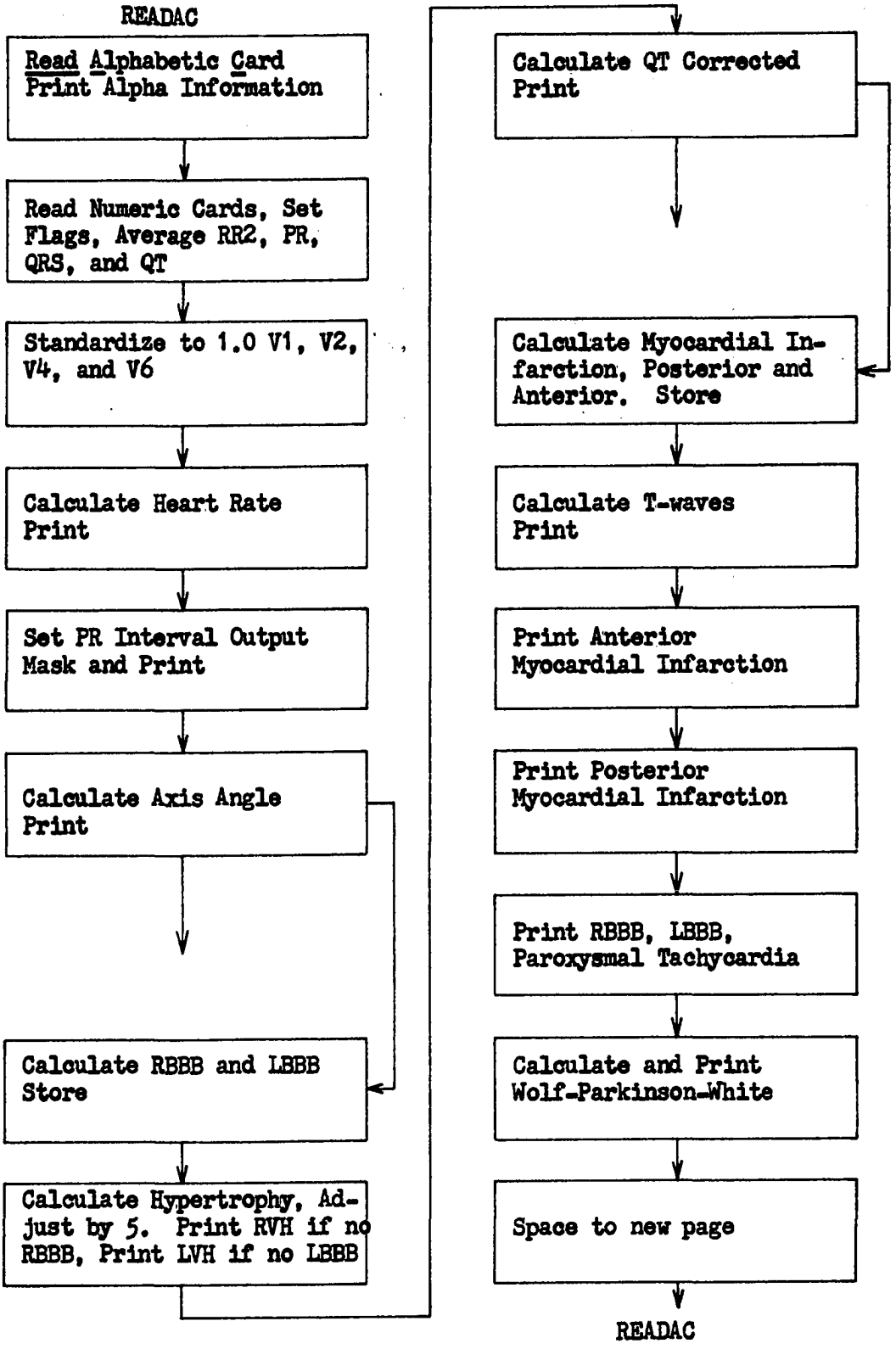
READAC
Read Alphabetic Card Print Alpha Information
Read Numeric Cards, Set Flags, Average RR2, PR, QRS, and QT
Standardize to 1.0 V1, V2, V4, and V6
Calculate Heart Rate Print
Set PR Interval Output Mask and Print
Calculate Axis Angle Print
Calculate RBBB and LBBB Store
Calculate Hypertrophy, Adjust by 5. Print RVH if no RBBB, Print LVH if no LBBB
Calculate QT Corrected Print
Calculate Myocardial Infarction, Posterior and Anterior. Store
Calculate T-waves Print
Print Anterior Myocardial Infarction
Print Posterior Myocardial Infarction
Print RBBB, LBBB, Paroxysmal Tachycardia
Calculate and Print Wolf-Parkinson-White
Space to new page
READAC

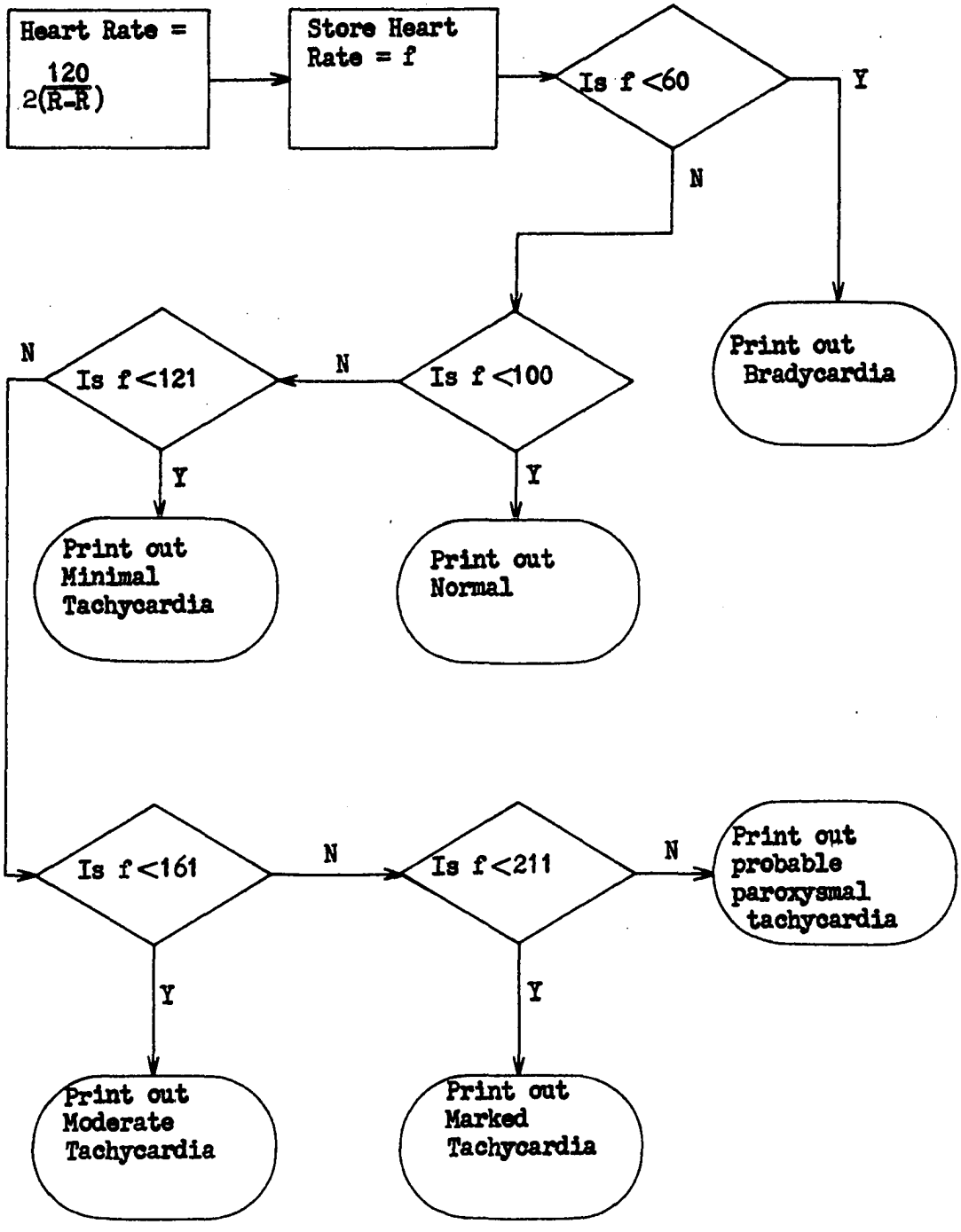

Figure 28. Heart rate

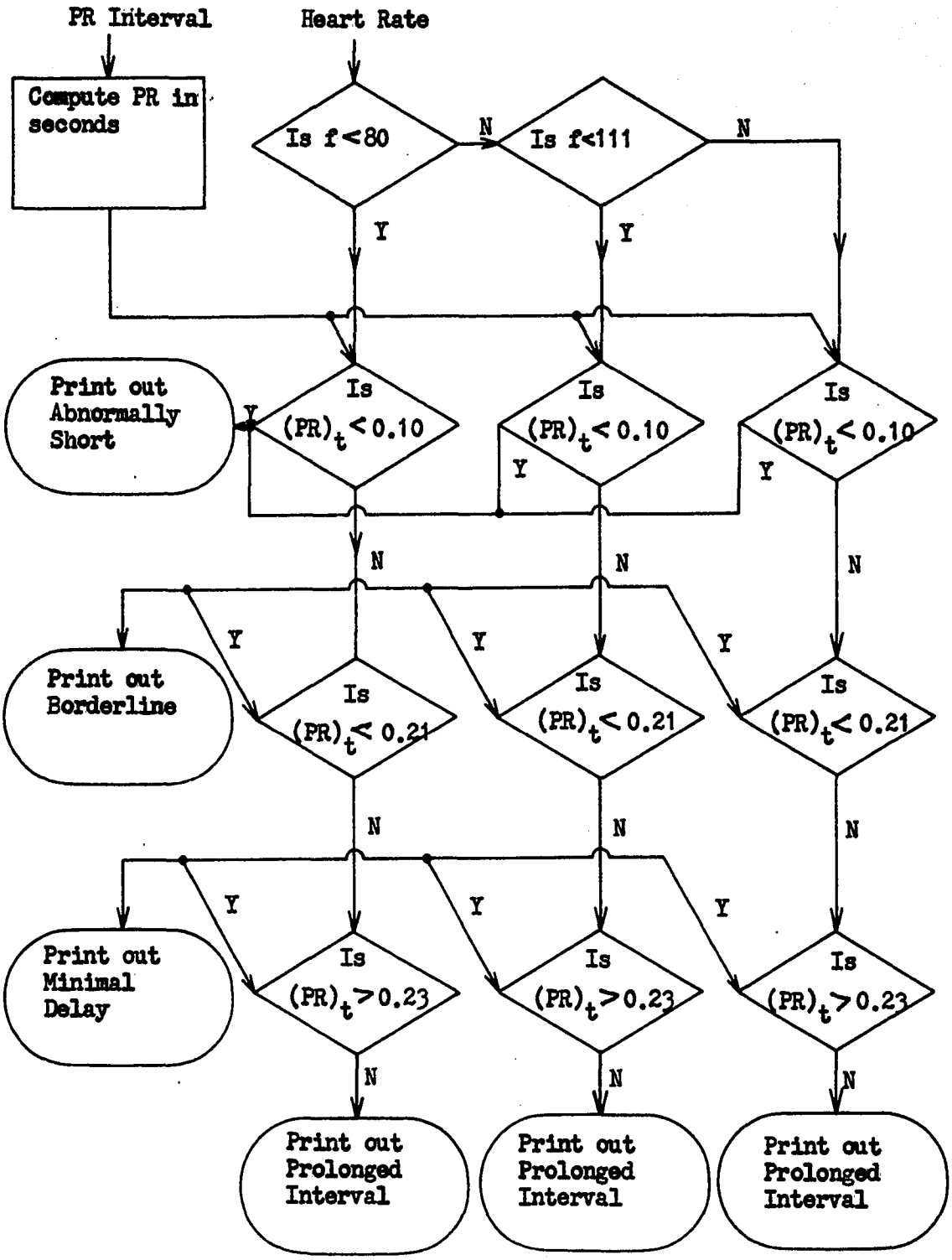

Figure 29. PR interval

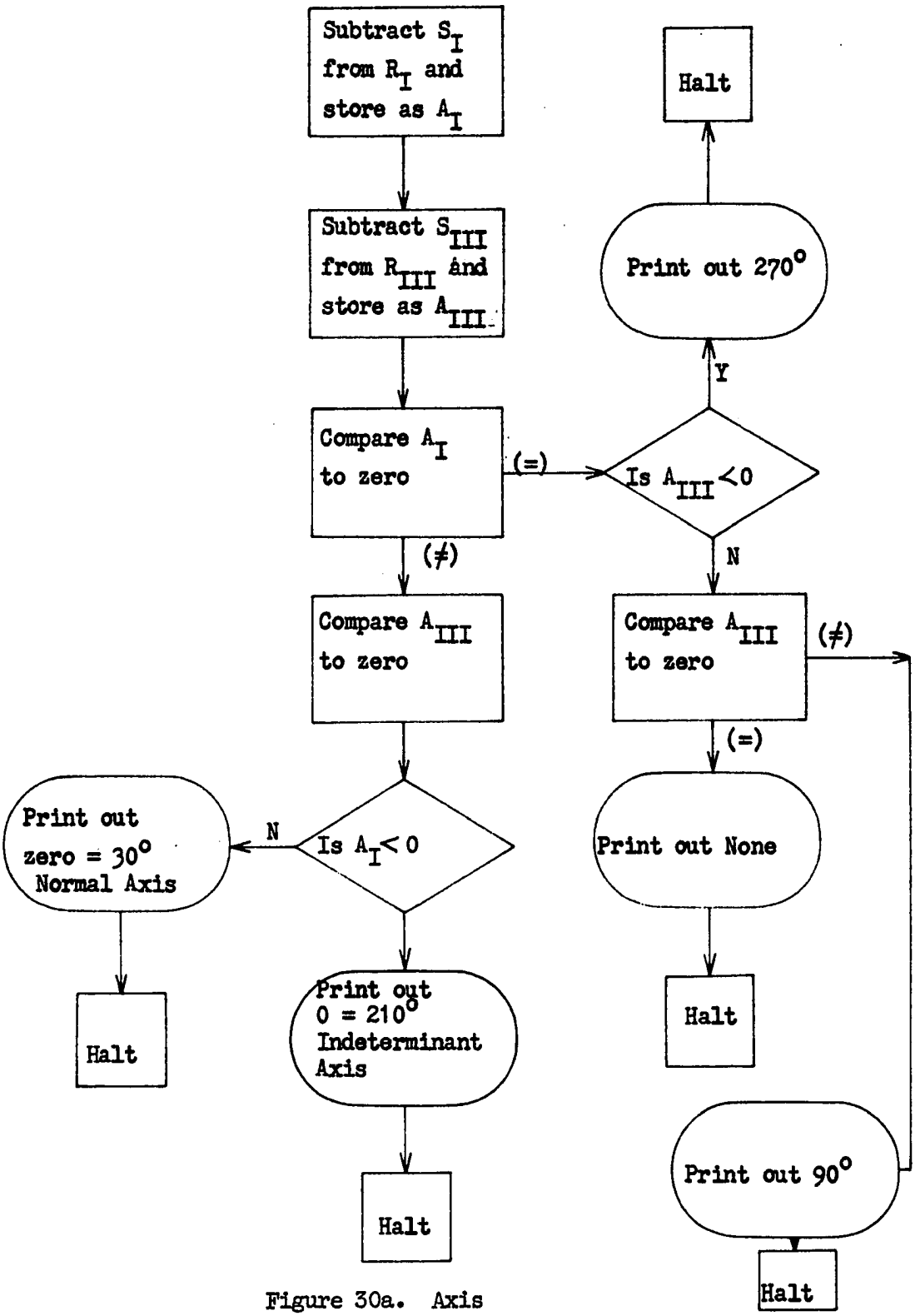

Figure 30a. Axis

From previous page

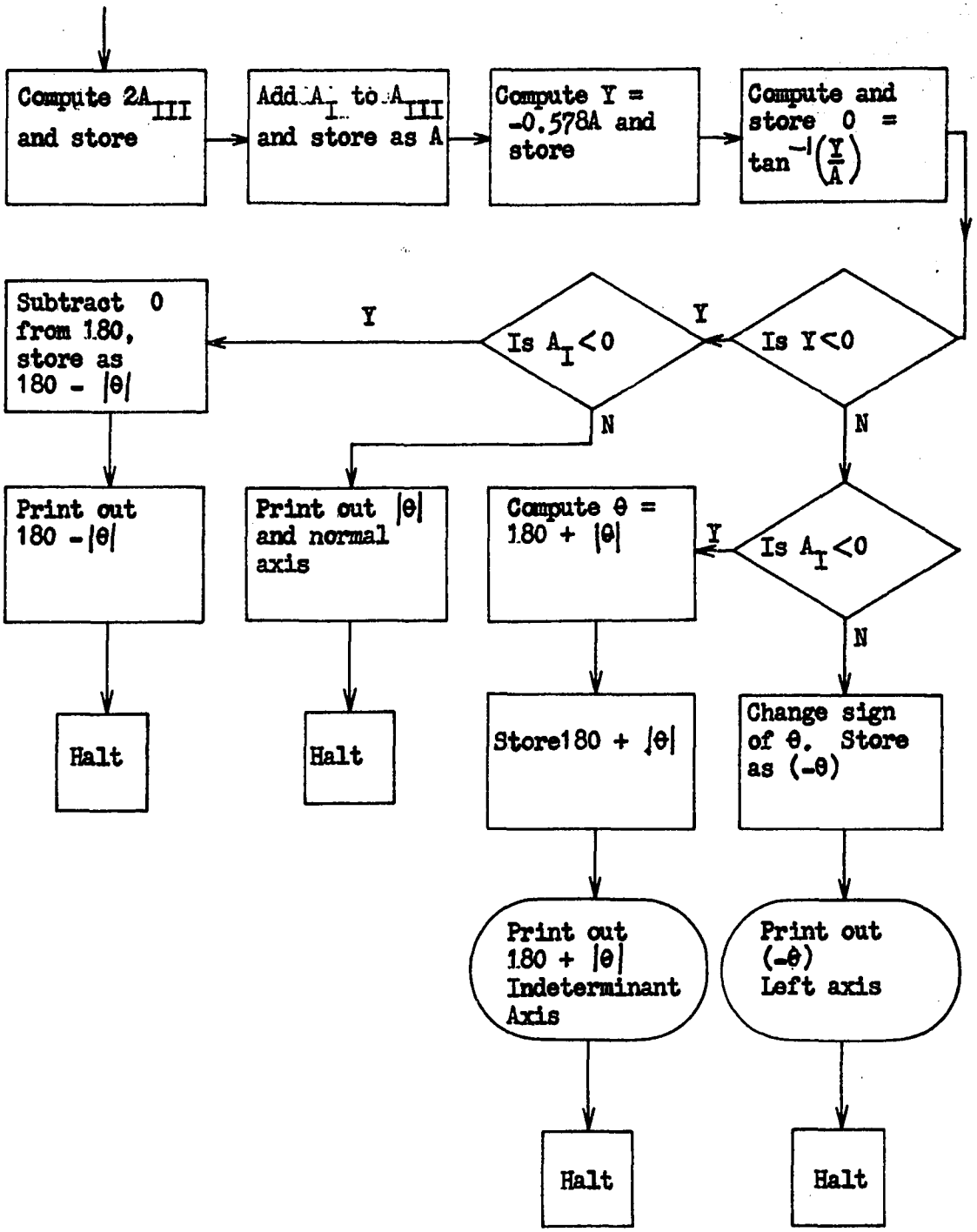

Figure 30b. Axis

Figure 31. Bundle branch block

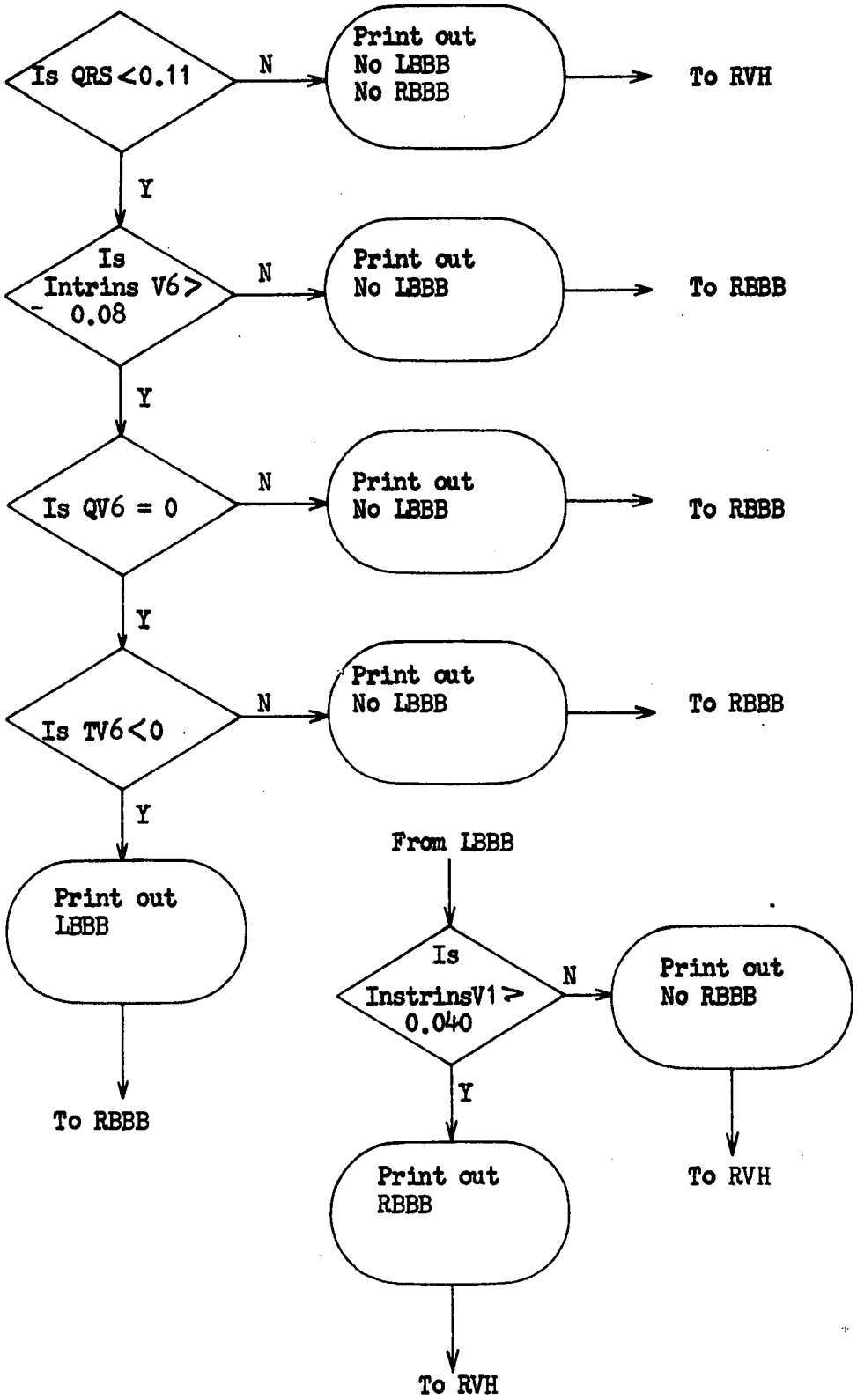
Is QRS<0.11
N
Print out
No LBBB
No RBBB
To RVH
Y
Is
Intrins V6>
0.08
N
Print out
No LBBB
To RBBB
Y
Is QV6 = 0
N
Print out
No LBBB
To RBBB
Y
Is TV6<0
N
Print out
No LBBB
To RBBB
Y
Print out
LBBB
To RBBB
From LBBB
Is
InstrinsV1>
0.040
N
Print out
No RBBB
To RVH
Y
Print out
RBBB
To RVH

Figure 32. Hypertrophy

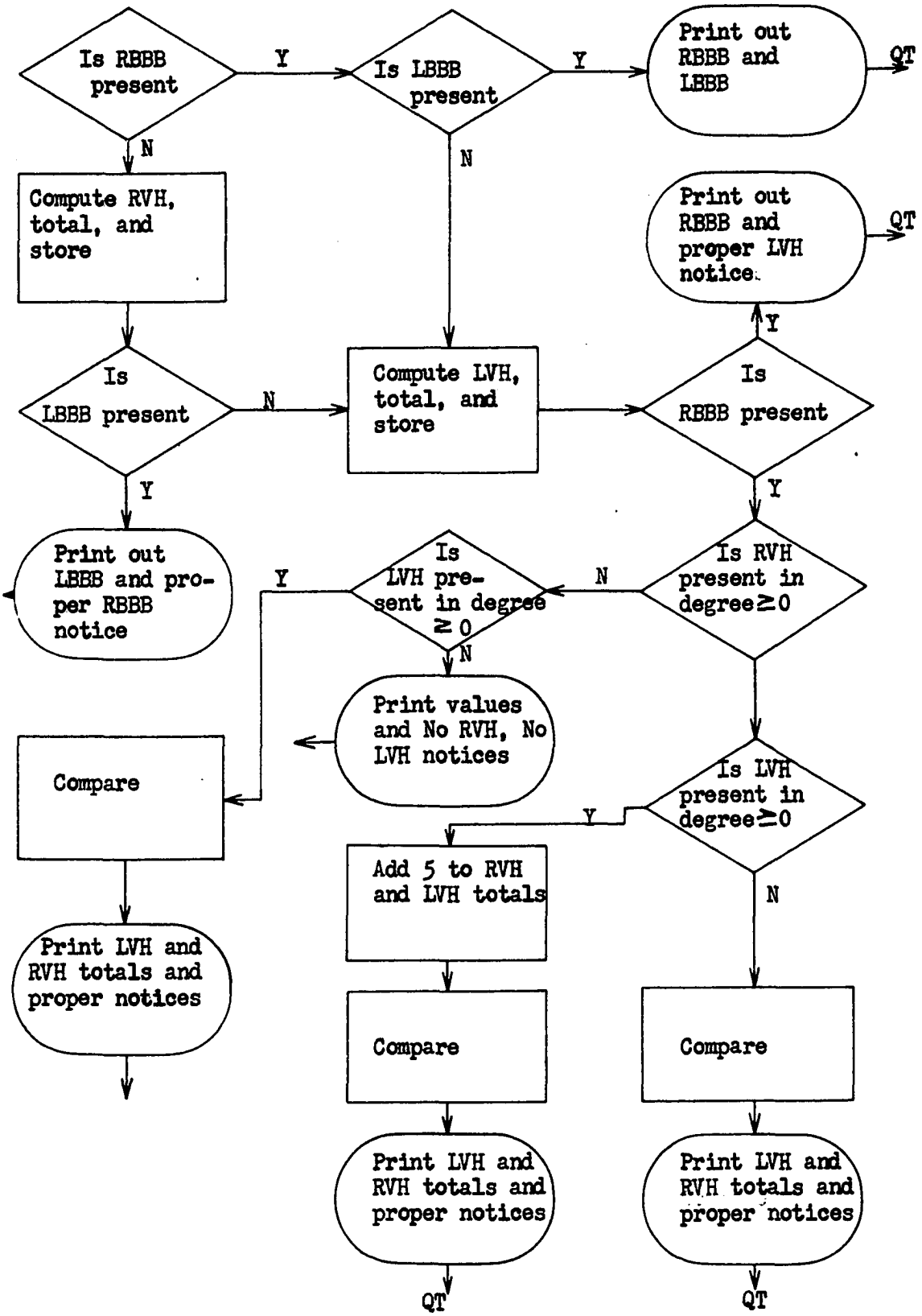
Is RBBB present
Y
Is LBBB present
Y
Print out RBBB and LBBB
QT
N
N
Compute RVH, total, and store
Print out RBBB and proper LVH notice
QT
Y
Is LBBB present
N
Compute LVH, total, and store
Is RBBB present
Y
Y
Print out LBBB and proper RBBB notice
Y
Is LVH present in degree ≥ 0
N
Is RVH present in degree ≥ 0
N
Print values and No RVH, No LVH notices
Compare
Is LVH present in degree ≥ 0
Y
Add 5 to RVH and LVH totals
N
Print LVH and RVH totals and proper notices
Compare
Compare
Print LVH and RVH totals and proper notices
Print LVH and RVH totals and proper notices
QT
QT

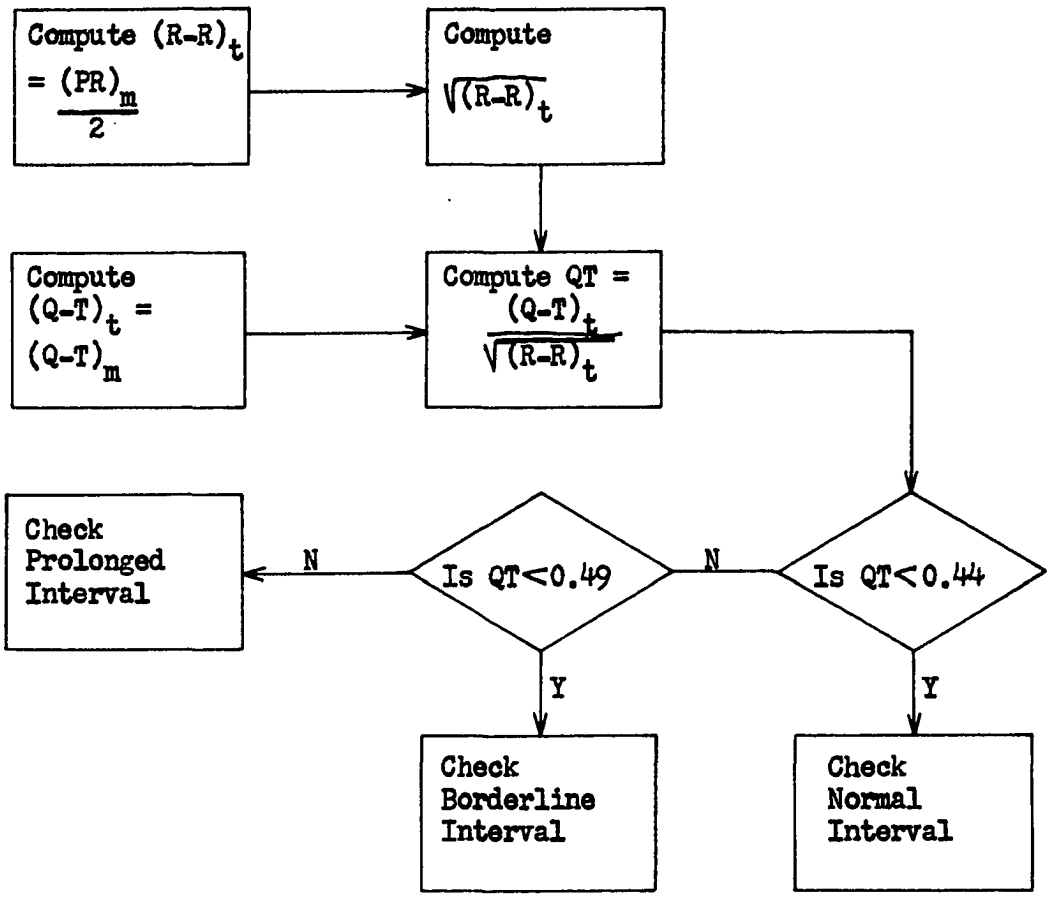

Figure 33. Q-T interval

Figure 34. Posterior myocardial infarction

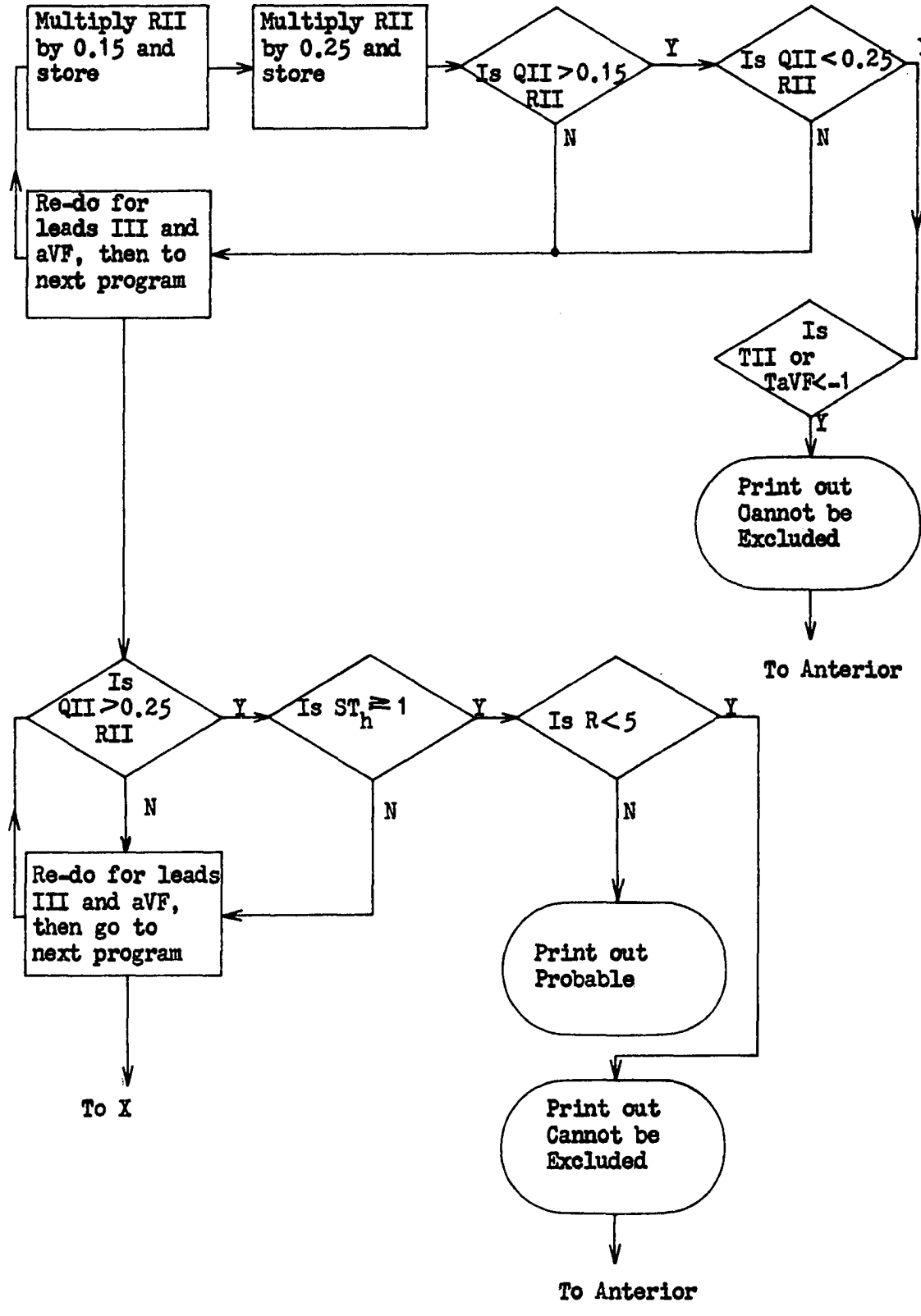
Multiply RII by 0.15 and store
Multiply RII by 0.25 and store
Is QII > 0.15 RII
Y
Is QII < 0.25 RII
Y
N
N
Re-do for leads III and aVF, then to next program
Is TII or TaVF < -1
Y
Print out Cannot be Excluded
To Anterior
Is QII > 0.25 RII
Y
Is $ST_h \geq 1$
Y
Is R < 5
Y
N
N
N
Re-do for leads III and aVF, then go to next program
Print out Probable
To X
Print out Cannot be Excluded
To Anterior

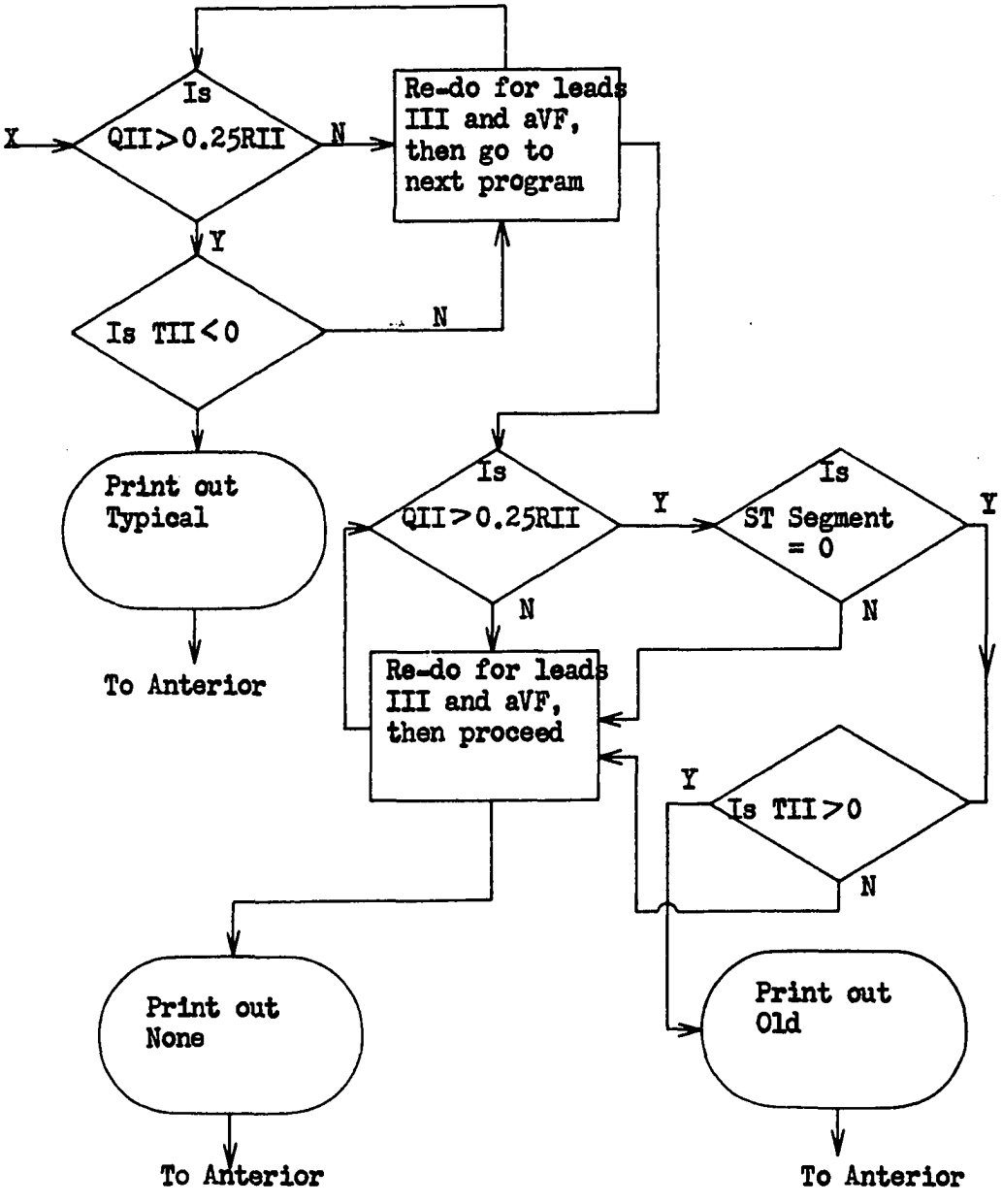

Figure 34. Posterior myocardial infarction (continued)

Figure 35a. Anterior myocardial infarction

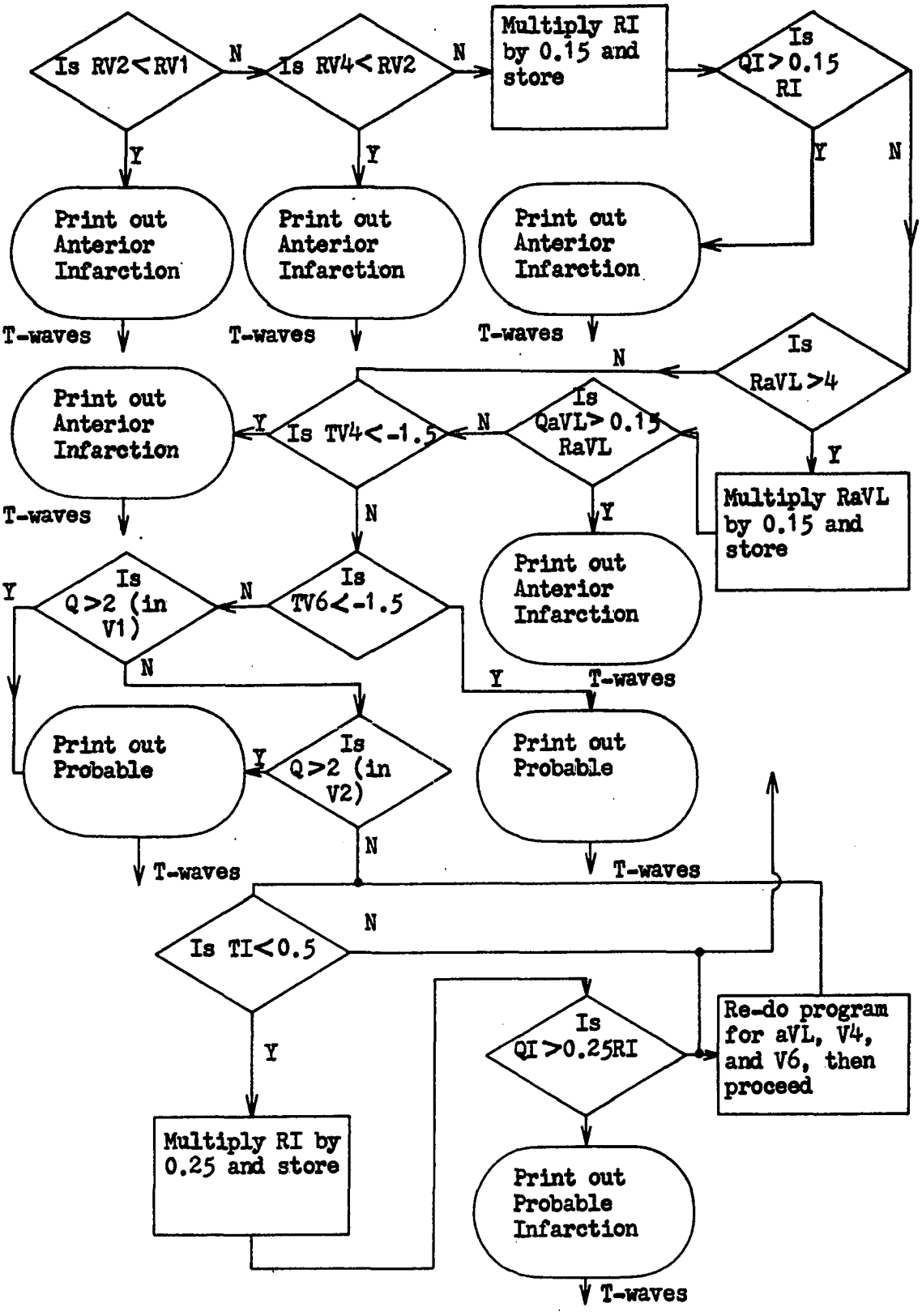
Is RV2<RV1
N
Is RV4<RV2
N
Multiply RI by 0.15 and store
Is QI>0.15 RI
Y
N
Y
Y
Print out Anterior Infarction
Print out Anterior Infarction
Print out Anterior Infarction
T-waves
T-waves
T-waves
Is RaVL>4
N
Y
Print out Anterior Infarction
Y
Is TV4<-1.5
N
Is QaVL>0.15 RaVL
Multiply RaVL by 0.15 and store
T-waves
N
Y
Print out Anterior Infarction
Y
Is Q>2 (in V1)
N
Is TV6<-1.5
Y
T-waves
N
Print out Probable
Y
Is Q>2 (in V2)
Print out Probable
N
T-waves
T-waves
N
Is TI<0.5
Y
Is QI>0.25RI
Re-do program for aVL, V4, and V6, then proceed
Multiply RI by 0.25 and store
Print out Probable Infarction
T-waves

Figure 35b. Anterior myocardial infarction

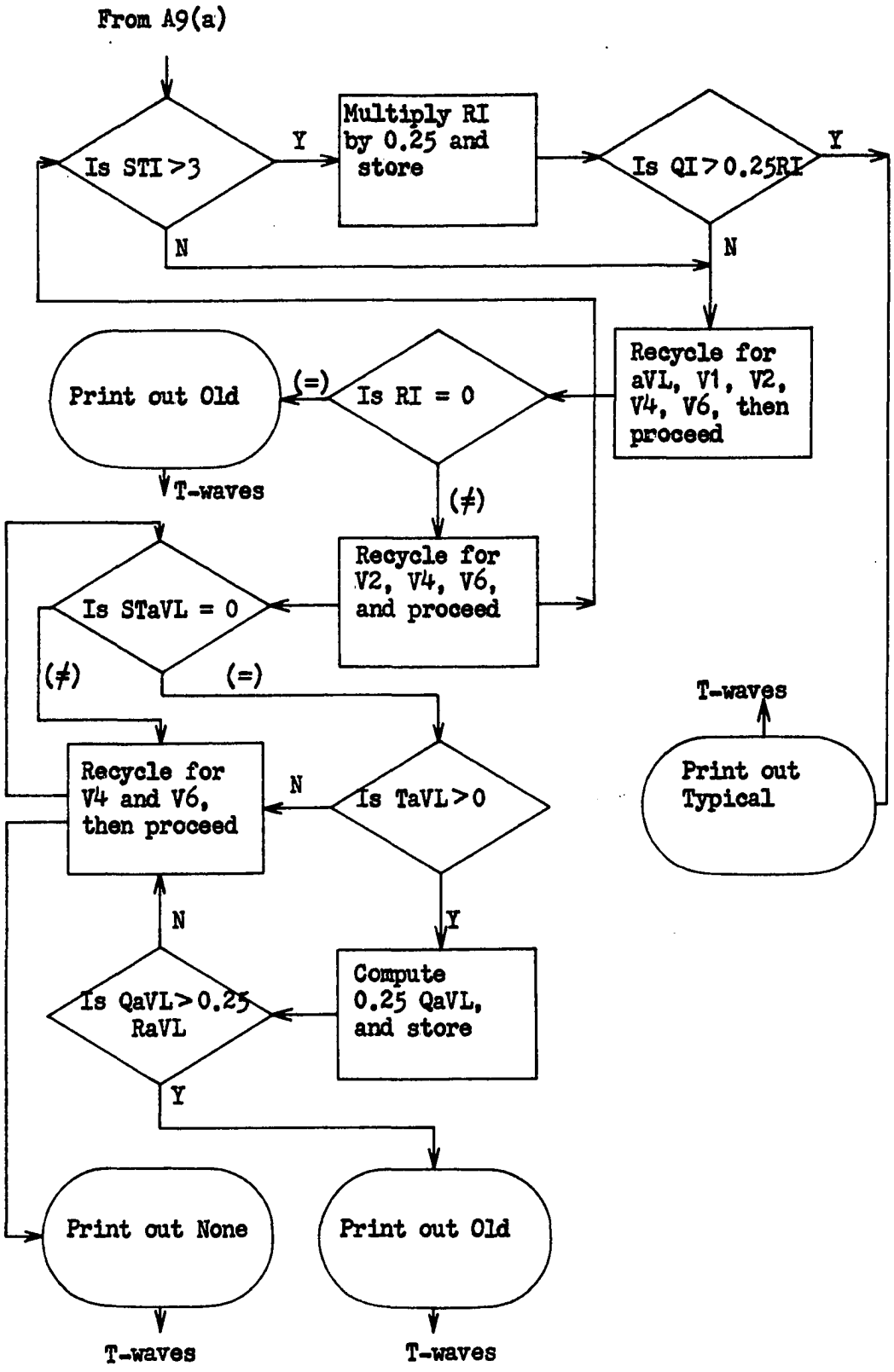
From A9(a)
Is STI > 3
Y
Multiply RI by 0.25 and store
Is QI > 0.25RI
Y
N
N
Recycle for aVL, V1, V2, V4, V6, then proceed
Print out Old
(=)
Is RI = 0
T-waves
(≠)
Recycle for V2, V4, V6, and proceed
Is STaVL = 0
(≠)
(=)
T-waves
Print out Typical
Recycle for V4 and V6, then proceed
N
Is TaVL > 0
Y
N
Compute 0.25 QaVL, and store
Is QaVL > 0.25 RaVL
Y
Print out None
Print out Old
T-waves
T-waves

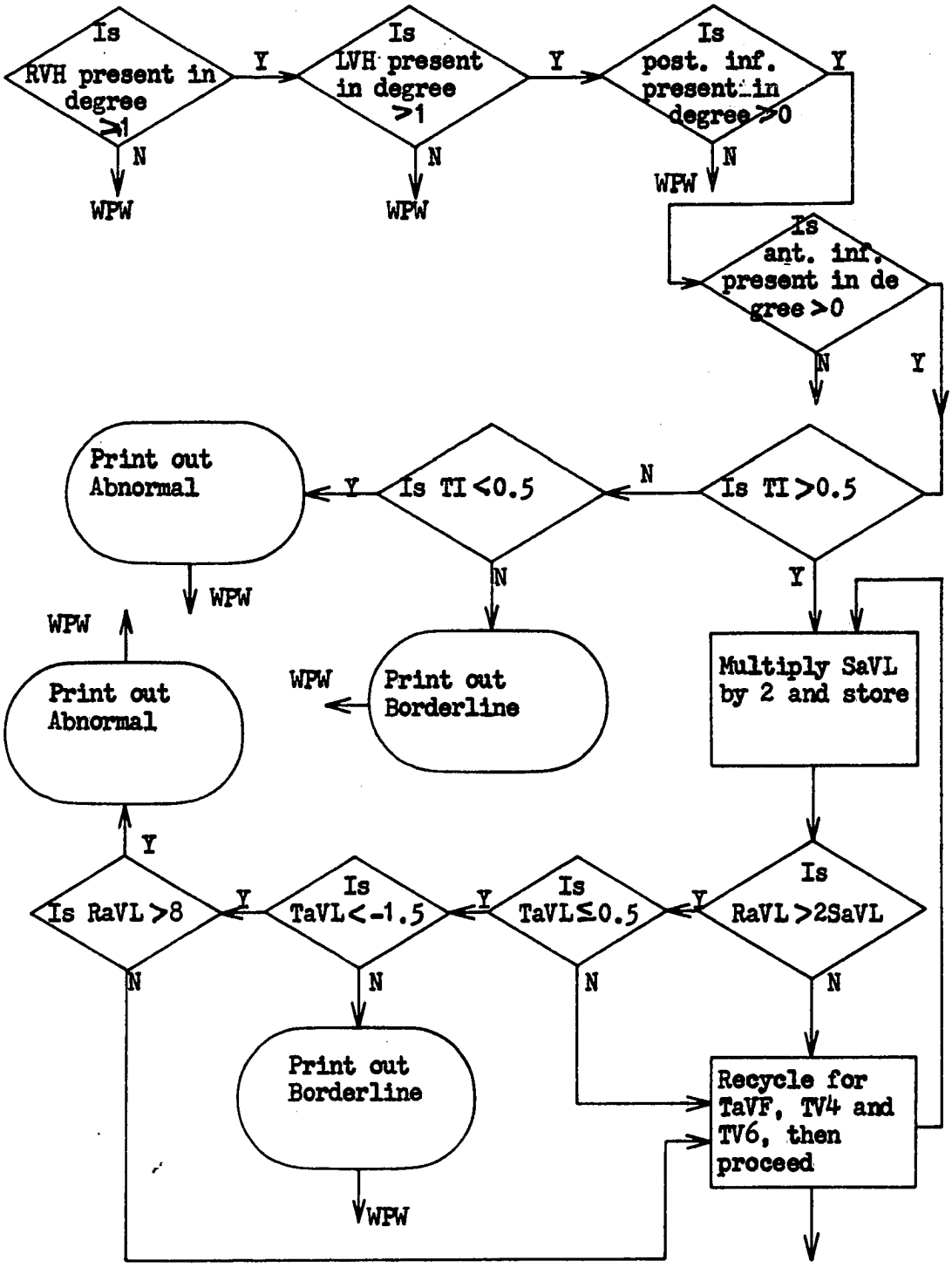

Figure 36a. T-waves

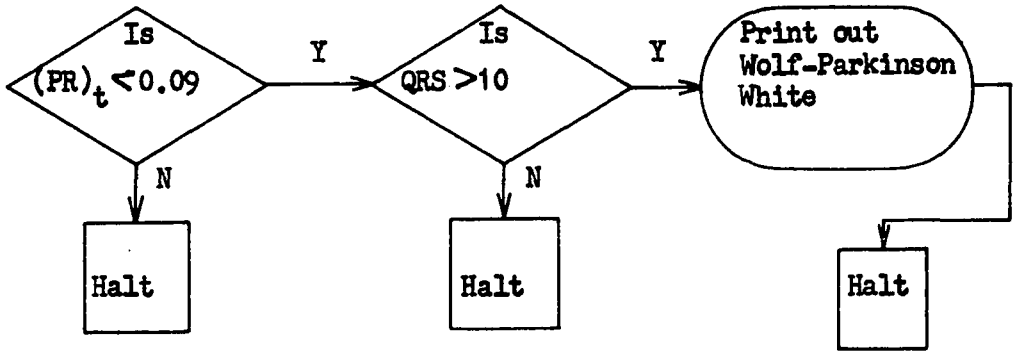

Figure 36b. Wolf-Parkinson-White

APPENDIX B

Determination of Sampling Frequency

In order to determine the sampling frequency of the proposed method, we shall investigate the frequency spectra of the pulses comprising the QRS complex of the electrocardiogram waveform. Since these are to be approximated by traingles, let us investigate the frequency spectrum of such a triangular pulse. The Fourier integral of a given pulse is

$$F(\omega) = \int_{-\infty}^{\infty} f(t)e^{-j\omega t}\, dt$$

Where $F(\omega)$ is the Fourier integral, and $f(t)$ the time function of the pulse under consideration.

In order to simplify computation, and in anticipation of future requirements for pulses not describable in an analytical manner, use is made of an approximation outlined in Papoulis (13). In this case, no approximation is required, since a triangular shape is assumed for the pulses of the QRS complex. If a relatively smooth waveform is present, it can be approximated by a series of polynomial segments. First, consider only straight line segments. Given, a smooth, general pulse of the type shown in Fig. 37. If straight line approximations are used, the resulting approximation is $\phi(t)$, as shown in Fig. 37a. The first and second derivatives, $\phi'(t)$ and $\phi''(t)$ of $\phi(t)$ are shown in Fig. 37b and 37c. Therefore, $\phi''(t)$ can be characterized by the series of impulses, and

$$\phi''(t) = \sum_{N=1}^{N} ki\, \delta(t - t_i),$$

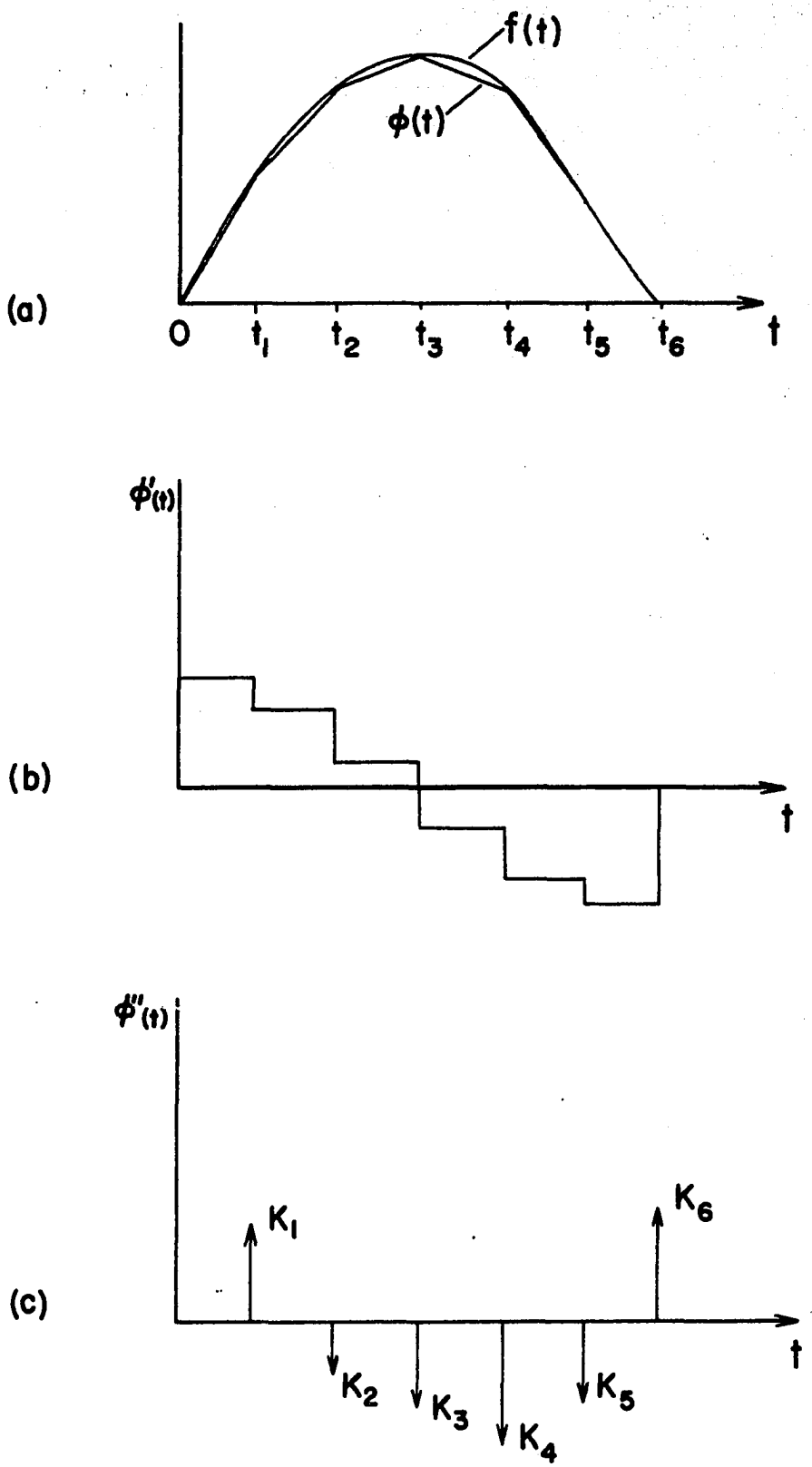

Figure 37. Polynomial approximation to Fourier integral

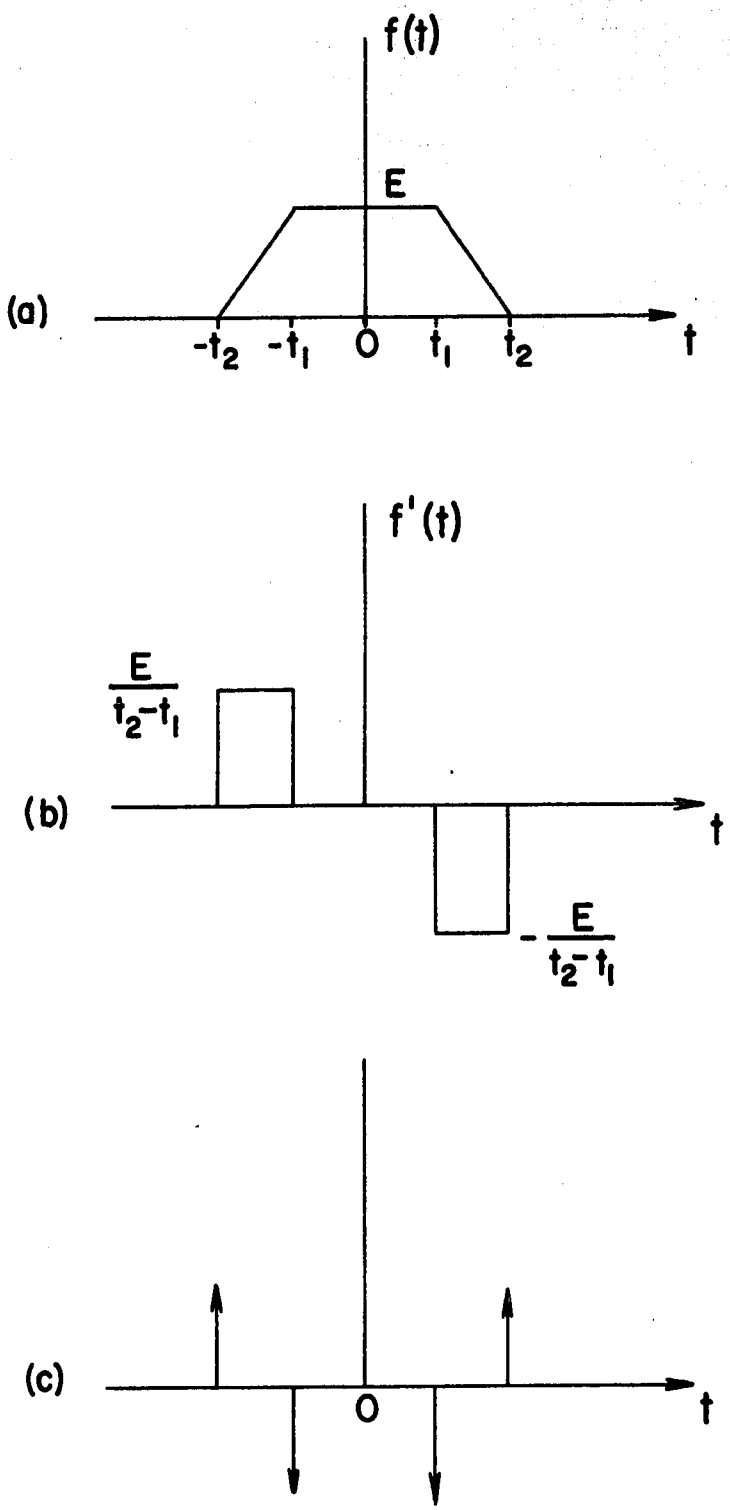

Figure 38. Trapezoidal computation

where k_i is the area of the ith pulse, and N is the total number of pulses.

Let us now consider the Fourier inversion integral

$$f(t) = \frac{1}{2\pi} \int_{-\infty}^{\infty} F(\omega) e^{j\omega t} \, d\omega$$

If we take the nth derivative of both sides of the above equation, we have

$$\frac{d^n f(t)}{dt^n} \longleftrightarrow (j\omega)^n F(\omega)$$

Now, with $\phi(\omega)$ the Fourier transform of $\phi(t)$, we conclude, with the use of the relationship $\delta(t - t_o) \quad e^{-j\omega t_o}$, (where the symbol $\longleftrightarrow$ indicates the Fourier transform), that

$$(j\omega)^2 \phi(\omega) = \sum_N k_i e^{-j\omega t_i}$$

therefore,

$$\phi(\omega) = -\frac{1}{\omega^2} \sum_N k_N e^{-j\omega t_i}$$

Thus, returning to the original time function, we can approximate the function in the following manner:

$$F(\omega) = -\frac{1}{\omega^2} \sum_N k_i e^{-j\omega t_i}$$

This is subject to the conditions that $\phi(\omega)$ does not contain singularities, namely $\delta(\omega)$ or $\delta'(\omega)$. In most applications, this will insure absence of singularities of $F(\omega)$.

Let us now apply this approximation to the trapezoidal pulses of the

type shown in Fig. 38, and allow t_2 to approach zero, which will yield the QRS complex triangular pulse. Since the trapezoid involves only straight lines, no approximation is involved. The process is carried out below, and shown in Fig. 38.

$$f''(t) = d''(t) = \frac{E}{t_2 - t_1}\left[\delta(t + t_2) - \delta(t - t_1) + \delta(t - t_2)\right]$$

$$\therefore F(\omega) = -\frac{E}{\omega^2(t_2 - t_1)}\left(e^{jt_2\omega} - e^{jt_1\omega} - e^{-jt_1\omega} + e^{-jt_2\omega}\right)$$

$$\lim_{t_1 \to 0} F(\omega) = -\frac{E}{\omega^2 t_2}\left[\frac{2(e^{jt_2\omega} + e^{-jt_2\omega})}{2} - 2\right]$$

$$= \frac{E}{\omega^2 t_2}(1 - \cos \omega t_2)$$

$$= \frac{4E}{\omega^2 t_2}\left[\frac{1 - \cos \omega t_2}{2}\right]$$

But, using the identify $\sin \frac{x}{2} = \pm \sqrt{\frac{1 - \cos 2x}{2}}$, we get

$$F(\omega) = \frac{4E}{\omega^2 t_2} \sin^2 \frac{\omega t_2}{2}$$

for the Fourier transform of the triangular pulse.

Now, this must be evaluated in order to determine the frequency spectrum of the pulse. This spectrum is shown in Fig. 39, for a pulse where $t_2 = 0.03$ seconds, and E has an amplitude of 10 units. These are the figures for the average values of the QRS complex R triangle. Then

$$F(\omega) = \frac{3333}{\omega^2} \sin^2 0.015\,\omega\ .$$

Figure 39. Frequency spectrum of Q-wave

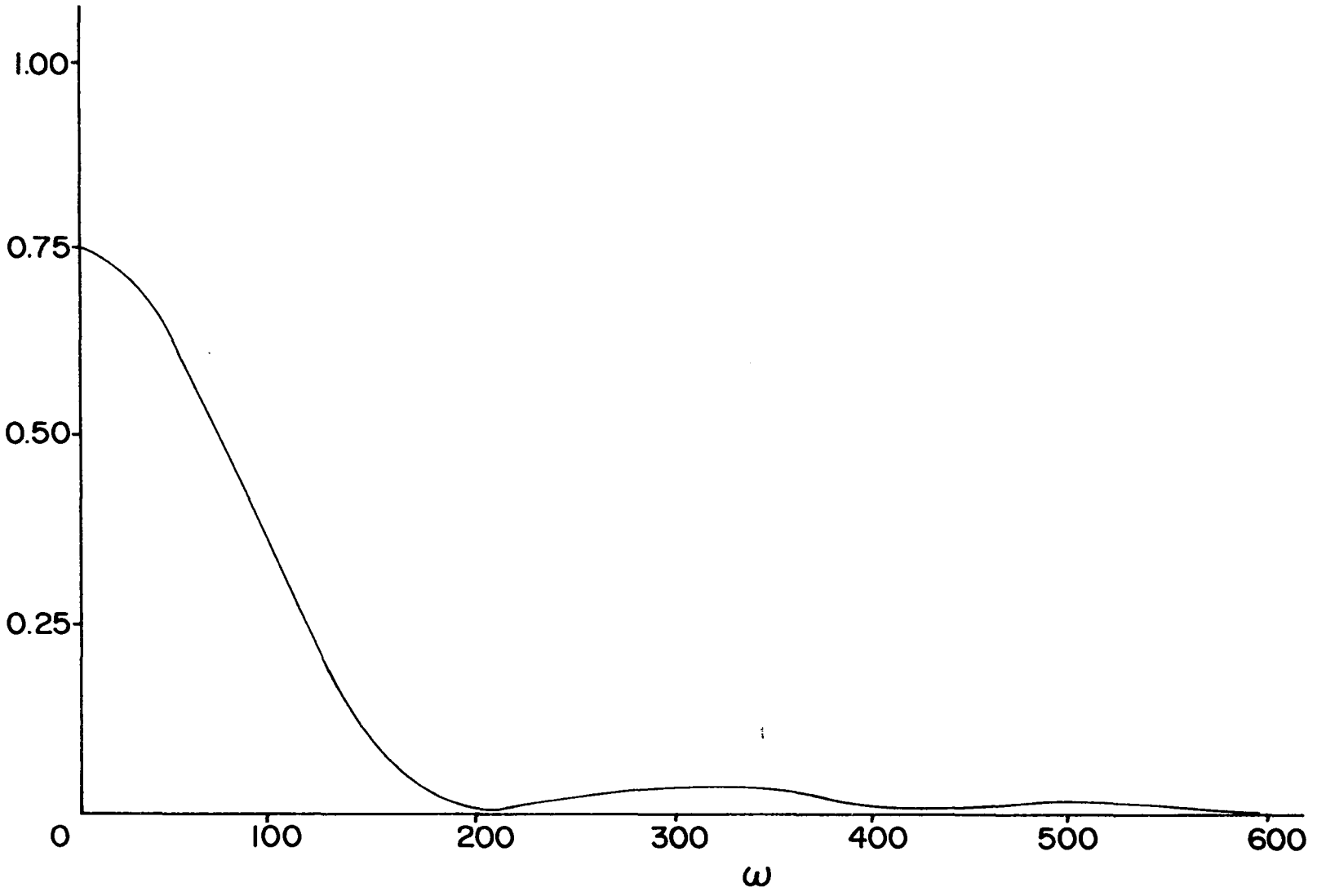
1.00
0.75
0.50
0.25
0
100
200
300
400
500
600
ω

Since the limit as $\omega \rightarrow 0$ is indeterminant, application of L'Hospital's rule yields the following limit at $\omega = 0$,

$$\lim_{\omega \rightarrow 0} \left\{F(\omega)\right\} = 0.750 \ .$$

As can be seen from the tabulation at the end of this section, $F(\omega)$ decreases rapidly with frequency. It will be noted that there is no arbitrary cutoff point in frequency beyond which all frequency components are zero, so an arbitrary cutoff point was selected, beyond which all components are considered negligible. The point selected was 628 radians per second, for a frequency of 100 samples per second. At an angular velocity of 723, the amplitude of the peak had decreased to 0.83% of the initial value. This represents a frequency of 115 samples per second. It was decided that practically no additional information would be lost if the maximum frequency was therefore decreased from 115 to 100 samples per second. Whereas the frequency selected above is that which will ultimately be used in this project, higher frequencies will be used during the study phases, so that the program in pattern recognition can be refined.

The sampling theorem in the time domain states: "If a function G(t) contains no frequencies higher than W cycles per second, it is completely determined by giving its ordinates at a series of points spaced 1/W seconds apart, the series extending throughout the time domain" [Goldman (8)]. Thus, a frequency of sampling of 2W is required, hence the data will be sampled 200 times per second. In the present investigation, sampling frequencies of 500, 250, and 125 samples per second will be utilized, in order to take advantage of the data furnished by the U. S. Public Health

Service.

ω	ω^2	$\frac{3333}{\omega^2}$	$\sin 0.015\ \omega$	$\sin^2 0.015\ \omega$	$F(\omega)$
0					0.750
1	1	333	0.015	2.25×10^{-4}	0.750
10	100	33.33	0.149	2.23×10^{-4}	0.742
20	400	8.33	0.295	8.7×10^{-2}	0.725
40	1600	2.08	0.565	0.319	0.663
60	3600	0.925	0.783	0.613	0.567
80	6400	0.52	0.932	0.868	0.452
100	10,000	0.333	0.997	0.995	0.331
120	14,400	0.231	0.973	0.946	0.219
140	19,600	0.170	0.866	0.750	0.128
160	25,600	0.130	0.749	0.560	0.0728
180	32,400	0.1026	0.423	0.180	0.0185
200	40,000	0.0833	0.139	0.0193	0.00161
250	62,500	0.0533	0.574	0.330'	0.0176
314	98,700	0.0337	-1.0	1.0	0.0337
418			0	0	0
523	275,000	0.0121	1.0	1.0	0.0121
732	536,000	0.0062	1.0	1.0	0.0062

APPENDIX C

Program to Compute Correlation Functions

It is desired to be able to crosscorrelate two waveforms with some degree of accuracy and flexibility. In this program, we shall try an initial rate of 500 samples per second. This is the highest rate at which the sampling will be made, and additional runs will be made at 250 and 125 samples per second, in order to determine the proper sampling frequency consistent with the accuracy requirements. After spectral analysis, 250 samples per second seem entirely adequate, but inspection of the electrocardiogram waveforms, indicates that some information might be lost in the QRS complex at this frequency.

The basic problem, then, is the correlation of two pulses shown in Fig. 40. Let it be assumes that $g_2(t) \neq g_1(t)$, but that the periods of T_p are equal in both waveforms. The manner in which the correlation is performed is to solve the following equation.

$$\phi_{12}(\tau) = \frac{1}{2T} \int_{-T}^{T} g_1(\tau) g_2(t + \tau)\, dt \ .$$

Thus, the crosscorrelation function $\phi_{12}(\tau)$ becomes a function of τ. Any reference can be taken, but one useful point is when the onset of the two waves coincides. Thus, if the waves are identical, and this was the point $\tau = 0$, the correlation function would have a value which would be maximum at $\tau = 0$. In the case outlined above, the total interval over which correlation would be performed would be from $-T_p$ to $+T_p$. Outside these

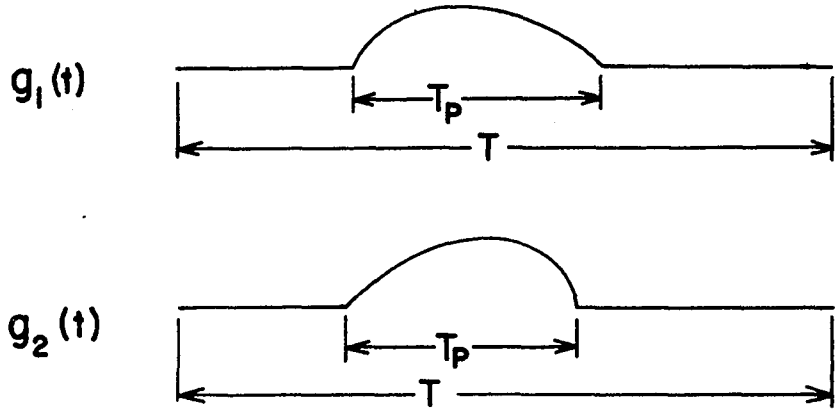

Figure 40. Two waveforms to be correlated

limits, the correlation function would be equal to zero, as the pulses are defined to be zero outside their own boundaries.

Now, in the discrete case under consideration, it is necessary to mechanize the following equation:

$$\phi_{12(j)} = \frac{1}{2N + 1} \sum_{K = -N}^{+N} x_K y_{K + j}$$

where x is the ordinate of one pulse, and y the ordinate of the other pulse. Now, if the sampling rate is W samples per second, and that period if T seconds, the total number of samples, since we are performing the same function as that above, is 2WT. Thus, N becomes WT, and the equation becomes

$$\phi_{12(j)} = \frac{1}{2WT_p + 1} \sum_{K = 1}^{K = WT_p} x_K y_{K + j}$$

Now, we want j to vary from $-WT_p$ to $+WT_p$. Thus, the expression for the corsscorrelation function will be

$$\phi_{12(j)} = \frac{1}{2WT + 1} \sum_{K = 1}^{K = WT_p} x_K y_{K + j} \qquad -WT_p \leq j \leq WT_p$$

For use in this initial program, the samples will be labeled consecutively upward from 1 at the onset of the pulse to WT_p at the end of the pulse.

The flow chart for mechanization of the correlation functions is shown in Fig. 41. The terminology is explained thereon. This particular routine correlates waves with up to 600 data points.

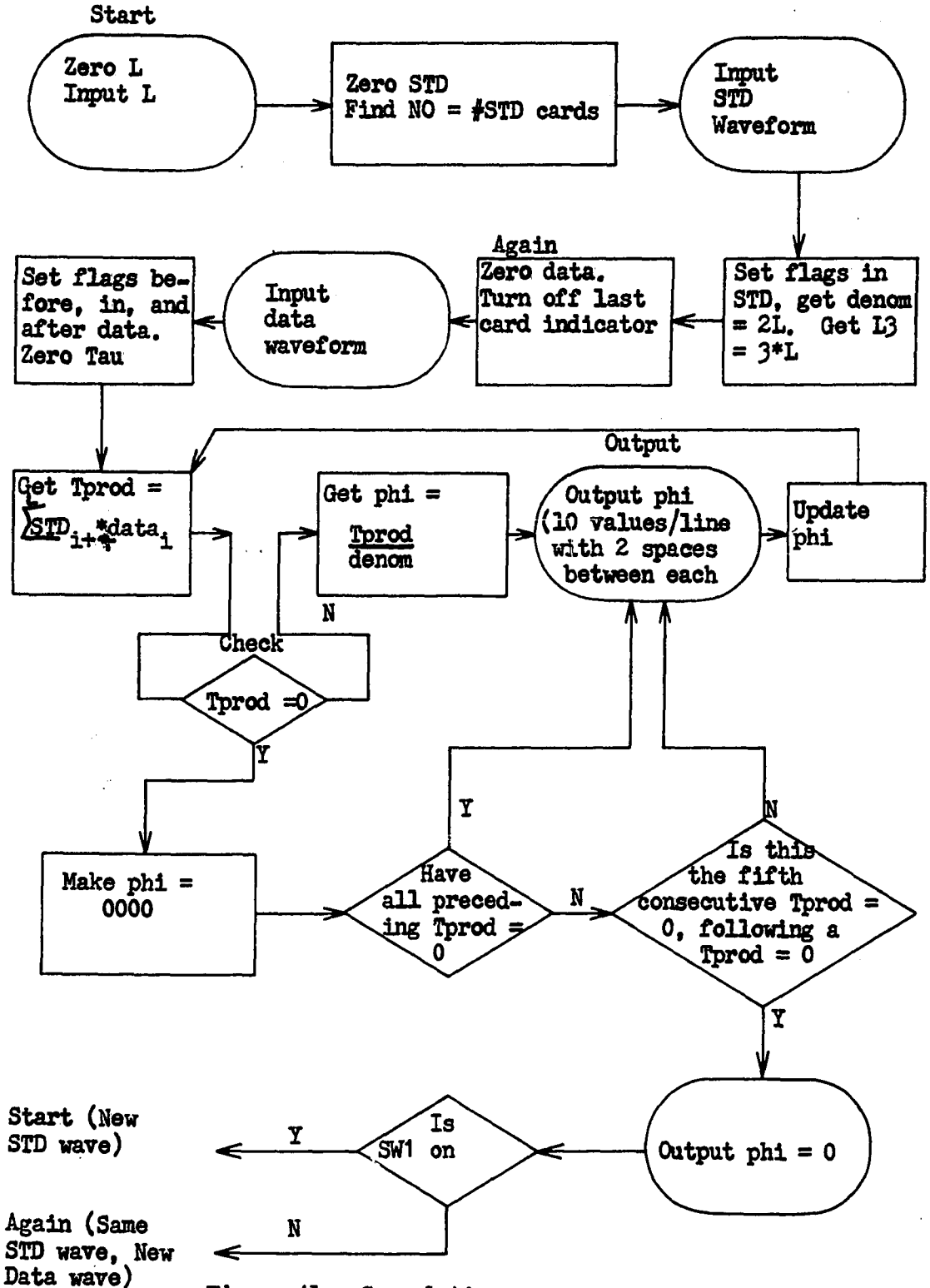

Figure 41. Correlation program

APPENDIX D

1. Recapitulations of average normal intervals and amplitudes with their normal ranges.

P-Wave (Adults)	Avg. amplitude in mm.	Range in mm.
Lead I	0.55	0 - 1.1
Lead II	1.25	0.3 - 2.5
Lead III	0.80	-1.0 - 2.0
	Avg. width in sec.	Range in sec.
Lead II	0.08	0.06 - 0.11
QRS Complex (Adults)	Avg. duration in sec.	Range in sec.
	0.08	0.06 - 0.10
Q-Wave	Avg. amplitude in mm.	Range in mm.
Lead I	0.36	0 - 2.0
Lead II	0.58	0 - 2.5
Lead III	0.61	0 - 3.0
R-Wave		
Lead I	5.5	1.5 - 12.0
Lead II	11.5	4.0 - 23.0
Lead III	7.0	1.0 - 20.0
Lead 4V		
Men	12.0	2.0 - 40.0
Women	7.5	1.2 - 35.0
S-Wave		
Lead I	1.5	0 - 6.0
Lead II	1.7	0 - 6.0
Lead III	1.5	0 - 6.5
Lead 4V	14.0	0 - 35.0

T-Wave		
Lead I	2.0	-0.5 - 5.5
Lead II	3.0	0 - 8.0
Lead III	1.2	-2.0 - 5.5
Lead 4V		
Men	5.0 or 6.0	1.0 - 13.0
Women	3.5 or 4.5	1.0 - 9.0

Upper limits of the normal P-R intervals (duration in seconds)

Rate	Below 70	71 - 90	91 - 110	111 - 130	Above 130
Large adults	0.21	0.20	0.19	0.18	0.17
Small adults	0.20	0.19	0.18	0.17	0.16

Duration of QRS (Distribution)

Duration of QRS (sec.)	Lead I, %	Lead II, %	Lead III, %
0.06	3	0.8	1.8
0.07	26	19.0	17.0
0.08	46	43.0	43.0
0.09	13	25.0	24.0
0.10	4	10.0	10.0
0.11	1	1.0	1.8
0.12	0	0.8	0.4

Upper limits of the ST segment in lead with highest T-wave (duration in seconds)

Rate	Men and Children	Women
40	0.155	0.170
50	0.150	0.165
60	0.145	0.160
70	0.135	0.150
80	0.125	0.140
90	0.115	0.130
100	0.100	0.115
110	0.080	0.095
120	0.060	0.095
130	0.040	0.055

Rate	Men and Children	Women
140	0.015	0.030
150	0.000	0.000

Normal Variations of the Q-T Interval

		Mean		Upper Limit	
Rate	Lower Limit	Men & Child	Women	Men & Child	Women
40	0.42	0.45	0.46	0.49	0.50
43	0.39	0.44	0.45	0.48	0.49
46	0.38	0.43	0.44	0.47	0.48
48	0.37	0.42	0.43	0.46	0.47
50	0.36	0.41	0.43	0.45	0.46
52	0.35	0.41	0.42	0.45	0.46
55	0.34	0.40	0.41	0.44	0.45
57	0.34	0.39	0.40	0.43	0.44
60	0.33	0.39	0.40	0.42	0.43
63	0.32	0.38	0.41	0.41	0.42
67	0.31	0.37	0.38	0.40	0.41
71	0.31	0.36	0.37	0.38	0.41
75	0.30	0.35	0.36	0.38	0.39
80	0.29	0.34	0.35	0.37	0.38
86	0.28	0.33	0.34	0.36	0.37
93	0.28	0.32	0.33	0.35	0.36
100	0.27	0.31	0.32	0.34	0.35
109	0.26	0.30	0.31	0.33	0.33
120	0.25	0.28	0.29	0.31	0.32
133	0.24	0.27	0.28	0.29	0.30
150	0.23	0.25	0.26	0.28	0.28
172	0.22	0.23	0.24	0.26	0.26

APPENDIX E

Correlation Functions - Probabilistic Development

A different approach to the development of the correlation functions is the use of probabilistic methods. This directly develops the discrete correlation functions, and directly shows that the mean square error is minimized. This supplements the previous development of the correlation functions through the matched filter approach.

If we are given two random variables, x, and y, and plot them on a plane, with the vertical axis representing x, the horizontal axis representing y, the outcome, at different times would be represented as points on the plane. If the variables were random and independent, one would expect the pattern of points representing x and y at given times to randomly scattered throughout the entire plane. However, if the variables were strongly dependent on each other, the expectation would be that the sample points would be clustered in the vicinity of a curve describing the dependence. The simplest case of dependence is linear dependence, where the curve is a straight line. This is of considerable practical importance, and is discussed in Feller (6), and Davenport (5) at some length.

If it is assumed that the variables have a strong linear dependence, the points will be clustered a straight line, called the regression line, whose general equation is $y_p = a + bx$. It is desired to determine the "best" predicted value y_p of the variable y, based on the mean square difference (error) e_{ms} between the true sample value y and its predicted value y_p. This is given by

$$e_{ms} = E[(y - y_p)^2] = E\{[y - (a + bx)]^2\}$$

where E is the expectation value of the difference squared. The line so determined is known as the linear mean square regression line.

It is now necessary to determine the values of a and b to find the equations of this line. The expression for the mean square error will be differentiated with respect to a and b, and the results equated to zero. The definition of the expectation value of a general function g(x,y) is given by

$$E[g(x,y)] = \int_{-\infty}^{\infty} \int_{-\infty}^{\infty} g(x,y)\, P(x,y)\, dx\, dy$$

Substituting this value for the expectation value gives

$$e_{ms} = \int_{-\infty}^{\infty} \int_{-\infty}^{\infty} [y - (a + bx)]^2 P(x,y)\, dx\, dy$$

$$= \int_{-\infty}^{\infty} \int_{-\infty}^{\infty} [y^2 - 2y(a + bx) + a^2 + 2abx + b^2x^2] P(x,y)\, dx\, dy$$

Differentiating this with respect to a gives

$$\frac{\alpha e_{ms}}{\alpha a} = \int_{-\infty}^{\infty} \int_{-\infty}^{\infty} (-2a)yP(x,y)\, dx\, dy + 2b \int_{-\infty}^{\infty} \int_{-\infty}^{\infty} xP(x)\, dx\, dy$$

$$+ 2a \int_{-\infty}^{\infty} \int_{-\infty}^{\infty} P(x,y)\, dx\, dy = -2aE(y) + 2a + 2b\, E(x) = 0$$

Differentiating the same expression with respect to b gives

$$\frac{\alpha e_{ms}}{\alpha a} = \int_{-\infty}^{\infty} \int_{-\infty}^{\infty} (-2b)xyP(x,y)dxdy + 2a\int_{-\infty}^{\infty} \int_{-\infty}^{\infty} xP(x,y)dxdy$$

$$+ 2b\int_{-\infty}^{\infty} \int_{-\infty}^{\infty} x^2P(x,y)dxdy = -2E(x,y) + 2aE(x) + 2bE(x^2) = 0$$

After solution of the simultaneous equations, the solutions for a and b are

$$b = \frac{E(xy) - E(x)\,E(y)}{E(x^2) - E(x)^2} \quad , \qquad a = \frac{E(y)\,E(x^2) - E(xy)\,E(x)}{E(x^2) - E(x)^2}$$

However, it is noted that the denominator of both expressions is the variance of x, σ_x^2. Inspecting the numerator of b, it is found, by application of the identity $E(xy) - E(x)E(y) = E(x - m_x)E(y - m_y)$, that the numerator of $b = \mu_{11}$ where μ_{11} is the covariance of the variables x and y. Similarly, inspection of the numerator of a, using the identity $E(x^2) = \sigma_x^2 + m_x^2$, and of the identity used in the numerator of b, we find

$$b = \frac{E(x - m_x)\,E(y - m_y)}{\sigma_x^2} = \frac{\mu_{11}}{\sigma_x^2} \quad ,$$

$$a = \frac{m_y(\sigma_x^2 + m_x^2)}{\sigma_x^2} - \frac{m_x(\mu_{11} + m_x m_y}{\sigma_x^2} = m_y - \frac{\mu_{11} m_x}{\sigma_x^2}$$

where m_x and m_y are the mean values of x and y. Now, substituting these values in the equation for the prediction line, we get

$$y_p = \frac{\mu_{11}}{\sigma_x^2}\,x + m_y - \frac{\mu_{11} m_x}{\sigma_x^2} = m_y + \frac{\mu_{11}}{\sigma_x^2}\,(x - m_x)$$

as the equation for the best prediction line.

Now, it is convenient to introduce the standardized variable corresponding to $\xi = \frac{x - m_x}{\sigma_x}$. Under these conditions, the following are true

$$E(\xi) = 0, \text{ and } \sigma^2 = 1$$

In terms of this standardized variable, we define a standardized prediction $n_p = (y_p - m_y)/\sigma_y$, the previously derived expression for the best prediction line in the mean square sense is $n_p = \rho$, where ρ is the standardized correlation coefficient defined by

$$\rho = E(\xi n) = \frac{\mu_{11}}{\sigma_x \sigma_y}$$

in which n is the standardized variable corresponding to y. Now this correlation coefficient can be expressed in the following manner.

$$\rho = \frac{\sum_{N=1}^{n} x_i y_i}{\sqrt{\sum_{N=1}^{N} x_i^2 \sum_{i=1}^{N} y_i^2}}$$

For our purposes, it is often of greater use to drop the normalization afforded by the denominator of the correlation coefficient, and deal with the numerator only, giving

$$r = \frac{1}{n} \sum_{i=1}^{n} x_i y_i$$

Since we are dealing with sequential samples, and a shift in sample number defines a shift in time, the autocorrelation function of a sequence of n numbers is defined as

$$\phi_{xx}(j) = \lim_{N \to 0} \frac{1}{2N + 1} \sum_{K = -N}^{N} x_K x_{K+j}$$

And the crosscorrelation function between the x and y sequence is

$$\phi_{xy(j)} = \lim_{N \to \infty} \frac{1}{2N + 1} \sum_{K = -N}^{N} x_K y_{K+j}$$

These represent the correlation functions for the discrete case, which is applicable to the sampled data used in this investigation. The discrete case can be extended to the continuous case, for which it is a satisfactory representation if the sampling frequency is sufficiently high. The autocorrelation function becomes

$$\phi_{xx}(\tau) = \lim_{\tau \to \infty} \frac{1}{2\tau} \int_{-\tau}^{\tau} x(\tau)x(t + \tau)d\tau$$

and the crosscorrelation function becomes

$$\phi_{xy}(\tau) = \lim_{\tau \to \infty} \frac{1}{2\tau} \int_{-\tau}^{\tau} x(\tau)y(t + \tau)d\tau.$$

APPENDIX F

This appendix includes the list of logic of recognition first utilized to perform the search required for the normalization and data location for application of the correlation techniques. This list of search operations is shown in the first two pages. The last page shows the search program consisting of the 5-point moving average. This flow chart shows the flow chart for the program for the digital computer.

Also included are the results of the application of the logic of recognition to the six waveforms considered to date. These results are used in later sections to supplement the data on diagnosis.

Logic of Recognition

1. Select first, second, third, and fourth flagged samples as maximum negative derivatives.
2. Count total number of samples between first and fourth flags = N.
3. Compute heart rate f = 1500/N and store.
4. Locate the third flagged sample. (This is the maximum negative derivative of the center waveform, which will be analyzed.)
5. Designate third sample as No. 400 on a counter.
6. Move to sample No. 100, and take moving average from sample 100 forward until 3 successive increases (decreases) are noted.
7. Move to sample No. 100, and take moving average from 100 backward until e successive increases (decreases) are noted.
8. Flag the sample showing the first increase (three back from that found in step 6).
9. Store value of constant moving average. This is the base point.
10. Subtract the base value from the values of each sample between second and fourth maximum negative derivatives.

11. Start correlation routing No. 1 for sine wave, 50 samples less than the value flagged in step No. 8.

12. Evaluate correlation function from flagged point until it equals zero. Store all values.

13. In evaluation of the correlation function, set all values of samples greater than 350 equal to zero.

14. Flag maximum value of correlation function, after determining it, and sample at which it occurs (N_1).

15. Flag sample at which correlation coefficient becomes zero (N_2).

16. Flag sample at start of correlation when coefficient becomes other than zero (N_3).

17. Store ϕ_1 max, N_1, N_2, N_3, and Y_1, determining Y_1 as equal to the average of samples $N_1 - 2$, $N_1 - 1$, N_1, $N_1 + 1$, and $N_1 + 2$. Set other values of correlation function = 0.

18. Take moving average between sample 350 and 450 (5 samples wide).

19. Note points between sample 360 and 430 where average changes sign. Flag samples at which sign changes.

20. Start correlation routing No. 2 at sample 350, and continue until correlation function is zero.

21. Perform correlation with all samples zero after first flagged sample for change of sign.

22. Flag sample at which correlation function first becomes different from zero (N_4).

23. Search for maximum correlation coefficient, $\phi_2$max, and flag sample (N_5).

24. Flag sample at which correlation coefficient first becomes zero (N_6).

25. Pick value of sample at $N_5 = Y_2$.

26. Store $\phi_2$max, N_4, N_5, N_6, and Y_2.

27. Set all sample values to zero before first change of sign flag.

28. Start correlation routine No. 3 at sample 360, and continue until correlation function is equal to zero.

29. Set all sample values to zero after second change of sign flag.

30. Flag sample at which correlation coefficient first becomes different from zero (N_7).

31. Search for maximum correlation coefficient, $\phi_3$max, and flag sample (N_8).

32. Flag sample at which correlation coefficient becomes zero (N_9).

33. Pick value of sample at $N_8 = Y_3$.

34. Store $\phi_3$max, N_7, N_8, N_9, and Y_3.

35. Set all sample values to zero before second change of sign flat.

36. Start correlation routine No. 2 at sample 390, and continue until correlation function equals zero.

37. Set all samples to zero after sample No. 415.

38. Flag sample value at which correlation coefficient first becomes different from zero (N_{10}).

39. Search for maximum correlation coefficient, $\phi_4$max, and flag sample at this point (N_{11}).

40. Flag sample at which correlation coefficient becomes zero N_{12}.

41. Pick value of sample at $N_{11} = Y_4$.

42. Store $\phi_4$max, N_{10}, N_{11}, N_{12}, and Y_4.

43. Start moving average (5 samples wide) at sample 410, continue until sample No. 415 + N_r. (N_r is determined from heart rate on subroutine) or until slope of moving average increases three times in a row at a rate greater than the previous three times.

44. Pick value of ST segment to be either last average at 415 + N_r or at point at which increased slope begins, this is stored as ST. Call this sample N_{13}.

45. Set all samples in ST segment, determined above, to zero.

46. Start correlation routine No. 4 at sample No. 415, and continue until correlation function is zero.

47. Flag sample at which correlation coefficient becomes zero (N_{15}).

48. Search for maximum correlation coefficient, $\phi_5$max, and flag as N_{14}.

49. Flag sample at which correlation coefficient becomes different than zero (N_{16}).

50. Take average of N_{14}-2, N_{14}-1, N_{14}, N_{14}+1, and N_{14}+2 and call Y_5.

51. Store $\phi_5$max, N_{13}, N_{14}, N_{15}, and Y_5.

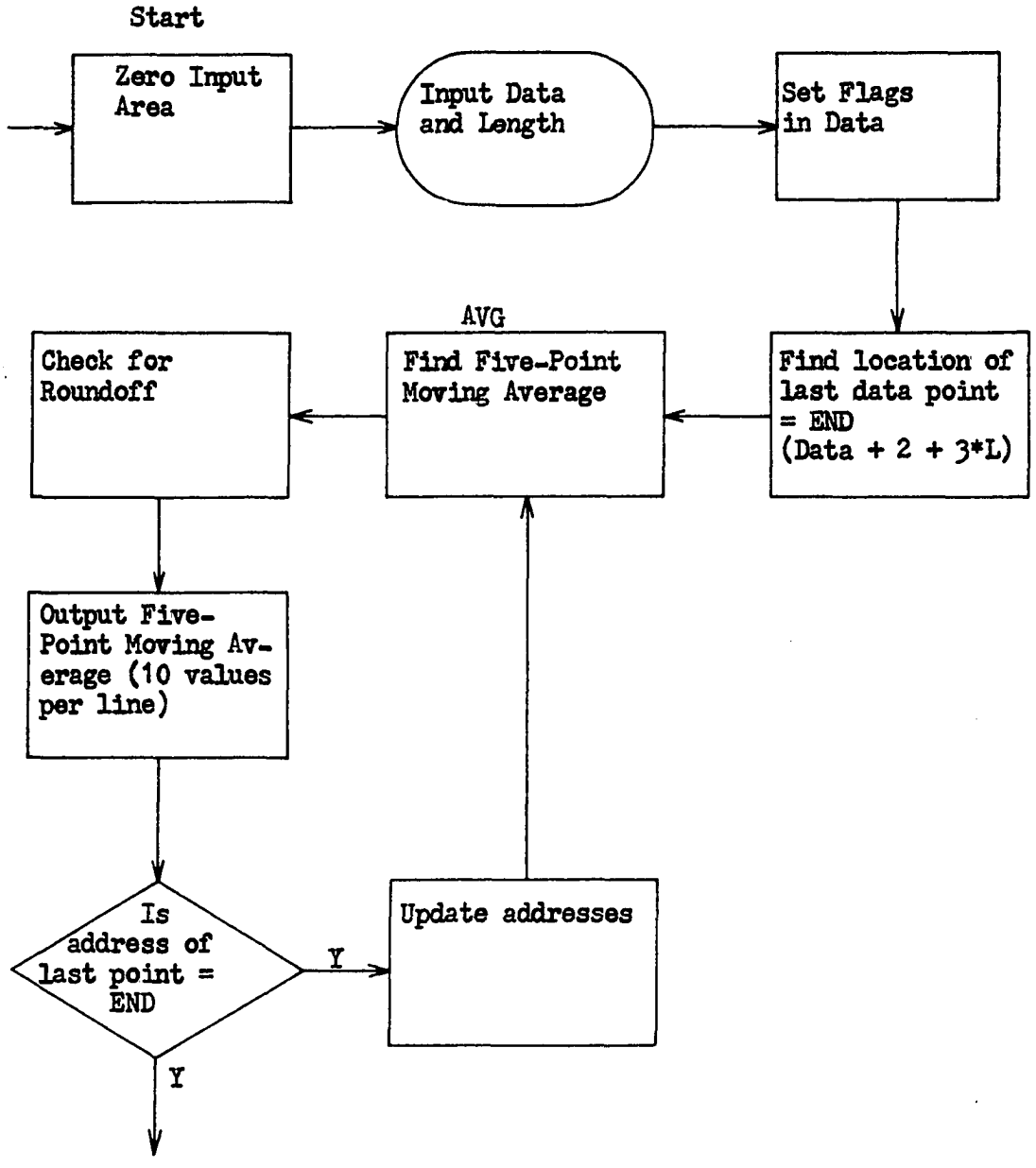

Figure 42. Moving average